Tobias Bollian

Localization of Rovers on the Lunar Surface using the Monopulse Technique

MASTER'S THESIS

to achieve the university degree of

Master of Engineering (MEng)

Master's programme: Space Systems and Business Engineering (SpaceTech)

submitted to

Graz University of Technology

Supervisors:

Univ.-Prof. Dipl.-Ing. Dr.techn. Philipp Berglez
Institute of Communication Networks and Satellite Communications
Graz University of Technology

Prof. Dr.-Ing. Marwan Younis
Institute of Radio Frequency Engineering and Electronics
Karlsruhe Institute of Technology

LIFE LONG LEARNING

Graz, September 2023

Affidavit

I declare that I have authored this thesis independently, that I have not used other than the declared sources/resources, and that I have explicitly indicated all material which has been quoted either literally or by content from the sources used. The text document uploaded to TUGRAZonline is identical to the present master‘s thesis.

23.08.2023

Date

Signature

Abstract

The interest in the Moon has significantly increased in the recent years due to the fact that the International Space Station will retire in the near future and because of the increased space activity of private companies. However, one major challenge of currently planned Lunar missions is the provision of cheap and reliable energy, restricting most missions to short durations and reducing mobility.

In order to overcome this problem, the LunarSpark company envisions launching a space-based power plant to orbit the Moon. This system can provide energy via laser to customers on the Lunar surface and thus eliminates the problem of cheap and reliable energy. Further, the system shall autonomously detect the coarse relative position between the satellite and the customer. This is needed in order to trigger a laser-based localization of the exact customer position, as it is already commonly performed in laser-based communication systems.

LunarSpark decided to deploy a Radio-Frequency (RF) beacon on the customer system. This beacon is used to retrieve a coarsely estimated customer position via microwaves and is investigated in this thesis. The monopulse technique is used for this purpose because unlike a radar measuring Doppler and distances, which is sensitive to topography and spatial position uncertainties when converting to the relative angular position, the monopulse technique allows to directly measure the angular direction. Thus, this work analyzes the requirements that such an RF beacon needs to fulfill for the monopulse technique, as well as how its operation fits into the overall operational timeline of the LunarSpark system. In addition, it also establishes the design parameters of this beacon. The work is supported with theoretical and simulated performance analyses to derive the final design parameters.

Zusammenfassung

Das Interesse am Mond hat in den letzten Jahren signifikant zugenommen, weil die Internationale Raumstation in naher Zukunft außer Betrieb genommen wird und aufgrund der erhöhten Weltraumaktivitäten von privaten Unternehmen. Allerdings ist eine große Herausforderung bei den derzeit geplanten Mondmissionen die Bereitstellung von günstiger und zuverlässiger Energie, was die meisten Missionen auf kurze Dauer beschränkt und die Mobilität einschränkt.
Um dieses Problem zu überwinden, plant das Unternehmen LunarSpark, ein weltraumbasiertes Kraftwerk in den Orbit des Mondes zu starten. Dieses System kann Energie per Laser an Kunden auf der Mondoberfläche liefern und beseitigt somit das Problem der kostengünstigen und zuverlässigen Energieversorgung. Weiterhin soll das System die grobe relative Position zwischen dem Satelliten und dem Kunden autonom erkennen. Dies ist notwendig, um eine Laser-basierte Ortung der genauen Kundenposition auszulösen, wie es bereits bei Laser-Kommunikationssystemen üblich ist.
LunarSpark hat beschlossen, einen Radiofrequenz (RF) -Funksender auf dem Kundensystem einzusetzen. Dieser Sender wird verwendet, um eine grob geschätzte Kundenposition über Mikrowellen zu ermitteln und wird in dieser Arbeit untersucht. Zu diesem Zweck wird die Monopulstechnik verwendet, da die Monopulstechnik im Gegensatz zu einem Doppler- und Entfernungsmessradar, das bei der Umrechnung in die relative Winkelposition empfindlich auf Topographie und räumliche Positionsunsicherheiten reagiert, eine direkte Messung der Winkelrichtung ermöglicht. Die Arbeit analysiert die Anforderungen, die ein solcher RF-Funksender erfüllen muss, wie sein Betrieb in den gesamten Betriebsablauf des LunarSpark-Systems passt und legt auch die Designparameter für diesen Sender fest. Die Arbeit wird durch theoretische und simulierte Leistungsanalysen unterstützt, um die endgültigen Designparameter abzuleiten.

Contents

List of Figures

List of Tables

Acronyms

GNSS Global Navigation Satellite System

PRF Pseudo-Random Noise

PRN Pulse Repetition Frequency

RF Radio-Frequency

SNR Signal-to-Noise Ratio

1 Introduction

1.1 Lunar Exploration

With the International Space Station set to retire in the near future [1], the Lunar market offers attractive alternative opportunities for a sustainable space economy through in-situ resource utilization [2]. Therefore, the Moon has again become an interesting mission target for multiple countries who want to explore and utilize the Moon's resources. The area around the Lunar South Pole is receiving special attention from many mission concepts [3]. Examples for current plans include exploration missions needed before establishing a long-term human presence, like studying the Moon's geological composition and finding potential resources for water [4].
However, the main challenge for all these efforts, and to make the Lunar economy feasible in general, is the access to energy on the Moon. Current missions are limited to short durations and come with a high cost and limited mobility, thus hindering exploration [5]. This is the case because of the high entry barrier for nuclear energy or radioisotope thermoelectric generators on the Moon, which results in many missions relying on solar energy. However, the long Lunar night, with an average length of 14 days, provides no energy source for such power generation [6]. As seen in Fig. 1, requiring sun illumination constrains the feasible operation area to a fraction of the Lunar surface. A human outpost and extended research on the Moon therefore only becomes feasible with a proper Lunar power infrastructure [7].

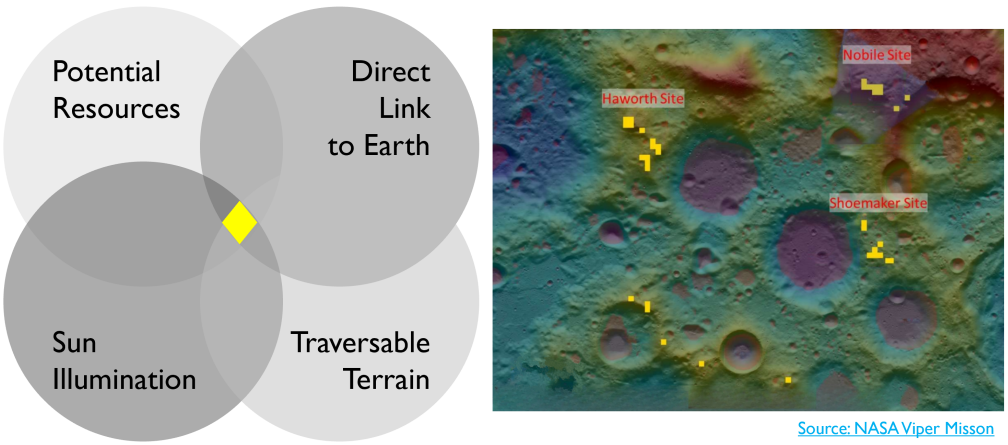

Figure 1: Selecting a spot for Lunar missions is challenging as the spot needs to provide sun illumination for energy. Only a fraction of the surface is suitable for the operation of a mission. Image from [8].

1.2 A Space-Based Power System around the Moon

In order to overcome the constraint of being dependent on sun illumination, the LunarSpark company (cf. Appendix) plans to operate a space-based power system in the Lunar orbit. This system can provide power for surviving the Lunar night without the customer having to traverse into a safe heaven of sun illumination. The goal of this system is to collect and convert the sun energy, which is then delivered via laser to customers operating in the LunarSpark servicing area at the Lunar South Pole. This servicing area was selected based on the large scientific interest in this region of the Moon, with many mission concepts currently investigating the operation of systems in this area [3]. The laser was selected as means for transmitting power due to the small receive and transmit aperture that becomes feasible in the optical region, despite its low efficiencies. This is a key design factor in the LunarSpark system, which focuses on customer mobility and therefore discarded the use of more mature microwave technology, as microwaves would result in significantly larger transmit and receive apertures. Fig. 2 shows the concept of operations of LunarSpark. The satellite is converting the solar energy into laser energy and is distributing it to customers on the Lunar surface. A periodic exchange with the ground segment on Earth is performed for optimizing the servicing timeline.

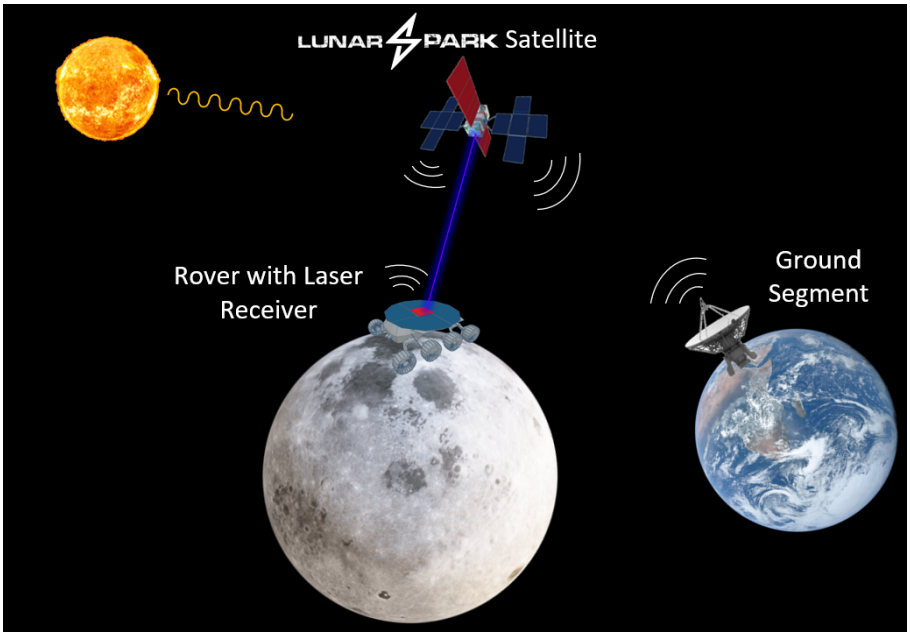

Figure 2: LunarSpark concepts of operation. The satellite relays the energy from the Sun via laser to the customer on the ground. Image from [8].

1.3 The Pointing Challenge for Wireless Power Transmission from the Lunar Orbit

The main challenge of the system presented in the previous subsection is the high pointing accuracy required to hit the small receive aperture of the customer with the fine laser beam at distances of many hundreds of kilometers. This could be overcome with a larger beamwidth that increases the footprint on the ground and thus reduces the pointing accuracy needed to point at the receiver. However, a larger beamwidth also increases the geometrical losses, as the receiver makes up a smaller percentage of the footprint (cf. Fig. 3). The beamwidth therefore needs to be kept reasonably small in order to reduce these losses and provide sufficient power to the customer. This trade-off between pointing accuracy and losses resulted in a targeted pointing accuracy of 36 microdegrees [9].

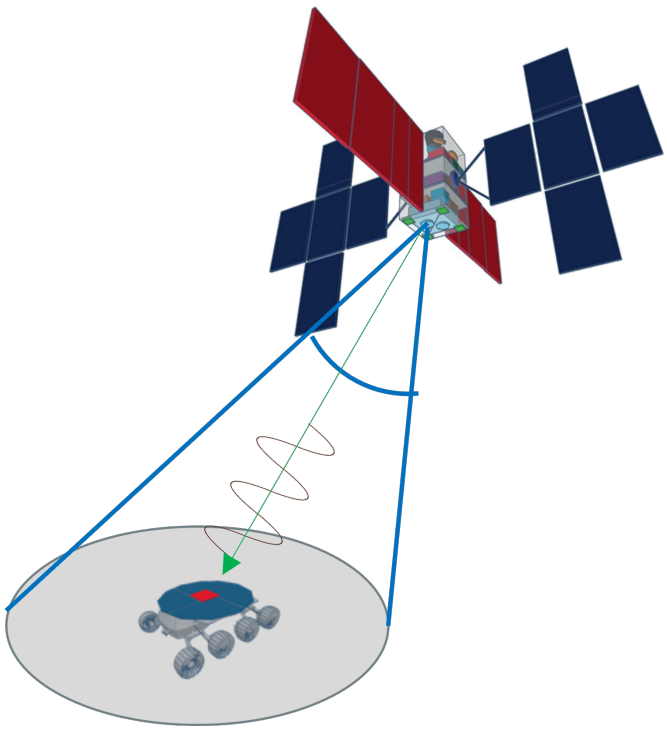

Figure 3: The footprint of the laser on-ground depends on the beam divergence. A larger footprint reduces the required pointing accuracy which places the customer inside the footprint. However, the larger the footprint, the more energy is wasted as the receiver only extracts a fraction of the energy inside the footprint. Image from [8].

All this needs to be achieved with a customer system that might be constantly moving between repeat-passes of the satellite. The LunarSpark satellite solves this with a pointing mechanism that functions only based on a coarse estimate of the relative receiver position. Based on this coarse estimate, a spiraling laser establishes the fine position of the satellite receiver. Once the receiver is detected, the laser beam is maintained on top of the receiver with a closed-loop tracking of the laser beam, during which the customer communicates the instantaneously received energy to the satellite. With this customer feedback, the satellite pointing is adjusted in order to maximize the received energy (further details provided in Chapter 3).

1.4 Scope and Motivation of this Thesis

In order to deal with the pointing challenge described in the previous subsection, LunarSpark has decided to use an RF beacon on top of the customer system that communicates with a small microwave antenna mounted on the satellite. This RF-link is used to retrieve a coarse estimate on the relative position and also to close the loop of the fine tracking. To achieve these goals, certain requirements have been identified for the RF waveform transmitted by the customer:

- Differentiation between customers: The satellite needs to be able to distinguish between different customers present on the Lunar surface.
- Modulated communication signal: The waveform should be capable of carrying a modulated communication signal.
- Processing gain for improved signal quality: The ability to apply processing techniques like pulse compression is necessary to enhance the signal-to-noise ratio, particularly for estimating the rough position between the satellite and the customer.

The motivation of this work is to select an appropriate communication scheme that fulfills all these requirements and allows for an estimation of the coarse relative position with sufficient accuracy. This work is structured as follows: first, a summary of the monopulse technique and the required theoretical background for the understanding of this thesis is given in Chapter 2. Chapter 3 provides a brief introduction into the LunarSpark system elements that need to interact with the RF beacon. In addition, Chapter 3 will also derive the optimum timeline of operation for the coarse position

estimation. This is followed by Chapter 4 which contains a detailed theoretical and simulated analysis of the localization accuracy that results from the selected technique, as well as a proposed design solution for the LunarSpark system. The work is concluded in Chapter 5.

2 Theoretical Background

This chapter presents the theoretical background needed in order to understand this thesis. Section 2.1 presents a basic overview of the monopulse technique as it is used in this work. Section 2.2 introduces the properties of common Global Navigation Satellite System (GNSS) signals, as these types of signals were selected for the LunarSpark RF Beacon in the trade-analysis performed for this thesis. Finally, Section 2.3 covers the link budget theory needed for the analysis performed in Chapter 4.

2.1 Monopulse Technique

The monopulse technique [10, 11] is a well-proven technique that has already been employed in a wide variety of radar systems and allows for the angle-of-arrival estimation of incoming signals. Therefore, this radar technique plays a crucial role in tracking systems [12].
Unlike other methods [13, 14], the monopulse technique not only offers a good robustness and reliability but can also be implemented with a low computational load. For the application of the monopulse technique, the antenna needs to be split into two channels in the one-dimensional case. In the two-dimensional case, the antenna needs to be split into four channels and the one-dimensional monopulse technique can be applied twice, once in each dimension. This is also illustrated in Fig. 4, which shows how two different signals $s_1(t)$ and $s_2(t)$ are extracted from the antenna channels. Both signals

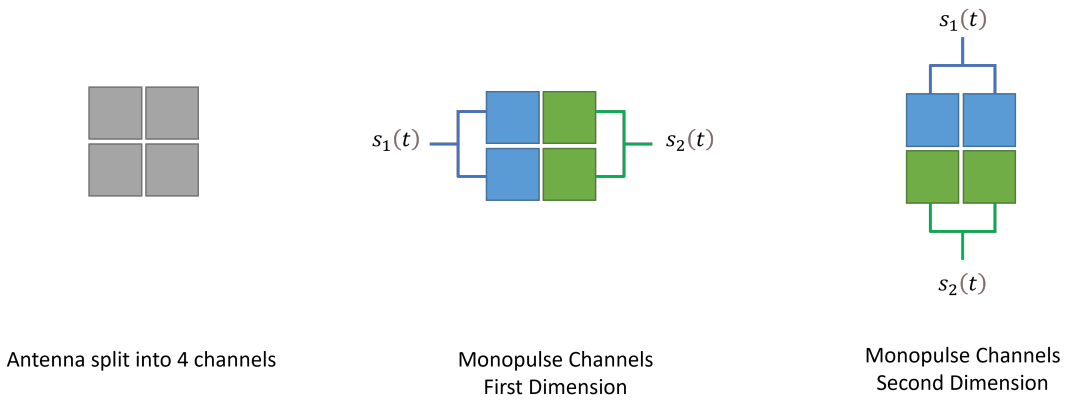

Figure 4: Required antenna for application of the two-dimensional monopulse technique (left), channel combination needed for monopulse in first dimension (middle), channel combination needed for monopulse in second dimension (right).

can then be combined to a sum signal and a delta signal according to

$$s_{\text{sum}}(t) = s_1(t) + s_2(t) \tag{2.1}$$

and

$$s_{\text{delta}}(t) = s_1(t) - s_2(t). \tag{2.2}$$

Using these two artificial signals, a ratio can be formed as follows:

$$s_{\text{ratio}}(t) = \frac{\text{Imag}\left[s_{\text{delta}}(t)\right]}{\text{Real}\left[s_{\text{sum}}(t)\right]}. \tag{2.3}$$

This ratio depends on the angle-of-arrival of the signal as shown in the following with simulated data.

Fig. 5 shows the simulated monopulse patterns and output from a tool developed in the framework of this thesis (in u and v antenna coordinates that are commonly used in antenna literature). The plots were simulated for an exemplary antenna operating at 24 GHz and a 7 cm by 7 cm antenna (3.5 cm by 3.5 cm size of each channel). Fig. 5a shows the output of Eq. 2.1 and thus the sum pattern. The output of Eq. 2.2 and thus the delta pattern is shown in Fig. 5b. Finally, Fig. 6 shows the monopulse ratio of Eq. 2.3. The ratio changes only in one dimension, as expected. For computing the angle-of-arrival in the other dimension, the monopulse needs to be applied with a different channel combination (see Fig. 4).

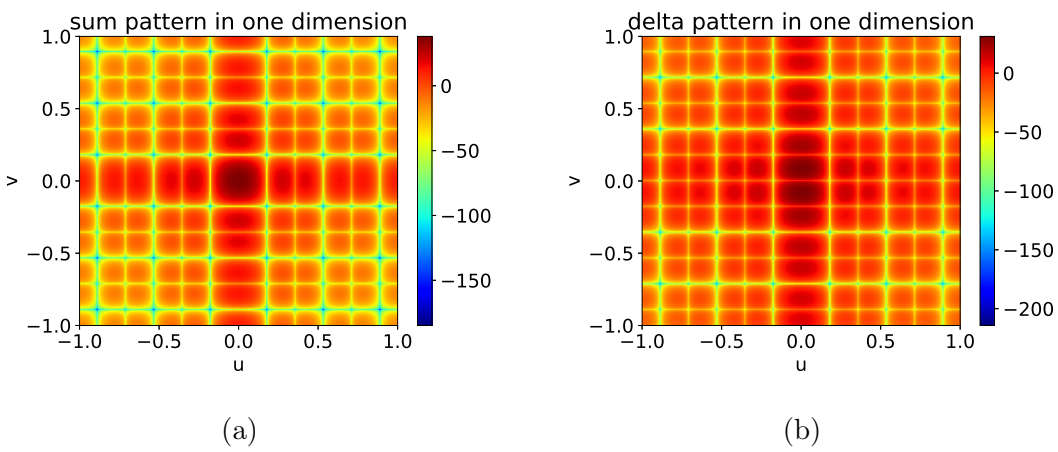

Figure 5: a) Two-dimensional antenna pattern of sum-signal plotted versus u and v, b) Two-dimensional antenna pattern of delta-signal plotted versus u and v.

The monopulse ratio in Fig. 6a shows a repetitive pattern. Thus, a proper angle-of-arrival estimation with this method is only possible if it can be assumed that the signal direction is within the mainlobe. In this case, the

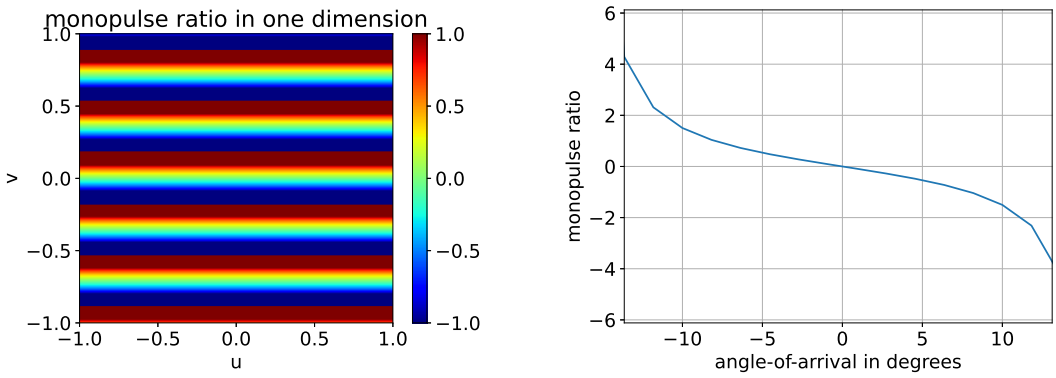

(a) (b)

Figure 6: a) Monopulse ratio resulting from the patterns shown in Fig. 5 plotted versus u and v, b) Zoom of monopulse ratio over main beamwidth shows linear relation between angle-of-arrival and estimated monopulse ratio.

ratio is unique (as shown in Fig. 6b) and can be approximated linearly within the mainlobe.

2.2 GNSS Signals

Global Navigation Satellite Systems (GNSS) have first been launched by the US in 1973 and were used for military purposes. Nowadays they are being used on a daily basis by the civil population and their technique has been well-proven. GNSS enables precise positioning and navigation worldwide. It consists of a constellation of satellites around Earth, continuously transmitting signals that can be received by GNSS devices. The main idea behind GNSS is that the user device can estimate its position by triangulating signals from multiple satellites.

To allow a separation of the signals from different satellites at the user, the satellites modulate a pseudo-random noise (PRN) code onto the GNSS carrier frequency as shown in Fig. 7. In addition, data (navigation message) is modulated onto the signal as shown further below.

The signals transmitted by GNSS satellites also carry information about the satellite positions and precise clock data. This is necessary in order to improve the user's estimated position. Thus, the same transmit pulse is repeated multiple times with a phase shift in order to modulate the information onto the signal. This is shown in Fig. 8.

Note that the PRN coding spreads the occupied spectrum, allowing the user to reverse the process and achieve an improved signal-to-noise ratio while

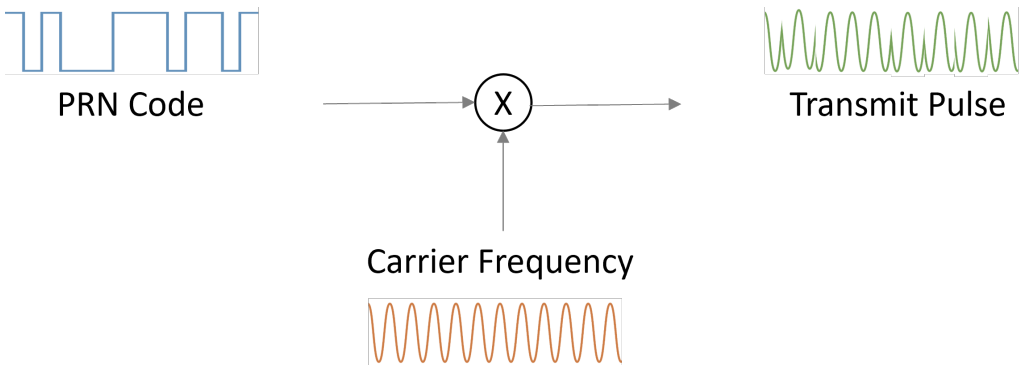

Figure 7: Zoom of monopulse ratio over main beamwidth shows linear relation between angle-of-arrival and estimated monopulse ratio.

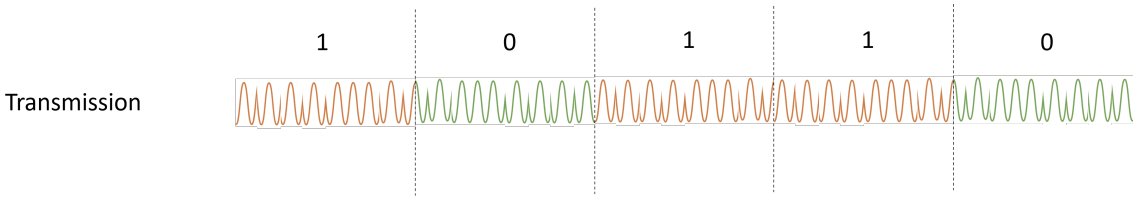

Figure 8: Zoom of monopulse ratio over main beamwidth shows linear relation between angle-of-arrival and estimated monopulse ratio.

separating the individual satellite signals. Fig. 9 shows the received signal after processing, which results in a compression of the signal in the time-domain.

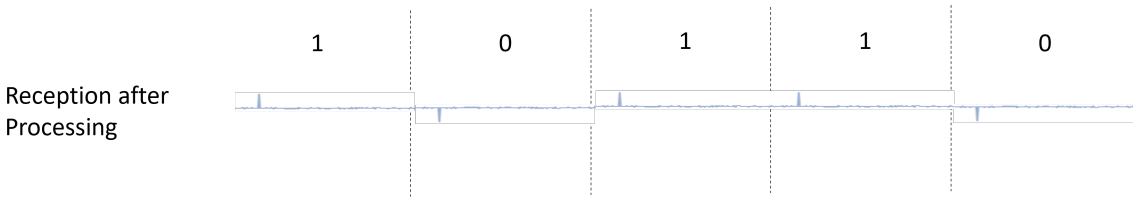

Figure 9: Zoom of monopulse ratio over main beamwidth shows quasi-linear relation between angle-of-arrival and estimated monopulse ratio within the mainlobe.

The properties of a typical GNSS signal, as used and relevant in this work[1], are summarized in Table 1.

[1] A high processing gain and small noise bandwidth are beneficial for the RF beacon performance. Thus, this type of GNSS signal was selected.

Parameter	Value
Pulse duration	1 ms
Bandwidth	2 MHz
Processing Gain	46 dB

Table 1: Typical GNSS signal properties that are used in this work.

2.3 Link Budgets

A powerful tool when designing microwave systems, for radar systems as well as communication systems, is the link budget. A link budget systematically takes into account all gains and losses encountered by a signal as it travels through the transmission channel. This allows for a prediction of the signal attenuation and the noise imposed onto the signal (cf. Fig. 10). Thus, the link budget helps with determining the required power levels for a successful reception at the receiver with a given Signal-to-Noise Ratio (SNR).

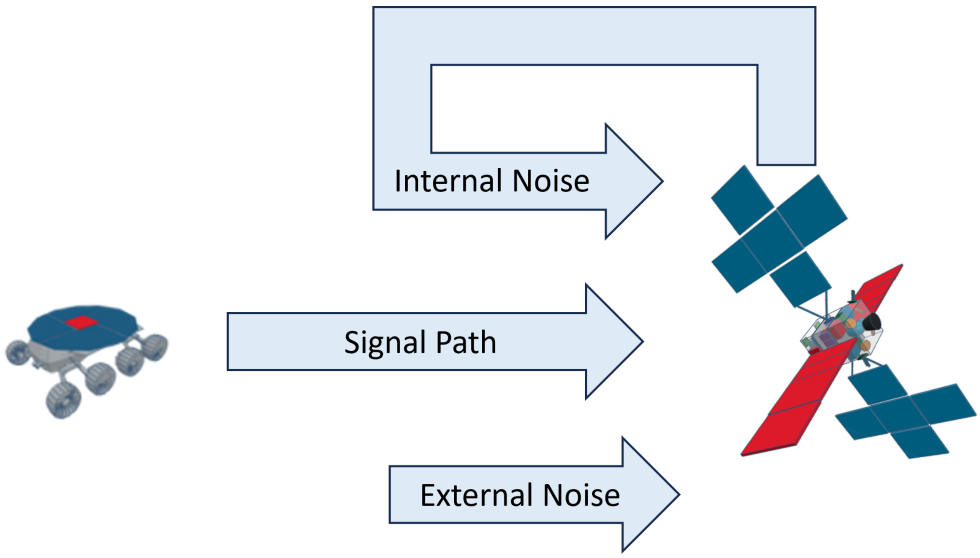

Figure 10: The link budget provides information about the power of the transmitted signal after it has propagated through the transmission channel and arrives at the receiver, as well as the power of the internal and external noise.

This section introduces the theoretical equations of the link budget and presents all the factors that affect the one-way trip of the microwave signal, as it is commonly required for communication signals. A summary of all considered components for the signal transmission is shown in Fig. 11.
A signal of peak transmit power P_{tx} is radiated from an antenna with gain G_{tx}. Depending on the angular direction θ and ψ and the shape of the transmit radiation pattern $C_{\text{tx}}(\theta, \psi)$, a different amount of power density

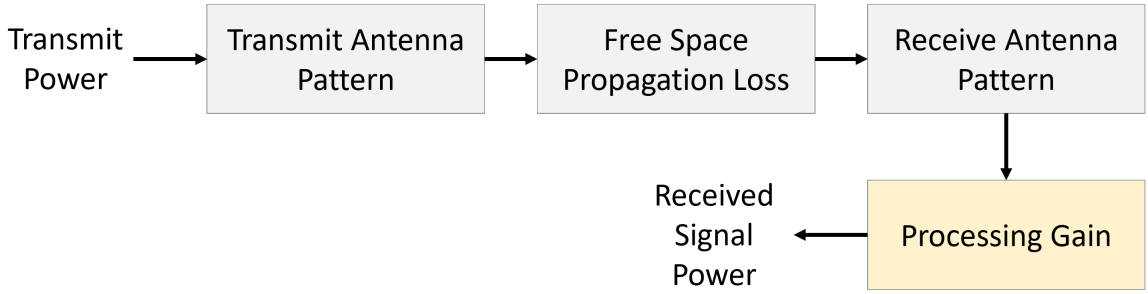

Figure 11: Chain affecting the amount of transmit power that arrives at the receiver.

S_{rad} is radiated from the antenna according to

$$S_{\text{rad}} = P_{\text{tx}} G_{\text{tx}} |C_{\text{tx}}(\theta, \psi)|^2. \tag{2.4}$$

The power density reduces as the signal propagates away from the transmitter on an ideal sphere, such that the power density S_{rx} at the receiver at distance R is given by

$$S_{\text{rx}} = \frac{S_{\text{rad}}}{4\pi R^2}. \tag{2.5}$$

The extracted receive power P_{rx} depends on the effective antenna aperture area A_{rx} of the receiver. The receive power is thus

$$P_{\text{rx}} = S_{\text{rx}} A_{\text{rx}}. \tag{2.6}$$

The effective antenna aperture depends on the receiver gain G_{rx} and receiver radiation pattern[2] $C_{\text{rx}}(\theta, \psi)$:

$$A_{\text{rx}} = G_{\text{rx}} |C_{\text{rx}}(\theta, \psi)|^2 \frac{\lambda^2}{4\pi}. \tag{2.7}$$

Finally, the total received power P_{rx} can be expressed as

$$P_{\text{rx}} = P_{\text{tx}} G_{\text{tx}} |C_{\text{tx}}(\theta, \psi)|^2 \frac{\lambda^2}{16\pi^2 R^2} G_{\text{rx}} |C_{\text{rx}}(\theta, \psi)|^2. \tag{2.8}$$

In addition, the receiver also perceives a noise signal that can be described with

$$P_{\text{n}} = k T_0 NF B, \tag{2.9}$$

where k is the Boltzman constant, $T_0 = 290$ K, NF is the noise figure, and B is the noise bandwidth.

[2]Different variables θ and ψ are generally used for transmit and receive. For simplicity, the same variables are used here.

The ratio between Eq. 2.8 and Eq. 2.9 results in the SNR of the received signal before processing:

$$SNR_{\text{raw}} = \frac{P_{\text{tx}} G_{\text{tx}} |C_{\text{tx}}(\theta, \psi)|^2 \lambda^2 G_{\text{rx}} |C_{\text{rx}}(\theta, \psi)|^2}{16\pi^2 R^2 k T_0 N F B}. \tag{2.10}$$

If processing is applied to the received signal, resulting in a processing gain of G_{proc} of the impulse response function peak, then this improves the SNR to

$$SNR_{\text{proc}} = \frac{P_{\text{tx}} G_{\text{tx}} |C_{\text{tx}}(\theta, \psi)|^2 \lambda^2 G_{\text{rx}} |C_{\text{rx}}(\theta, \psi)|^2 G_{\text{proc}}}{16\pi^2 R^2 k T_0 N F B}. \tag{2.11}$$

3 RF Beacon Concept Design

This chapter discusses the aspects that need to be taken into consideration for the successful implementation of the LunarSpark RF Beacon. First, a mathematical description of the viewing geometry is introduced in Section 3.1, which serves as the starting point for defining the optimum operation timeline and the performance analysis performed in Chapter 4. Next, all the elements of the LunarSpark system that interact with the RF beacon are described in Section 3.2. Using this as a foundation, Section 3.3 then defines the optimum operation timeline.

3.1 Operation Geometry

Fig. 12 shows a simplified version of the observation geometry that impacts the RF beacon. Three different (but related) angles can be defined to describe the geometry by which the RF-link is established. The elevation angle θ_e represents the angle between the surface tangent and the line-of-sight. The requirements provided by the team designing the laser power transfer are provided in this angle. This angle can easily be converted to the more commonly used incidence angle θ_i in the field of radar. Finally, the look angle θ_l is useful in order to evaluate the radiation pattern with which the satellite receives the signals emitted by the RF beacon.
In order to better understand the requirements for the operation timeline, it is useful to analyse the time-behavior of these three angles. For this purpose, $t = 0$ is defined as the very first time instance that the satellite needs to transmit power. This time occurs for a receiver that is located at the edge of the servicing area on the South Pole. The service area is defined as latitudes greater than 80 degrees. Thus, $t = 0$ commences the power transfer for a receiver at 80 degrees latitude.
Fig. 13 shows the relevant parameters in order to derive the time-behaviour of all angles. From this figure, it is possible to derive the following equations.

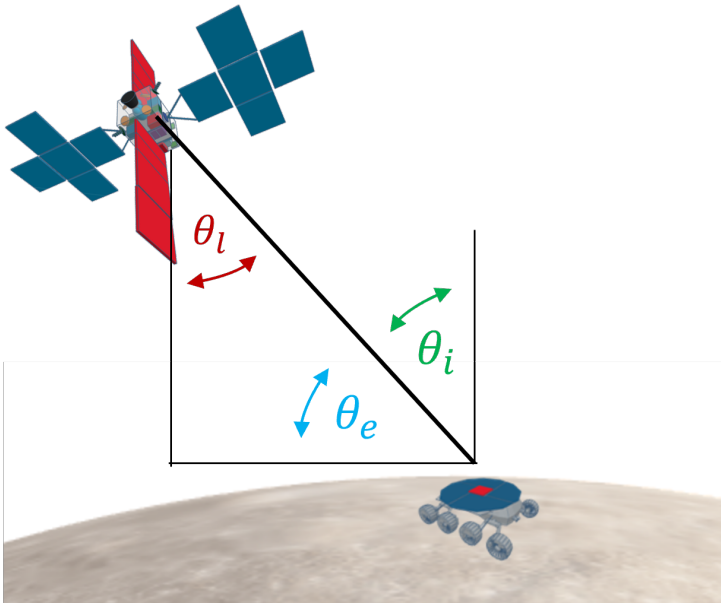

Figure 12: Simplified viewing geometry under which the LunarSpark satellite views the customer's RF beacon.

Given the elevation angle θ_e at $t = 0$ (start of power transfer), the look angle θ_l at $t = 0$ can be computed via

$$\theta_l(0) = \arcsin\left(\frac{R_M}{R_M + H}\cos[\theta_e(0)]\right). \tag{3.1}$$

Thus, as evident from Fig. 13, this directly results in the Moon angle at $t = 0$

$$\theta_M(0) = \frac{\pi}{2} - \theta_l(0) - \theta_e(0) + 10\,\mathrm{deg}\,. \tag{3.2}$$

Because θ_M changes by 360 degrees within one orbit period T_O, the Moon angle at all times is given by

$$\theta_M(t) = \theta_M(0) - \frac{t}{T_O}2\pi, \tag{3.3}$$

where

$$T_O = 2\pi\sqrt{\frac{(R_M + H)^3}{\mu_M}}. \tag{3.4}$$

Fig. 13 then allows for writing the distance R between satellite and RF beacon as

$$R(t) = \sqrt{(R_M + H)^2 + R_M^2 - 2R_M(R_M + H)\cos(\theta_M - 10\,\mathrm{deg})}. \tag{3.5}$$

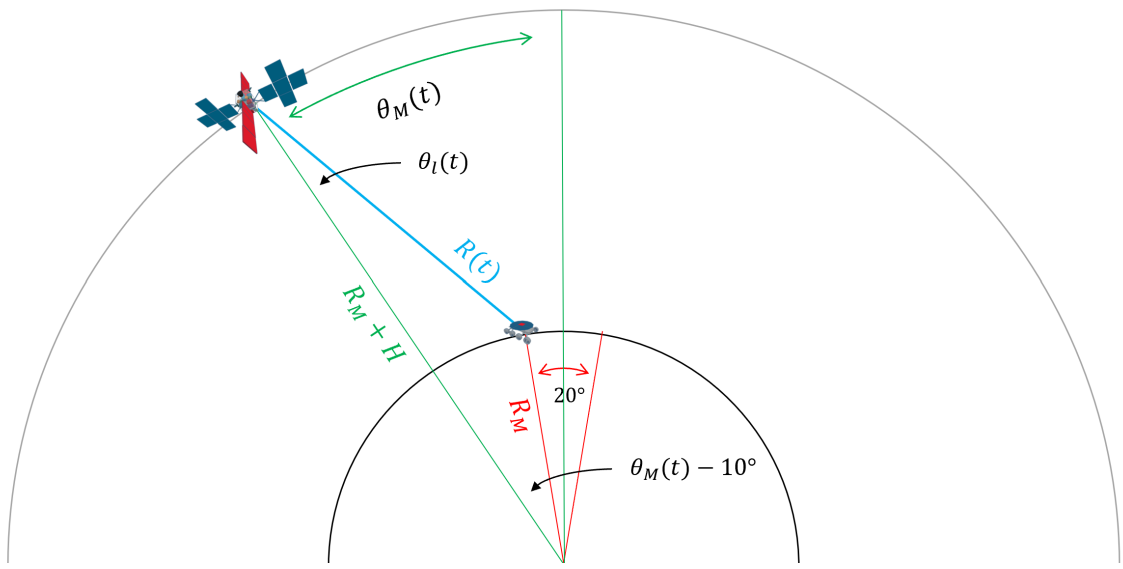

Figure 13: Geometric relations between distances and angles in the viewing geometry between satellite and RF beacon.

And thus the instantaneous look angle is given by

$$\theta_l(t) = \arcsin\left(\frac{R_M \sin[\theta_M(t) - 10\,\mathrm{deg}]}{R(t)}\right), \tag{3.6}$$

which results in the instantaneous elevation angle

$$\theta_e(t) = \arccos\left(\frac{[R_M + H]\sin[\theta_M(t) - 10\,\mathrm{deg}]}{R(t)}\right). \tag{3.7}$$

The elevation angle can be converted into the incidence angle via

$$\theta_i(t) = \frac{\pi}{2} - \theta_e(t). \tag{3.8}$$

Assuming a power transfer at $\theta_e(0) = 45\,\mathrm{deg}$ and orbit altitude $H = 700$ km, the angles change according to Fig. 14. It is evident that the elevation angle quickly becomes more shallow when moving away from $t = 0$. A too shallow elevation angle results in a strongly squinted geometry under which the antenna pattern of the customer's RF beacon is severely attenuated. It is therefore desired to perform the coarse localization for elevation angles greater than at least 20 degrees, which occurs around $t = -6.6$ min.

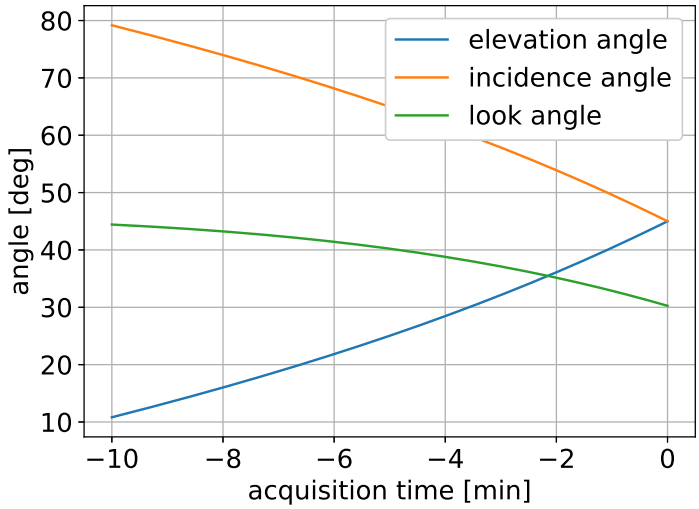

Figure 14: Simulated angles over time for an orbit height of 700 km and a power transfer starting at 45 degrees elevation angle.

3.2 Interaction with Other System Elements

This subsection provides a brief overview of all the interactions that need to be considered when defining the optimum operational timeline of the RF beacon.

3.2.1 Attitude Control

For each pass the satellite is oriented with an attitude control accuracy of ±1.75 mrad. This imperfect satellite pointing is then compensated with the optical fine-pointing capabilities of the laser (access range of ±2 mrad). Therefore, as a conservative measure, the coarse localization accuracy needs to be better than ±0.25 mrad (cf. Fig. 15) to guarantee that the actual position is still within the fine-pointing access range. Note that the slewing of the satellite, which brings it into the required orientation, spans a time window of up to 10 minutes and requires the coarse location retrieved with the RF beacon as input.

3.2.2 Laser Fine-Detection Mechanism

The LunarSpark satellite possesses the capability to perform a fine-detection of the receiver position using the laser beam itself. For this purpose, the laser performs an outward-spiraling movement over the search area, as shown in Fig. 16a. Note, that the coarse location retrieved by the RF beacon serves as

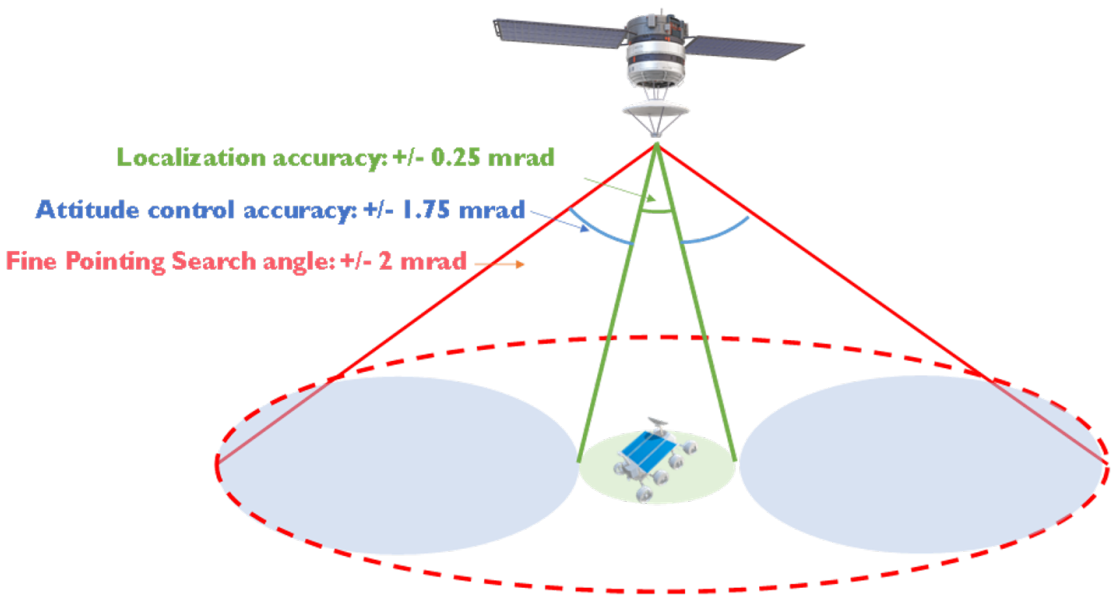

Figure 15: The error in the coarse estimation of the receiver position and the error in the attitude control result in the red-dashed search angle that needs to be accessible by the fine-pointing meachnism.

input. This allows for searching the entire circular area up until the customer is found (e.g., Fig. 16b). Note that this technique is operationally applied in laser communication and thus well-proven.

In order to speed up the spiraling duration, the satellite performs two separate spirals. A first spiral is performed with a widened laser beam (beam is spread with optical lens) as seen in Fig. 17 on the left. Once the receiver is found with this widened beam, a second spiral is performed with the nominal laser beam width over a smaller search area (cf. Fig. 17 on the right).

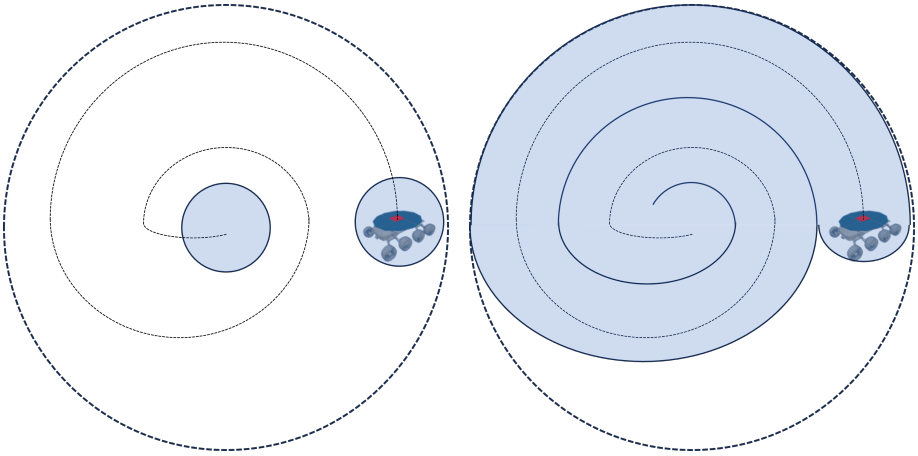

(a) (b)

Figure 16: a) Two-dimensional antenna pattern of sum signal plotted versus u and v, b) Two-dimensional antenna pattern of delta signal plotted versus u and v.

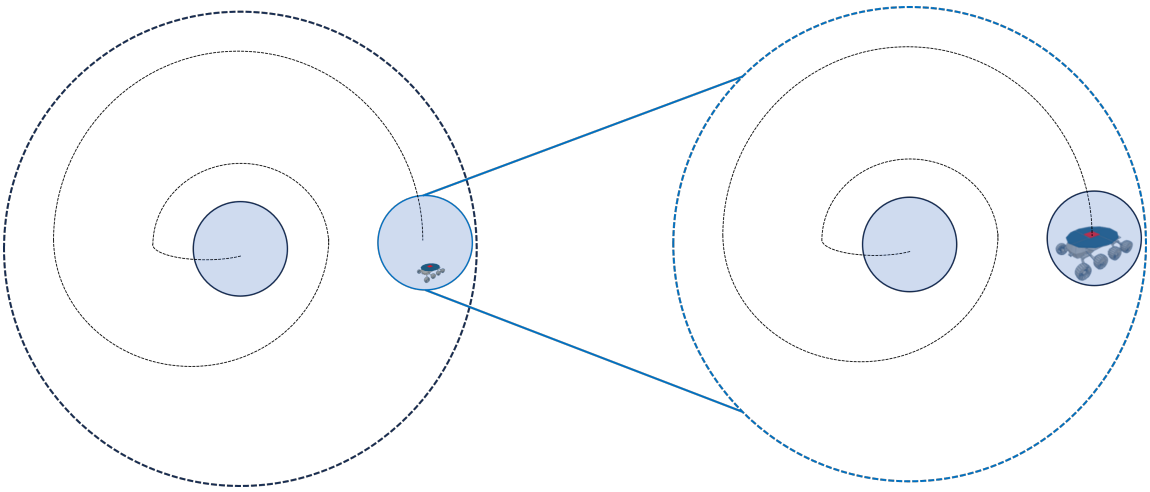

Figure 17: A first spiral with a wide beam over the entire search area is followed by a spiral with the nominal beam over a smaller search area.

3.2.3 Laser Fine-Tracking Closed Loop

Once the laser is pointed at the customer, the laser switches from the search mode into the tracking mode, which remains active during the entire power transmission window. This allows the laser to maintain a pointing at the customer even as the satellite flies over the servicing area. This is achieved with a closed loop during which the customer periodically relays the amount of received power (on different parts of the receiver surface, see next subsection) back to the satellite using the RF beacon. This concept is shown in Fig. 18.

Figure 18: The closed loop using the RF beacon maintains the correct pointing of the laser beam.

3.2.4 Customer Receiver

The RF beacon of this thesis is placed on top of the customer's receiver (red square in Fig. 19). The beacon antenna is limited to a length of maximum 20 centimeters in each dimension. As shown in Fig. 19, the laser cells of the receiver are segmented in four different modules (or quadrants). This allows for measuring the received power on four different surface areas which improves the closed link for a consistant laser pointing.

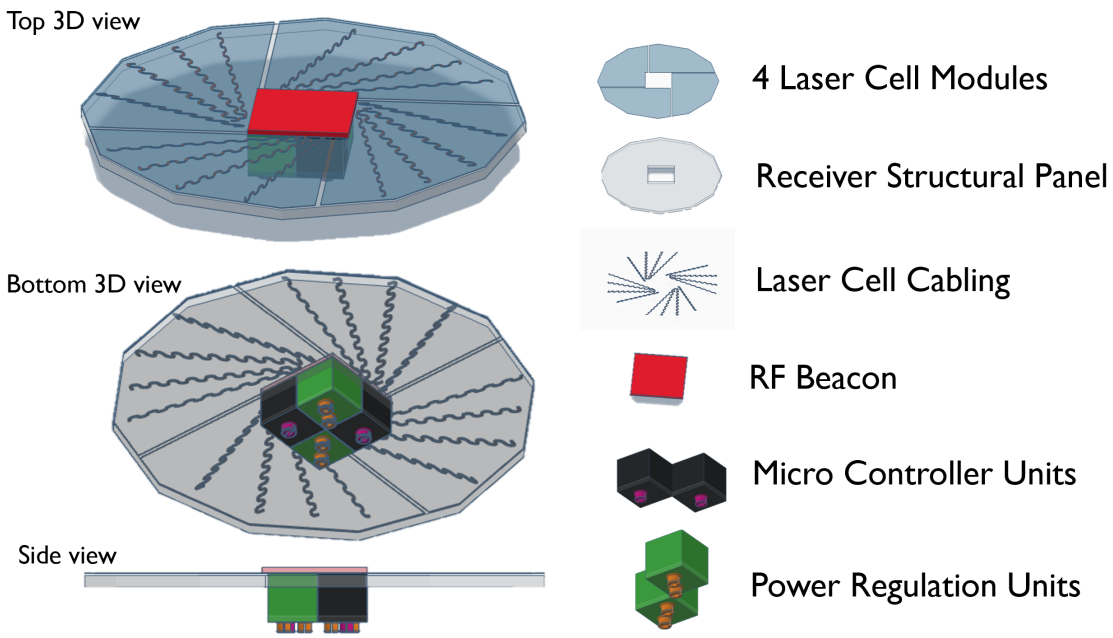

Figure 19: The LunarSpark receiver design that is placed on top of the customer.

3.3 Construction of Optimum Operational Timeline

With the information of the previous two subsections, it is now possible to construct the optimum operational timeline for the RF beacon localiza-

tion. Figure. 20 shows this timeline versus time for two successive orbits. In addition, Fig 21 shows an angular representation of the timeline that only includes the most basic events: customer servicing at the South Pole, communication with the Earth ground segment at the North Pole, as well as a constant collection of solar energy, radiation of excess heat, and orbit correction. The dashed area represents the desired elevation angle range for the RF beacon operation (cf. Section 3.1).

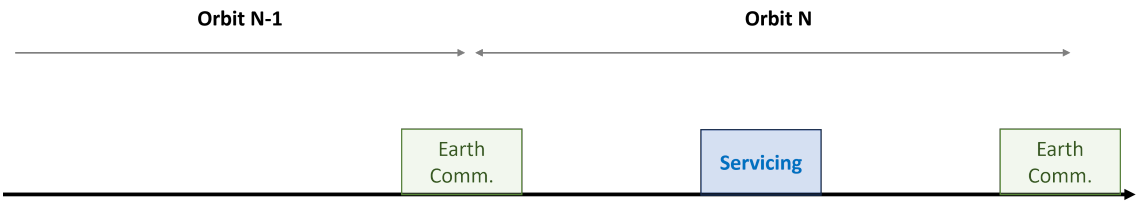

Figure 20: Time representation of the operational timeline that only includes the most basic events.

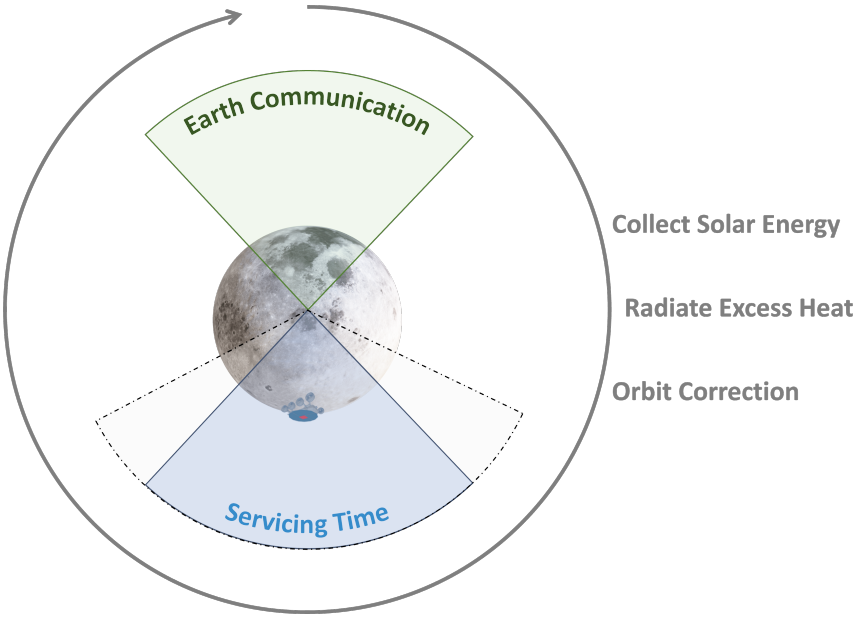

Figure 21: Angular representation of the operational timeline that only includes the most basic events. The dashed area represents the elevation angle range during which the RF beacon can be operated with sufficient gain.

As evident from Fig. 14, the RF beacon coarse localization needs to occur at least 6.6 minutes before the earliest power transmission. However, Section 3.2.1 states that the slewing of the satellite, which requires the coarse locaization to have been completed, takes at least 10 minutes. This represents a conflict (cf. Fig. 22) that can only be solved by using the coarse

localization from the previous orbit as input to the slewing. Using the position from the previous orbit is acceptable given that the customer position changes slowly between orbits, an assumption that is confirmed by [5]. The resulting operational timeline to overcome this problem is thus shown in Fig. 23.

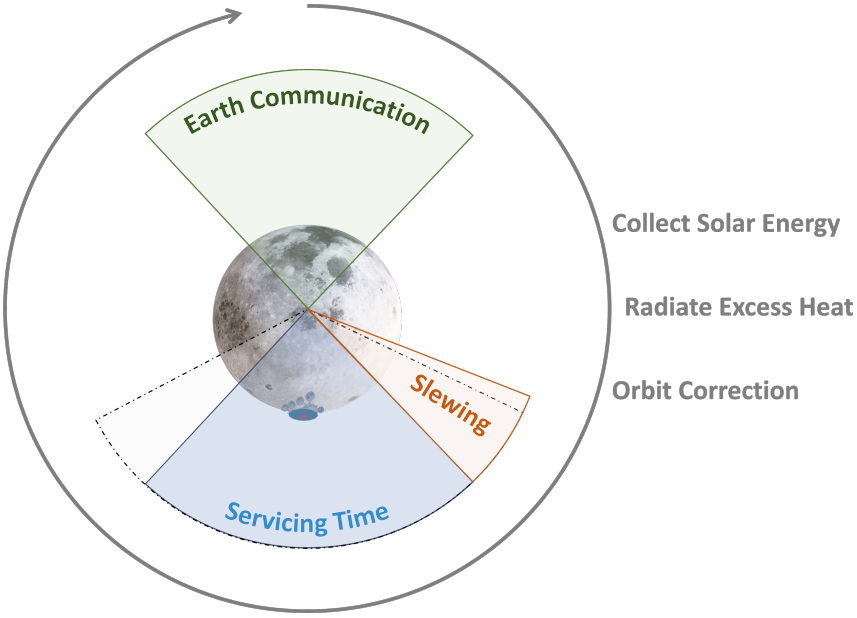

Figure 22: Angular representation of the operational timeline with a slewing directly before the servicing time window. The dashed area represents the elevation angle range during which the RF beacon can be operated with sufficient gain. It is evident that the RF beacon localization would occur during unfavorful elevation angles in this scenario.

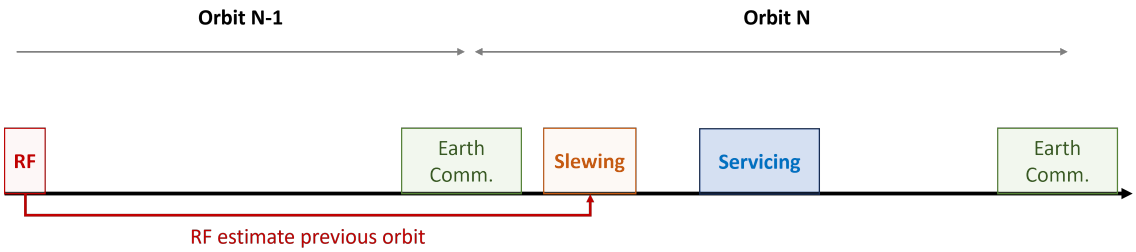

Figure 23: Time representation of the operational timeline that utilizes a coarse position estimate from the previous orbit to perform the satellite slewing.

A more realistic approach to finding the optimum timeline is to place the laser fine-detection mechanism before the servicing window (cf. Fig. 24). The implementation of both spirals (cf. Section 3.2.2) will take up to 4 minutes. Therefore, sufficient time remains for performing the coarse localization with the RF beacon, with the earliest coarse localization performed 4 minutes before the servicing window starts.

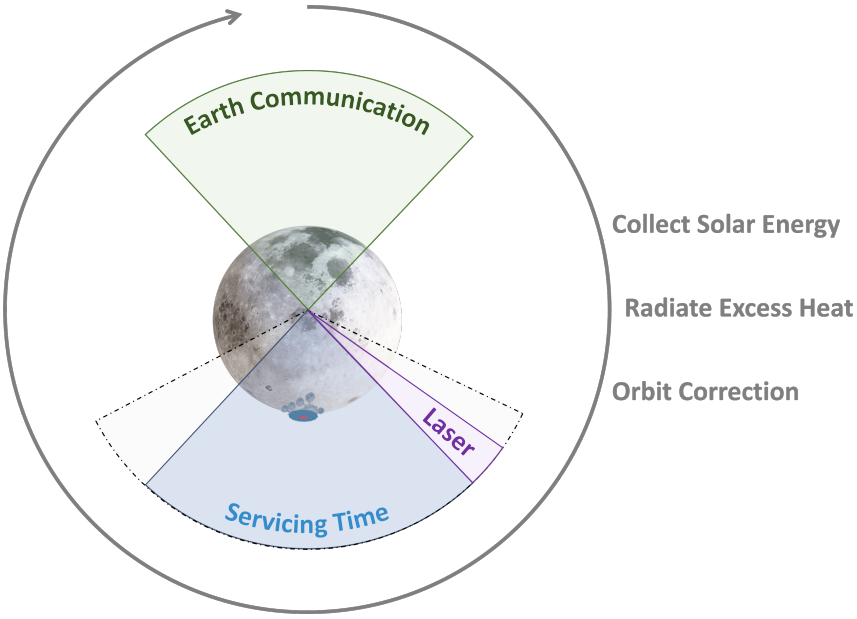

Figure 24: Angular representation of the operational timeline with the laser fine-detection before the servicing time window. The dashed area represents the elevation angle range during which the RF beacon can be operated with sufficient gain. It is evident that sufficient time for the RF beacon localization remains.

This results in the optimum operational timeline as shown in Fig. 25 and Fig. 26. The first coarse localization estimate is retrieved in the previous orbit and the satellite is oriented accordingly. Then, a second coarse localization estimate is obtained, which can be used to perform a slight correction of the satellite orientation and also serves as input for the fine-detection with the laser. Once the customer is found, the power transfer begins. The start and end times of each event are summarized in Table 2.
Note that further details on the attitude control can be found in [15]. More details on the laser fine-detection and closed-loop can be found in [16].

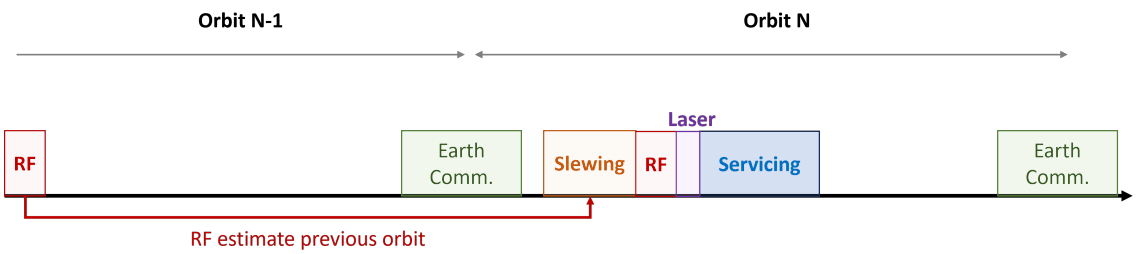

Figure 25: Time representation of the optimum operational timeline.

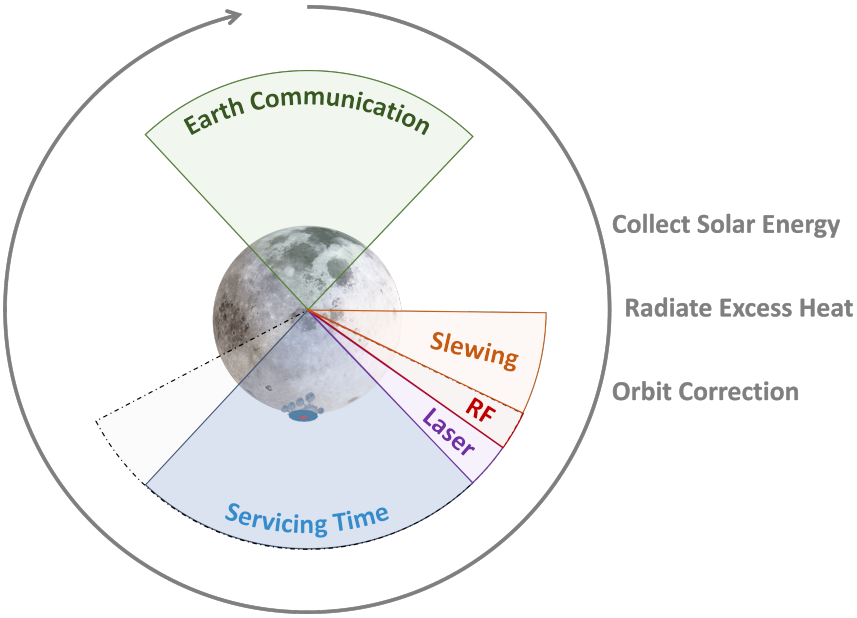

Figure 26: Angular representation of the optimum operational timeline.

Start Time	End Time	Event
-15 min	-5 min	Attitude control orients the satellite towards the expected receiver position obtained during the previous orbit
-5 min	-4 min	First coarse location estimate is obtained using RF beacon
-4 min	-4 min	Minor update of satellite attitude if needed based on new location estimate
-4 min	-2 min	Fine-detection with first laser spiral
-2 min	0 min	Fine-detection with second laser spiral
0 min		Power transfer begins

Table 2: Summary of the events in the optimum operational timeline and their corresponding start and end times.

4 RF Beacon Design and Performance Analysis

This chapter introduces the signals and transmission timeline of the RF beacon (Section 4.1), as well as the design choices that are proposed for the RF beacon based on geometrical considerations (Section 4.2). Section 4.3 derives the resulting link budget and SNR that directly affect the theoretical monopulse accuracy (presented in Section 4.4). In addition, constraints on the satellite transmit pulse repetition frequency are discussed in order to optimize the system for the worst case geometry in Section 4.5. Further, Section 4.6 demonstrates a simulation of the actual achieved monopulse accuracy and compares it to the expected theoretical performance. The chapter is concluded with Section 4.7, which presents the parameters selected for the LunarSpark implementation.

4.1 Concept

Fig. 27 gives a high-level view of the proposed RF beacon concept. As the satellite approaches the servicing area with the customer, the satellite transmits a wake-up signal (see signal timeline in Fig. 28). This signal arrives at a potential customer at distance R after a time duration of $\frac{R}{c}$, where c is the speed of light. After a certain delay τ_Δ, which is longer than the pulse duration of the transmit signal, the customer responds with a so-called response signal. Note, that no actual knowledge of τ_Δ is required for the position estimation with the monopulse technique and thus this delay does not need to be well calibrated in the customer's system. The response signal is a GNSS-like signal that was discussed in Section 2.2. The key parameters are repeated here for convenience in Table 3. Note that its duration τ_{rx} depends on the amount of information (or bits) that shall be transmitted according to Section 2.2 and is thus a multiple of 1 ms.
The response signal then arrives at the signal after a total round-trip time of $\frac{2R}{c} + \tau_\Delta$. The satellite removes the PRN code to reverse the spread spectrum technique (cf. Section 2.2), which increases the SNR via the processing gain and also allows to distinguish between different customers[3]. Then, the monopulse technique is applied.

[3]Note that each customer is assigned a unique PRN code by LunarSpark

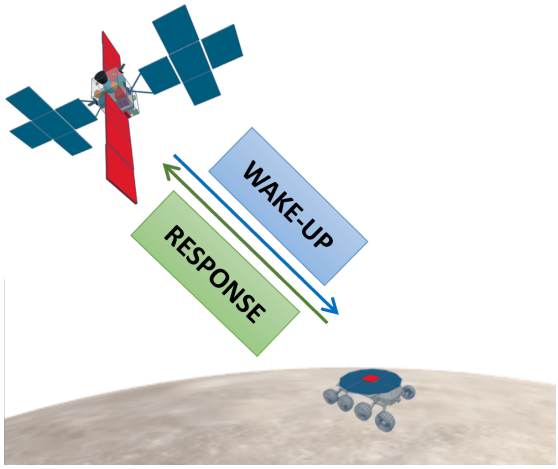

Figure 27: High-level view of RF beacon concept.

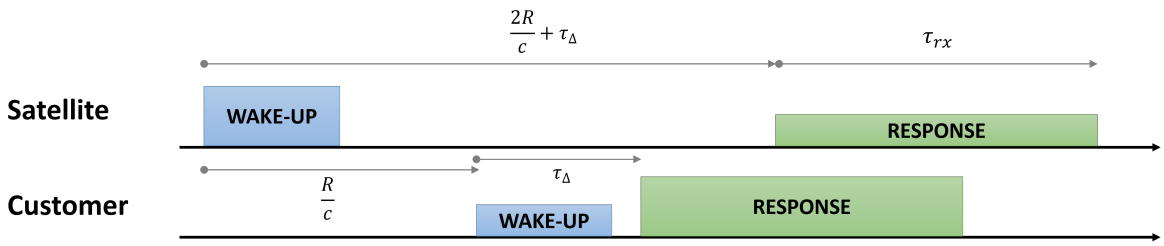

Figure 28: High-level view of the RF beacon signal timelines

Parameter	Value
Pulse duration	1 ms
Bandwidth	2 MHz
Processing Gain	46 dB

Table 3: Typical GNSS signal properties that are used in this work.

4.2 Antenna Sizing

This subsection takes a close look at the observation geometry and discusses the optimum size of the microwave antenna placed on the LunarSpark satellite. Fig. 29 shows the side on which the laser is located (orange circle) and thus on which the microwave antenna needs to be mounted in order to face the Lunar surface. Note that four possible locations have been identified (for the installation of redundant monopulse systems), marked by the blue squares. The microwave antenna dimensions are therefore limited to 25 cm by 25 cm.

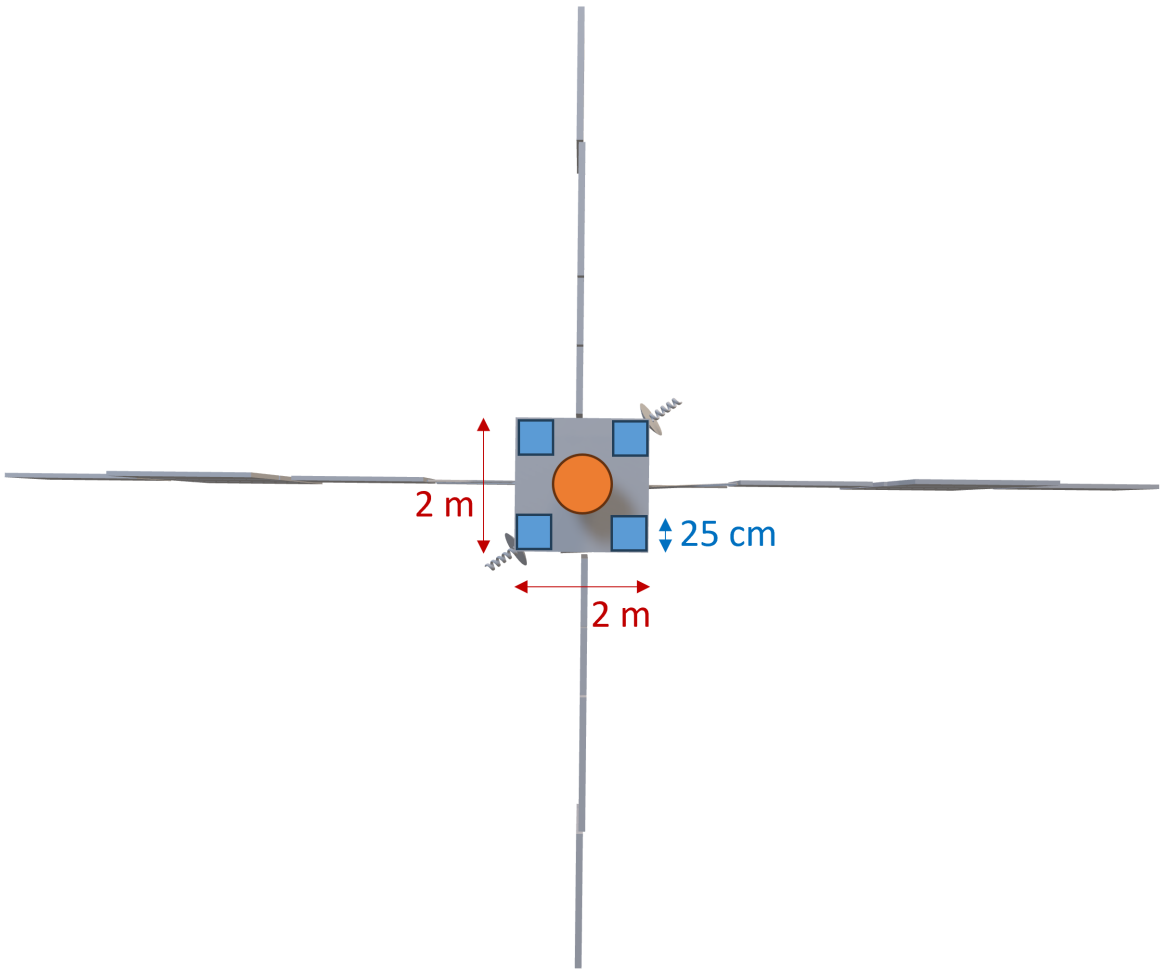

Figure 29: The microwave antenna (potential locations marked with blue squares) and laser system (orange circle) need to be mounted on the same satellite surface as both systems require a line of sight to the customer.

In order to determine the optimum antenna size, the (time-dependent) beamwidths required to cover the entire servicing area from the (time-dependent) satellite position are analysed. This is first performed in the elevation direction of the antenna. Hereby, the two extreme positions of the customer position occur when the customer is located at the edges of the servicing area. A mathematical expression for the edge closest to the satellite, distance R, was already derived in Section 3.1. Now, the equivalent for the far edge shown in Fig. 30 is derived.
From this figure, analog to the math in Section 3.1, $R_2(t)$ can be calculated with

$$R_2(t) = \sqrt{(R_M + H)^2 + R_M^2 - 2R_M(R_M + H)\cos(\theta_M - 10\,\mathrm{deg})}. \quad (4.1)$$

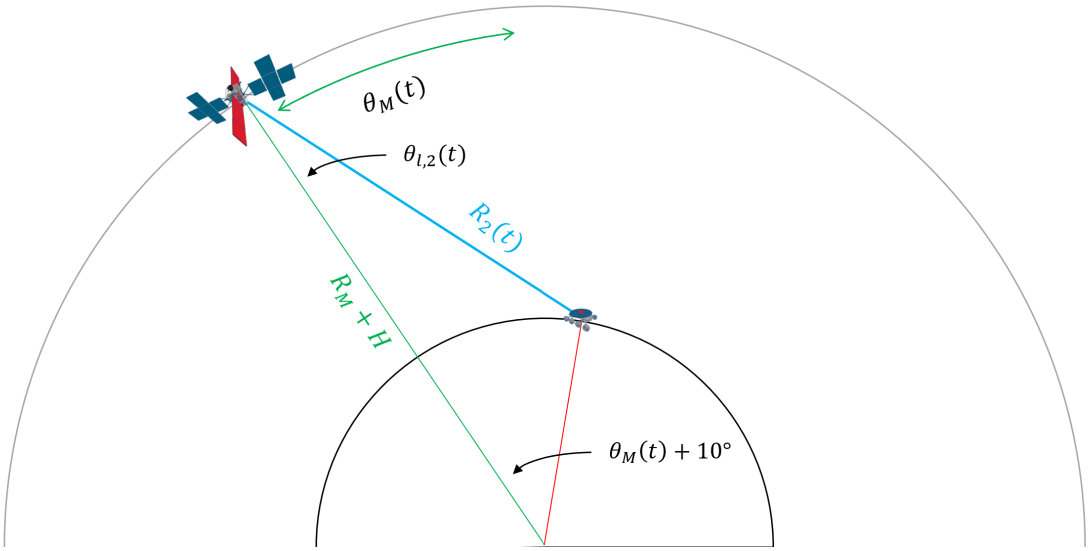

Figure 30: Geometric relations between distances and angles in the viewing geometry between satellite and furthest possible RF beacon position.

And thus the instantaneous look angle is given by

$$\theta_{l,2}(t) = \arcsin\left(\frac{R_M \sin[\theta_M(t) - 10\,\mathrm{deg}]}{R(t)}\right). \tag{4.2}$$

The difference between the look angles for both extreme positions, $\theta_{l,2}(t) - \theta_l(t)$, then results in the beamwidth required to cover the servicing area in elevation (cf. Fig. 31).

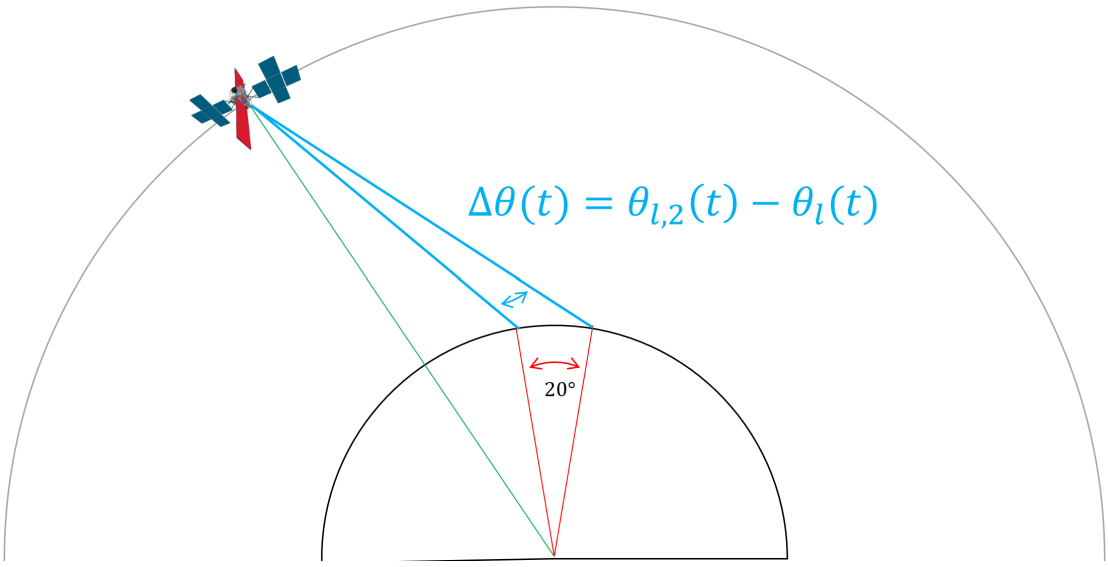

Figure 31: Geometric relations that result in elevation beamwidth required to cover service area.

The $\theta_{l,2}(t) - \theta_l(t)$ resulting from the equations is plotted in Fig. 32 for an

orbit altitude of 700 km. It is evident that a beamwidth of 6.62 degrees would be sufficient.

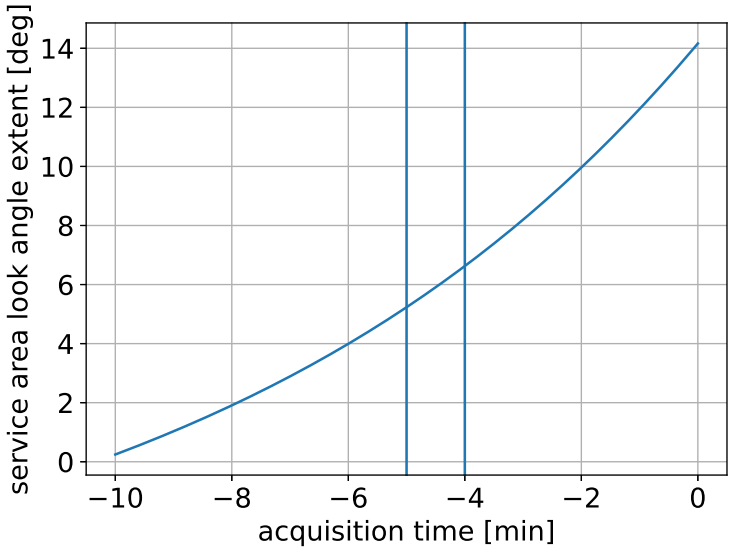

Figure 32: Angular extent of service area for the elevation look angle.

Next,

$$0.89 L_{\text{ant}} = \frac{\lambda}{\theta_{\text{BW}}} \tag{4.3}$$

is used to estimate the required antenna length L_{ant} for a desired beamwidth θ_{BW}. At a frequency of 24 GHz, this results in an antenna size of 10.81 cm by 10.81 cm. This size can easily be accommodated in the available space on the satellite surface and reflects the optimum dimensions (maximum gain) for the elevation direction.

Next, this analysis is repeated in the dimension orthogonal to elevation, which spans in the across-track direction of the LunarSpark observation geometry. Fig. 33 shows the geometry with the satellite moving into the page. As can be derived from this figure, the distance d spanned by the green line is

$$d = 2R_M \sin\left(\frac{20\,\text{deg}}{2}\right), \tag{4.4}$$

which can be approximated[4] to

$$d \approx R_M \frac{10\,\text{deg}}{180\,\text{deg}}\pi. \tag{4.5}$$

[4]The small angle approximation of the sine results in an error of less than 1% for angles up to 13 degrees.

Equivalently, the required θ_{BW} from the satellite perspective can be approximated to

$$\theta_{\mathrm{BW}} \approx \frac{d}{R}, \tag{4.6}$$

yielding

$$\theta_{\mathrm{BW}} \approx \frac{R_M}{R} \frac{10\,\mathrm{deg}}{180\,\mathrm{deg}} \pi. \tag{4.7}$$

Note that here the shortest distance R is assumed because Eq. 4.7 increases as the distance is reduced. The result of this analysis is shown in Fig. 34.

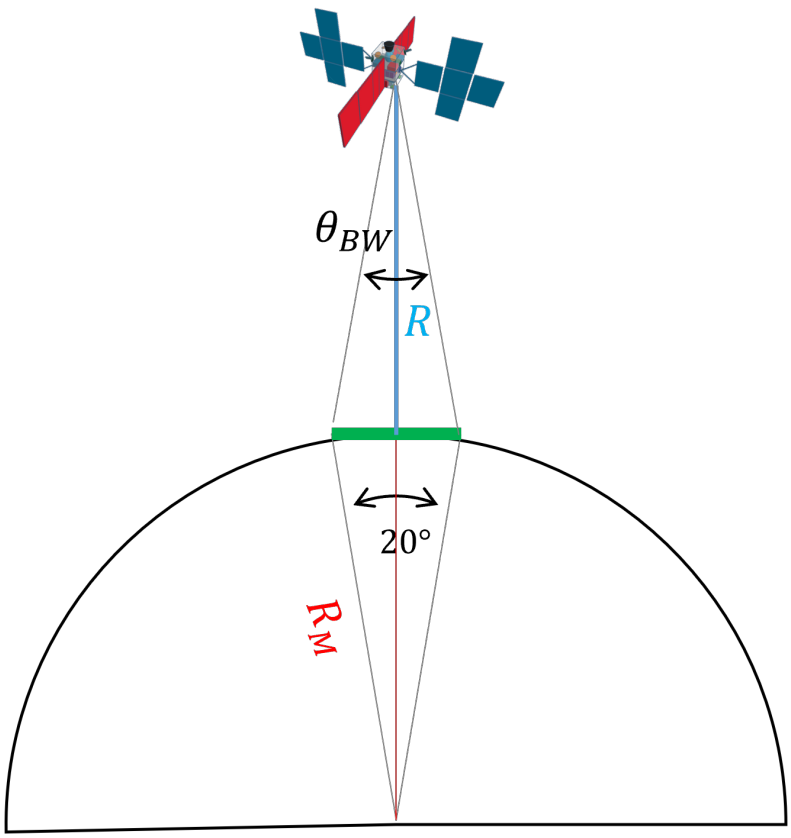

Figure 33: Observation geometry in across-track. The satellite flies into the plane. The green line represents the across-track distance spanned by the service area.

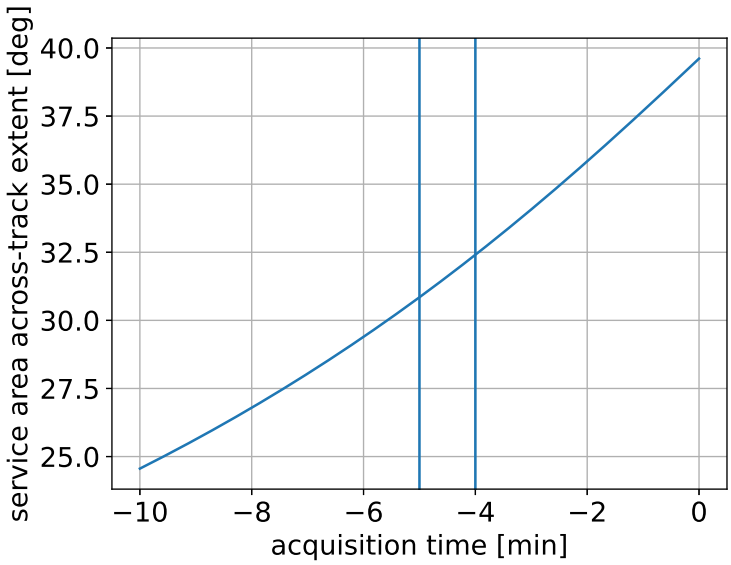

Figure 34: Angular extent of service area for the angle spanning in across-track.

It is evident that the across-track dimension is the driving parameter and thus the antenna beam needs to be widened at the cost of antenna gain. This is necessary so that the entire servicing area can be observed during one overpass without requiring a scanning of the microwave beam. Because the satellite attitude depends on the position of the currently serviced customer, the required beamwidth should be doubled to ensure that the entire service area is in view even when pointing to the edge of the service area. Further, the microwave antenna should be squared because the satellite attitude varies and cannot accommodate the orientation of the microwave antenna. Accounting for these effects, the recommended beamwidth is plotted in Fig. 35. The corresponding antenna dimensions are shown in Fig. 36. Thus, the antenna on the satellite is assumed to be of size 1.1 cm by 1.1 cm for the subsequent analysis[5].

[5]Note that this is referring to the size of the full antenna, as it is the sum beamwidth that needs to cover the full servicing area

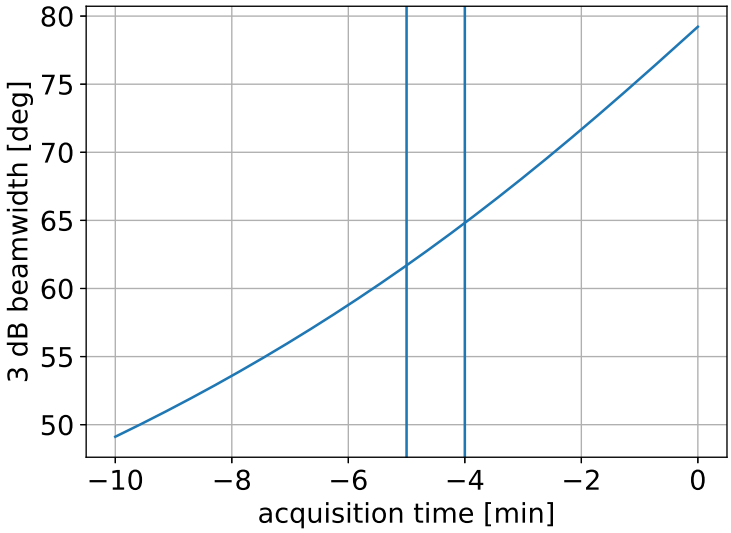

Figure 35: Required beamwidth to allow for an observation of the entire servicing area. The shown beamwidth accounts for a varying satellite attitude and thus orientation of the microwave antenna, as well as an arbitrary satellite pointing to a point within the servicing area.

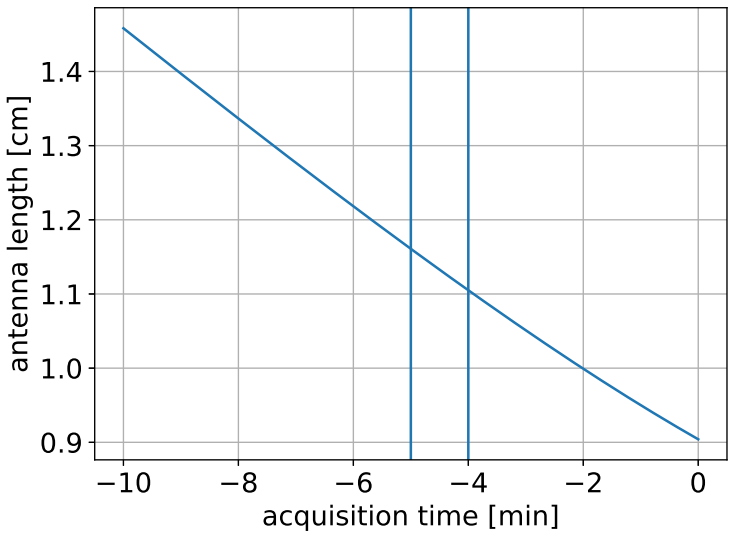

Figure 36: Required antenna length to account for a varying satellite attitude and thus orientation of the microwave antenna, as well as an arbitrary satellite pointing to a point within the servicing area.

4.3 Link Budget

This subsection investigates the achieved SNR for the satellite antenna size selected in the previous subsection. The equation for the link budget presented in Section 2.3 is repeated here for convenience:

$$SNR_{\text{proc}} = \frac{P_{\text{tx}} G_{\text{tx}} |C_{\text{tx}}(\theta, \psi)|^2 \lambda^2 G_{\text{rx}} |C_{\text{rx}}(\theta, \psi)|^2 G_{\text{proc}}}{16\pi^2 R^2 k T_0 N F B}. \tag{4.8}$$

The gain of the antennas can be replaced with the expression

$$G = \frac{4\pi L_{\text{ant}}^2}{\lambda^2}. \tag{4.9}$$

This results in

$$SNR_{\text{proc}} = \frac{P_{\text{tx}} L_{\text{ant,tx}}^2 |C_{\text{tx}}(\theta, \psi)|^2 L_{\text{ant,rx}}^2 |C_{\text{rx}}(\theta, \psi)|^2 G_{\text{proc}}}{R^2 k T_0 N F B \lambda^2}. \tag{4.10}$$

Note that using the full microwave antenna size results in the SNR of the sum beam and not the SNR of the individual channel.
Further, the customer radiation pattern can be expressed in dependence of the elevation angle, assuming symmetry, which results in

$$|C_{\text{rx}}(\theta_E(t))|^2 = \text{sinc}\left(\frac{L_{\text{ant,rx}} \cos\theta_E(t)}{\lambda}\right)^2. \tag{4.11}$$

A worst case attenuation of 3 dB (above, the satellite antenna is designed to contain the entire servicing area within the 3 dB beamwidth) is assumed for the satellite radiation pattern, which corresponds to the radiation pattern value at the edges of the main beam. This yields

$$SNR_{\text{proc}} = \frac{0.5 P_{\text{tx}} L_{\text{ant,tx}}^2 L_{\text{ant,rx}}^2 G_{\text{proc}}}{R^2 k T_0 N F B \lambda^2} \text{sinc}\left(\frac{L_{\text{ant,rx}} \cos\theta_E(t)}{\lambda}\right)^2. \tag{4.12}$$

Note that $\theta_E(t)$ was derived in Section 3.1 as Eq. 3.7 and is also plotted in Fig. 37.
Finally, the number of M pulses transmitted by the customer is accounted for via

$$SNR_{\text{proc}}(N) = \frac{0.5 M P_{\text{tx}} L_{\text{ant,tx}}^2 L_{\text{ant,rx}}^2 G_{\text{proc}}}{R^2 k T_0 N F B \lambda^2} \text{sinc}\left(\frac{L_{\text{ant,rx}} \cos\theta_E(t)}{\lambda}\right)^2. \tag{4.13}$$

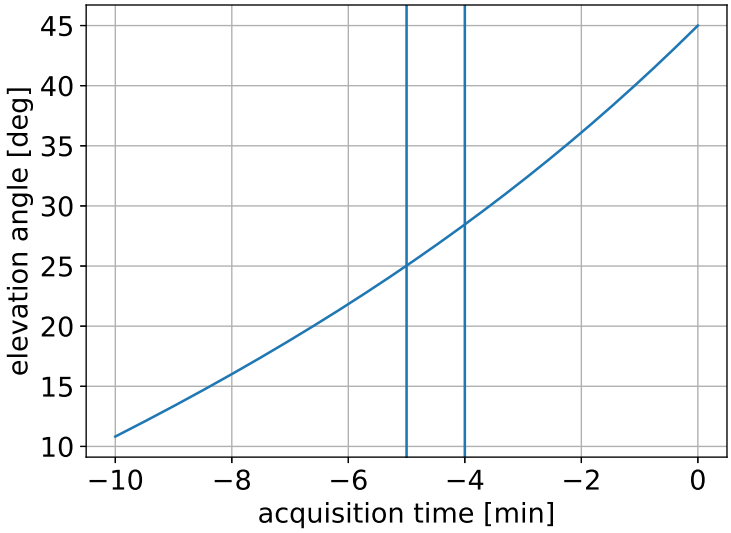

Figure 37: Elevation angle under which the customer is viewed for a satellite orbit of 700 km.

The sum beam SNR based on Eq. 4.13 for $M = 1$ and 240 mW peak transmit power is shown in Fig. 38. The optimum antenna length at the customer (as evident from the plot) is around 5 cm, which yields the highest shown SNR and is also the most robust against changes in the time of measurement. It is visible that a longer customer antenna does not contribute to the SNR. While the peak gain and thus SNR increases for longer antennas, this effect does not play a role for the low elevation angle under which the signal is sent. On the contrary, longer antennas create a larger sensitivity to the time of measurement due to the impact on the sidelobes. Thus, in the remainder of this work, a 5 cm by 5 cm antenna is assumed to be mounted on top of the customer system.

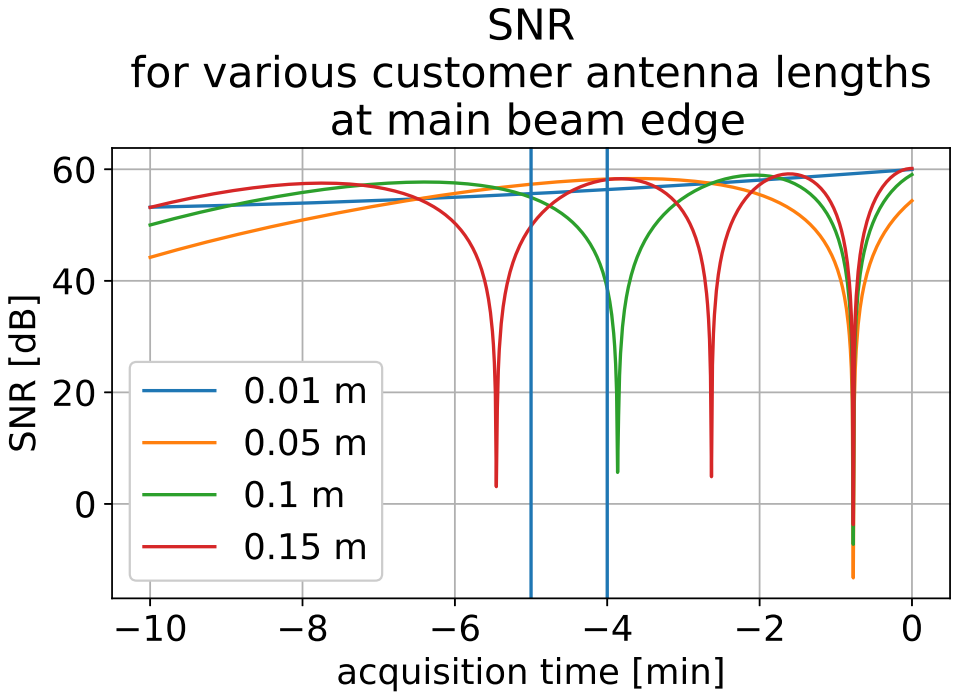

Figure 38: SNR of response signal received at satellite for various customer antenna lengths. The SNR is calculated for a signal that arrives at the main beam edge of the satellite (3 dB below the peak gain).

4.4 Theoretical Monopulse Accuracy

In this subsection, the sum beam SNR is calculated for a transmit power of 240 mW and with 150 pulses sent by the customer. The resulting sum beam SNR is then used to derive the theoretical 3-sigma monopulse accuracy $3\sigma_{\text{acc}}$ according to [17]:

$$3\sigma_{\text{acc}} = \frac{2.16\ \theta_{\text{BW}}}{\sqrt{2SNR_{\text{proc}}}}. \tag{4.14}$$

The result is shown in Fig. 39. It is evident that the selected parameters result in a 3-sigma accuracy that meets the requirements outlined in Chapter 3.

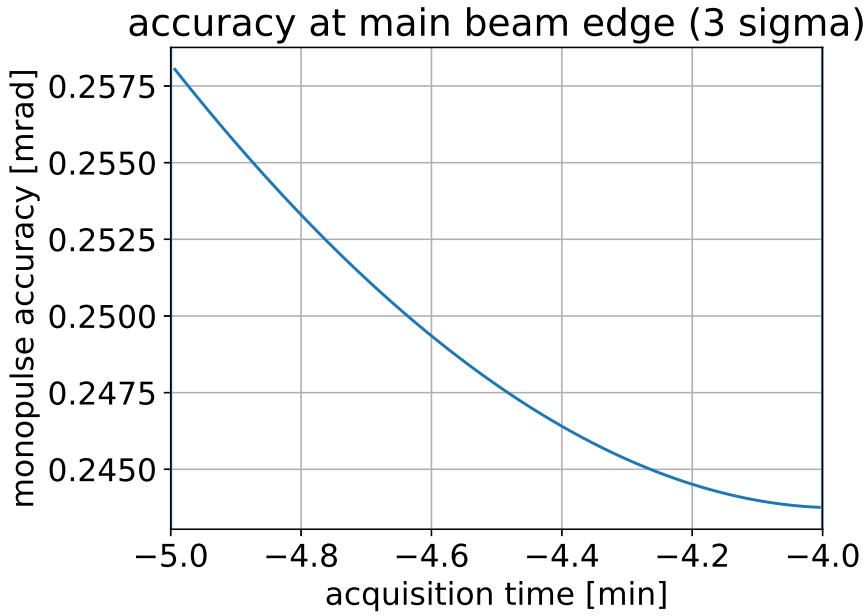

Figure 39: Theoretical monopulse accuracy for a signal that arrives at the main beam edge of the satellite (3 dB below the peak gain). The transmit power is set to 240 mW and the customer sends 150 pulses.

4.5 Satellite Pulse Repetition Frequency

This subsection investigates the selection of the pulse repetition frequency (PRF) of the satellite transmitter, which is sending the wake-up signal. Two different constraints are analysed: the minimum and maximum feasible PRF that allows for the operation of the RF beacon. Note that keeping the PRF as low as possible is favorable, as this would reduce the operational complexity of the LunarSpark RF beacon and satellite.

The first aspect to be considered is the minimum PRF. The SNR analysis in the previous subsections assumed the customer is located at the nearest possible position - namely the near edge of the servicing area. However, the SNR suffers for customers that are further inside the servicing area due to the increased distance R and the impact of the radiation patterns (arrival angles are further away from the antenna boresight direction). This effect could be avoided by periodically repeating the RF beacon operation as the satellite traverses over the servicing area.

The minimum PRF of the satellite wake-up signal which limits this SNR drop is estimate as follows:

1. The SNR to customers across the servicing area is estimated, accounting

for the varying geometry.

2. Using the SNR at the reference position (closest edge of servicing area), the relative SNR loss is computed across the servicing area.

3. The time when each customer position would be observed under the reference geometry is calculated.

4. The SNR loss is plotted against this time (reference position at time zero). This represents the sampling time needed in order to limit the SNR loss to a given value (assuming customers are always observed with look angles greater than the reference position look angle).

5. In order to approximate for the fact that customers can also be observed with look angles smaller than the reference position look angle, this calculated time is doubled.[6]

The result of this approximation is shown in Fig. 40. A sampling time of 50 seconds (minimum PRF of 0.02 Hz) would limit the SNR drop to 1.5 dB.

[6] Assuming an arbitrary position in the servicing area that would result in a 3 dB loss and assuming this position would be observed under the reference geometry after 45 seconds. It is now assumed, for a first order approximation, that this same position would also experience a 3 dB loss if a wake-up pulse is transmitted 90 seconds after the reference geometry. Note that the satellite will have rotated backwards for the power transmission at this new time instance.

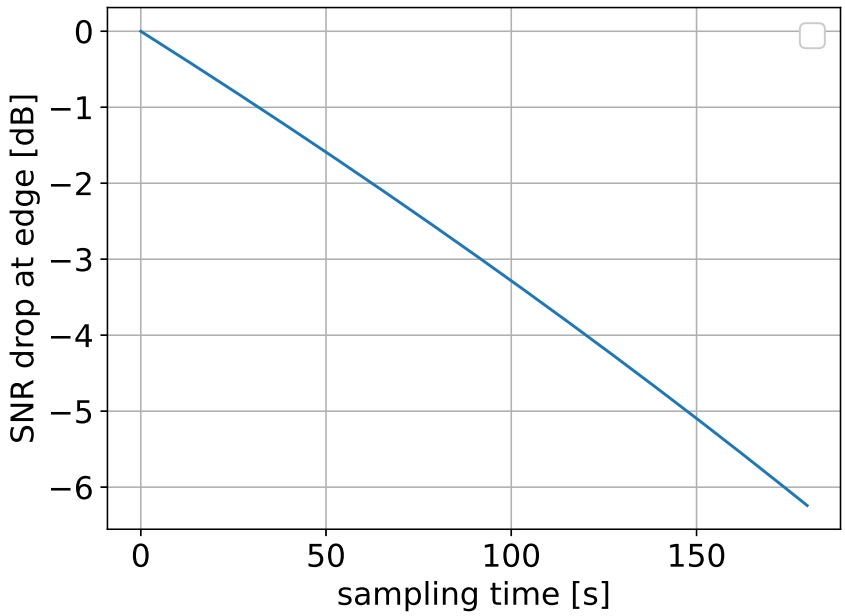

Figure 40: Approximation of the worst-case SNR drop (with respect to the reference geometry) for different repeat times of the wake-up signal. The SNR drops slowly due to the wide antenna patterns.

Next, the maximum feasible PRF is investigated. Because the satellite microwave antenna cannot receive the response signal while the wake-up signal is being transmitted, special care needs to be taken to avoid an overlap of both signals. This results in the following requirement:

$$\frac{1}{PRF} > \tau_{\text{tx}} + \tau_{\Delta} + M\ \tau_{\text{rx}} + \frac{2R_{\text{max}}(PRF)}{c}, \tag{4.15}$$

where PRF is the pulse repetition frequency, τ_{tx} is the duration of the wake-up signal, τ_{rx} is the duration of a pulse within the response signal, and M is the number of pulses within the response signal. Note that $R_{\text{max}}(PRF)$ represents the maximum customer distance that occurs given the selected PRF.

The result is plotted in Fig. 41. With the selected response signal parameters, a PRF of 1 Hz remains feasible for $M = 2000$. For the minimum PRF needed to limit the SNR loss to 1.5 dB (0.02 Hz), the response signal can consist of up to 100.000 pulses. Note that this would also allow for a significant amount of data exchange between the satellite and the customer and thus also makes the implementation of a data relay service with the LunarSpark satellite feasible, which has been intended as a later service.

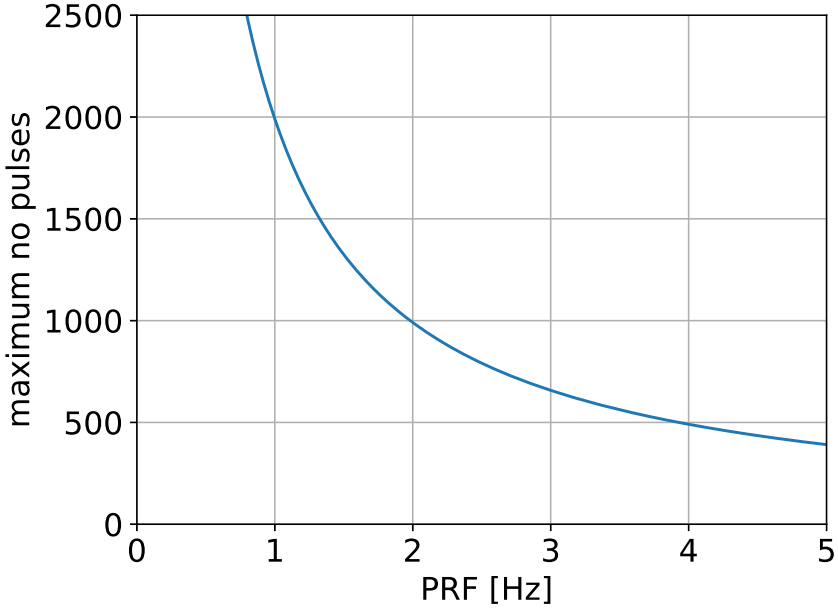

Figure 41: The amount of pulses that can be transmitted within the customer's response signal for a given PRF.

4.6 Simulated Monopulse Accuracy

This subsection simulates the monopulse performance for the selected microwave antenna sizes of 1.1 cm by 1.1 cm (satellite) and 5 cm by 5 cm (customer). The resulting sum and delta patterns of the monopulse implementation are shown in Fig. 42. It is evident that the beamwidths of the satellite are very wide.

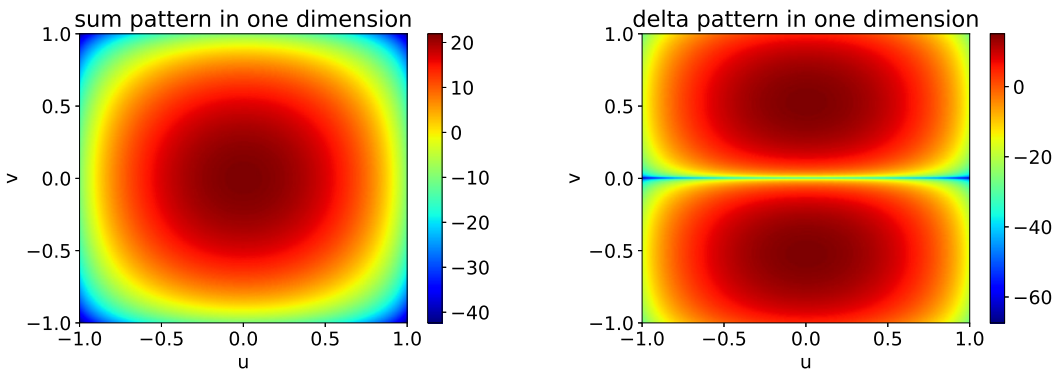

(a) (b)

Figure 42: Simulation results for the selected antenna dimensions: a) Two-dimensional antenna pattern of sum-signal plotted versus u and v, b) Two-dimensional antenna pattern of delta-signal plotted versus u and v.

The resulting monopulse ratios for different directions are shown in Fig. 43 and Fig. 44.

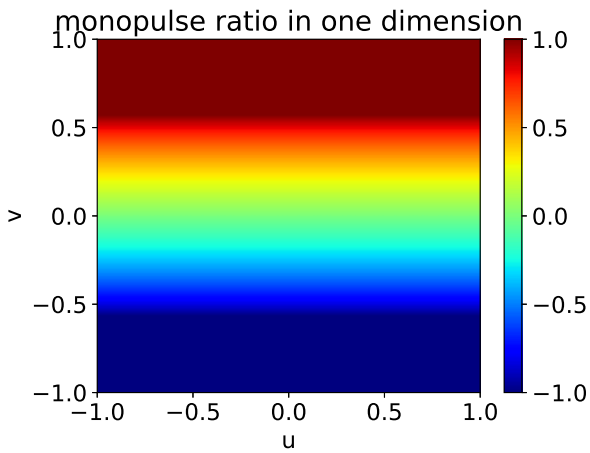

Figure 43: Simulation results for the selected antenna dimensions: Monopulse ratio resulting from the patterns shown in Fig. 5 plotted versus u and v.

Next, an actual signal with constant SNR is simulated. This simulated signal is fed into the different simulated channels of the simulated monopulse antenna with a varying phase difference to simulate different angles of arrival within the main lobe. The impact of the simulated antenna pattern then results in a varying SNR depending on the angle of arrival. The simulated monopulse accuracy is shown in Fig. 45 (red circles) together with the theoretically expected accuracy based on Eq. 4.14 (blue line). The plot shows that the simulation and theory match very well for the simulated signals

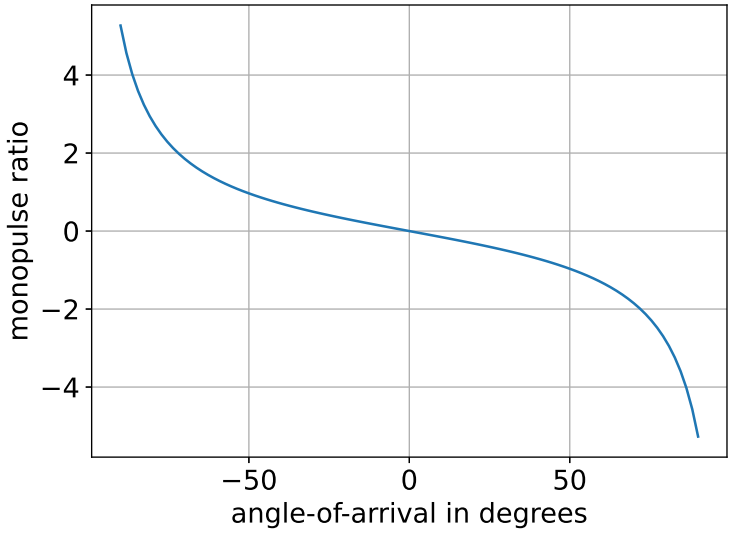

Figure 44: Simulation results for the selected antenna dimensions: Zoom of monopulse ratio over main beamwidth shows linear relation between angle of arrival and estimated monopulse ratio.

with the lowest SNR, which corresponds to signals that are received at the edges of the main lobe. Signals that are received further inside the main lobe show a simulated accuracy that outperforms the expected theoretical performance. This shows that Eq. 4.14 refers to the worst-case accuracy at the main beam edge.

The simulation is repeated for signals with varying SNR but with a fixed angle of arrival that corresponds to the main beam edge. The comparison of theoretical and simulated accuracy is shown in Fig. 46. Simulation and theory are well in agreement for SNR above 18 dB. A discrepancy between both curves starts to appear for SNR below 18 dB. Thus, Eq. 4.14 only seems to be valid for large SNR. However, given the large SNR achieved with the LunarSpark RF beacon (better than 50 dB), the results outlined in the previous subsections remain valid.

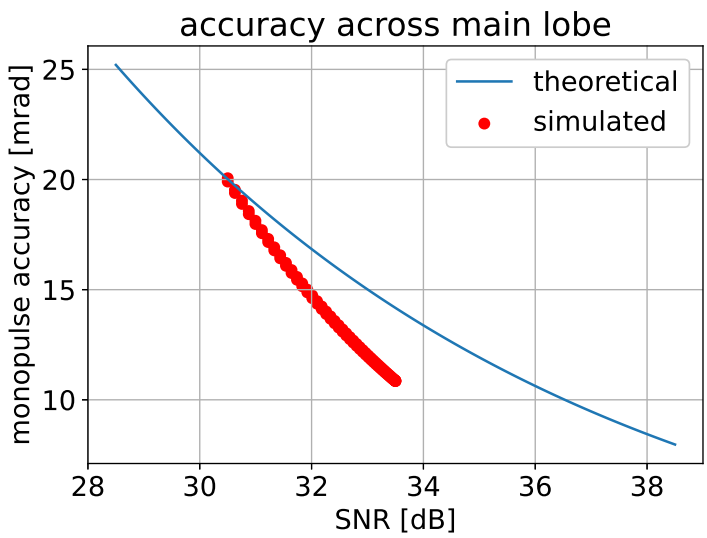

Figure 45: Comparison of simulated monopulse accuracy (red circles) and theoretical expectation (blue line) for a signal with constant SNR before the antenna. The SNR variation is due to the simulation of different angles of arrival within the main lobe.

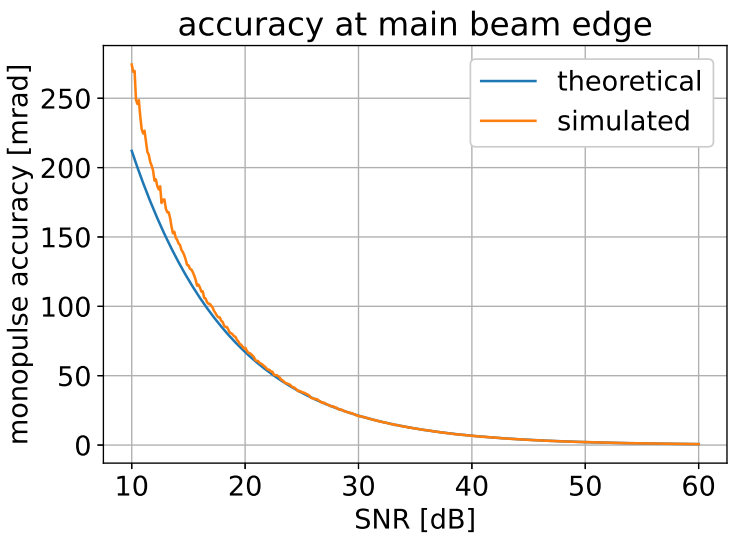

Figure 46: Comparison of simulated monopulse accuracy (orange line) and theoretical expectation (blue line) for simulated signals that are received at the main beam edge.

4.7 Proposed LunarSpark RF Beacon Design

Table 4 summarizes all relevant parameters for the implementation of the LunarSpark RF beacon based on the theoretical analysis and simulation presented in this work. The designed RF beacon can physically be accommodated by the satellite and customer architecture. Further, the required accuracy of 0.25 mrad (3-sigma) is successfully met in the worst-case scenario (customer signal arrives in main beam edge of satellite antenna). In the best case, which is more likely during the second position estimate due to the pre-pointing of the satellite, an accuracy of 0.145 mrad (3-sigma) is achieved.

Parameter	**Value**
Center Frequency	24 GHz
Satellite Receive Antenna	1.1 cm by 1.1 cm
Satellite Receiver Noise Figure	3 dB
Satellite PRF	0.02 Hz
Customer Transmit Antenna	5 cm by 5 cm
Peak Power	339 mW
Bandwidth	2 MHz
Pulse Duration	1 ms
Type	PRN-Code
No. Pulses	50
Transmit RF Energy per Pass	4.71 μWh
Worst SNR at Satellite	55.2 dB
3-Sigma Accuracy (Target)	0.250 mrad
3-Sigma Accuracy (Worst)	0.245 mrad
3-Sigma Accuracy (Best)	0.145 mrad

Table 4: Summary of selected parameters for the LunarSpark RF beacon implementation.

5 Conclusion and Outlook

In the framework of this thesis, it was demonstrated that the LunarSpark RF beacon is a viable concept. It was shown that both LunarSpark's physical satellite architecture as well as its operational timeline can accommodate an RF beacon for the estimation of the customer's position. Further, the proposed RF beacon concept serves not only as a means of locating the customer but also allows for a flow of information from the customer to LunarSpark, enhancing the overall customer experience. It also allows for closing the tracking loop of the laser and thus makes an optical laser communication terminal not necessary. This presents a significant advantage for the LunarSpark system, reducing the complexity of the customer system and operation chain.
Theoretical assessments of the link budget demonstrated the high signal-to-noise ratio that can be achieved while keeping the energy consumption of the customer low (4.71 μWh per pass). These also proved that the corresponding monopulse accuracy meets the required angular accuracy for the coarse estimation. These theoretical assessments were supported by simulations of the actual monopulse accuracy, which highlighted that the theoretical expressions actually represent a worst-case scenario when the customer is seen at the 3 dB edge of the microwave beam. An even better accuracy is thus achieved close to the peak of the mainlobe, where the customer should be located for the second position estimate after the satellite pre-pointing, which helps to speed up the fine-detection of the laser. Hence, the designed RF beacon retrieves the coarse position with an accuracy of 0.245 mrad (3 sigma) in the worst case and with an accuracy of 0.145 mrad (3 sigma) in the best case.
In conclusion, this work sucessfully showcased the potential of the LunarSpark RF beacon and derived the monopulse system design parameters that can be used for the final LunarSpark system.

A potential future improvement of this work could be achieved by investigating different transmit patterns of the customer's RF beacon. Here, the transmit pattern was assumed static and pointing upwards in this work. As a consequence, the radiation pattern drops signficiantly for small elevation angles, cancelling any gain improvement that could be achieved with a larger antenna. Solutions for this could either involve the use of two different an-

tenna patterns for low elevation angles and for large elevation angles, or could involve a beam scanning with a phased-array antenna. This would then further improve the SNR at the cost of an increased RF beacon complexity, thus significantly improving the coarse estimation accuracy.
Further, the fact that the LunarSpark satellite surface could accommodate four monopulse systems with a large spatial separation could be exploited with advanced processing techniques, also trading an improved accuracy against the need for more processing resources. It is worth noting that this accuracy improvement could then again be traded against a reduced energy consumption for the customer.

6 References

[1] "International Space Station Transition Report", *https://www.nasa.gov/sites/default/files/atoms/files/2022_iss_transition_report-final_tagged.pdf*, 2022

[2] Crawford, I. "Lunar resources: A review", *Progress in Physical Geography*, 2015

[3] Flahaut, J., Carpenter, J., Williams, J., Anand, M., Crawford, I., Westrenen, W., Füri, E., Xiao, L. & Zhao, S. "Regions of interest (ROI) for future exploration missions to the lunar South Pole", *Planetary and Space Science*, 2020

[4] Smith, K., Colaprete, A., Lim, D. & Andrews, D. "The VIPER mission, a resource-mapping mission on another celestial body", *SRR XXII MEETING Colorado School of Mines*, 2022

[5] Shirley, M., Balaban, E., Colaprete, A., Elphic, R., Sanchez, H., Falcone, L., Beyer, R., Banerjee, S. & Bradner, K. "VIPER Traverse Planning", *53rd Lunar And Planetary Science Conference*, 2022

[6] Ulamec, S., Biele, J. & Trollope, E. "How to survive a Lunar night", *Planetary And Space Science*, 2010

[7] Cataldo, R. & Bozek, J. "Power requirements for the first lunar outpost", *AIP Conference Proceedings*, 1993

[8] "Central Case Project LunarSpark - Final Presentation", *SpaceTech Class 2022/2023*, TU Graz, 2023

[9] "Central Case Project LunarSpark - System Engineering Package Document", *SpaceTech Class 2022/2023*, TU Graz, 2023

[10] Nickel, U. "Overview of generalized monopulse estimation", *IEEE Aerospace and Electronic Systems Magazine*, 2006

[11] Barton, D. "History of Monopulse Radar in the US", *IEEE Aerospace and Electronic Systems Magazine*, 2010

[12] Howard, D. "High range-resolution monopulse tracking radar", *IEEE Transactions on Aerospace and Electronic Systems*, 1975

[13] Schmidt, R. "Multiple emitter location and signal parameter estimation", *IEEE Transactions On Antennas And Propagation*, 1986

[14] Oumar, O., Siyau, M. & Sattar, T. "Comparison between MUSIC and ESPRIT direction of arrival estimation algorithms for wireless communication systems", *The First International Conference on Future Generation Communication Technologies*, 2012

[15] David Levacq "Attitude Determination and Control System for Lunar Space-Based Solar Power Satellite", *SpaceTech Class 2022/2023 Master Thesis*, TU Graz, 2023

[16] Miron Dulj "Fine Pointing Mechanism for Lunar Laser Power Transmission", *SpaceTech Class 2022/2023 Master Thesis*, TU Graz, 2023

[17] Takahashi, R., Hirata, K., Hara, T. & Okamura, A. "Derivation of monopulse angle accuracy for phased array radar to achieve Cramer-Rao lower bound", *2012 IEEE International Conference on Acoustics, Speech and Signal Processing (ICASSP)*, 2012

Appendix

SpaceTech

MASTER OF ENGINEERING (MEng)
IN SPACE SYSTEMS AND BUSINESS ENGINEERING

LUNAR PARK

Executive Summary

by
Carl TODD, Tobias BOLLIAN, Sidd GUNDDANNAVAR, Nuno SANTOS, Bernhard GOTTHART, Miron DULJ, David LEVACQ, Nathan UITENBROEK, Filip NOVOSELNIK, Leon NUSCHELE

27th June 2023

Graz University of Technology

Table of Contents

Figures

Tables

Acronyms

Acronym	Definition
ADCS	Attitude Determination and Control System
AIT	Assembly Integration and Test
AR	Acceptance Review
BR	Business Risk
CATR	Compact Antenna Test Range

CDR	Critical Design Review
CLPS	Commercial Lunar Payload Services
ECSS	European Cooperation for Space Standardization
EM	Engineering Model
EMC	Electromagnetic Compatibility Test
EPS	Electrical Power System
EQM	Engineering Qualification Model
ESA	European Space Agency
EUR	Euro
FPM	Fine Pointing Mechanism
GMAT	General Mission Analysis Tool
GNSS	Global Navigation Satellite Systems
GPS	Global Positioning Systems
GSE	Ground Support Equipment
ISP	Specific Impulse
ISS	International Space Station
KIP	Key Inspection point
LCL	Low Current Limiter
LEO	Low Earth Orbit
LOI	Lunar Orbit Insertion
LRO	Lunar Reconnaissance Orbiter
MMH	Mono-Methyl Hydrazine
MOE	Measure of Effectiveness
MPL	Mechanically Pumped Loop
N2O4	Di-Nitrogen Tetroxide
NASA	National Aeronautics and Space Administration
NH3	Ammonia
PCDU	Power Control and Distribution Unit
PFM	Proto Flight Model
PM	Protoflight Model
PTR	Post Test Review
QM	Qualification Model
QR	Qualification Review
RF	Radio Frequency
RR	Regulatory Risk
RTG	Radioisotope Thermoelectric Generators
SBSP	Space-Based Solar Power
STM	Structural Thermal Model
TCS	Thermal Control System
TLI	Trans Lunar Injection
TR	Technical Risk
TRR	Test Readiness Review

TT&C	Telemetry, Tracking, and Command
TTL	Time-To-Live
VIPER	Volatiles Investigating Polar Exploration Rover
WBS	Work Breakdown Structure

Table 1: Acronym Definitions

1. Introduction

Space technologies have revolutionized our understanding of the universe and brought countless benefits to our society. From satellite communications to GPS, Global Positioning System, our reliance on these technologies has become ingrained in our daily lives. As we push the boundaries of exploration further, the lunar surface will become the prime destination for scientific research in the coming years, aiming for an establishment of a permanent human outpost on the Moon. Robotic missions play a pivotal role in this endeavour, serving as precursors to human presence and enabling us to unlock the mysteries of the Moon while preparing for our next giant leap.

The Moon, as Earth's closest celestial neighbour, offers a unique laboratory for scientific exploration, free from the atmospheric disturbances and environmental factors that can hinder observations on Earth. One of the primary objectives of robotic missions on the lunar surface is to study the Moon's geological composition, its history, and its potential resources. Understanding the lunar environment is crucial for establishing a sustainable human outpost on the Moon. By sending robotic missions to investigate potential landing and resource utilization sites, scientists can evaluate the Moon's surface conditions, radiation levels, and potential hazards. This knowledge is vital for ensuring the safety and well-being of future human explorers. Robotic missions can also scout for resources, such as water ice, which can be utilized for life support systems, fuel production, and as raw materials for construction, thus reducing the dependence on Earth for essential supplies.

Thus, the quantity and quality of the data being generated by the robotic missions drives the timeline of the human exploration and the growth of the lunar market. This requires an efficient use of the rovers when being operated on the lunar surface. Within current projects that focus on finding in-situ resources, the mission design is mainly driven by the boundaries of direct earth communication, traversable terrain, and the availability of sunlight as the source of power.

Constraints related to Earth communication can be overcome by employing a satellite constellation in lunar orbit to facilitate data relay. Finding traversable terrain can be alleviated by charting alternative routes to navigate non-traversable terrain. The complex illumination conditions on the lunar surface remain, creating a persistent challenge to finding a reliable power source for these robotic explorers.

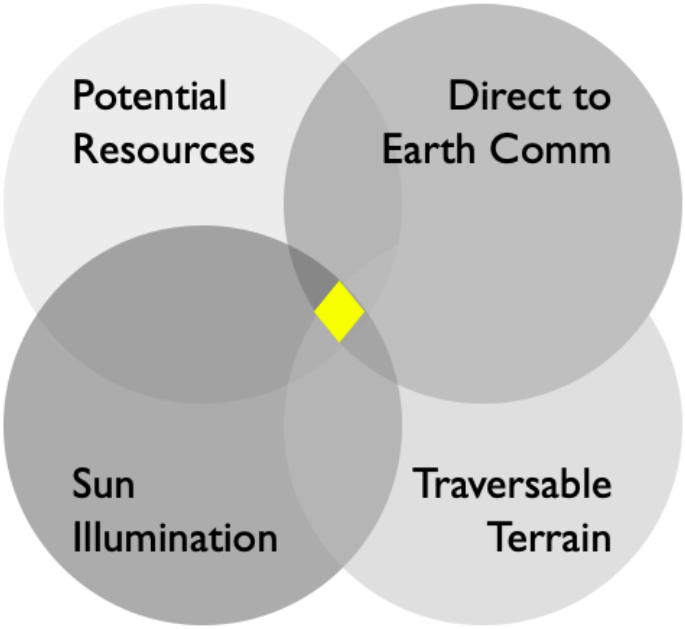

Figure 1: Primary Mission Constraints for Lunar Exploration

Addressing this challenge head-on, Lunar Spark, a pioneering company, providing a groundbreaking solution transforming the lunar market and enable lunar exploration missions.

2. Problem Statement

Robotic exploration of the lunar surface is crucial for establishing a continuous human outpost. However, the lunar environment presents daunting challenges due to its harsh conditions caused by the absence of an atmosphere. One of the major obstacles that robotic missions face is the lunar night, during which there is no available energy source for power generation.

The duration of the lunar night varies depending on the location on the moon. On average, the lunar night lasts for approximately 14 Earth days. This varies slightly by latitude. The local topography will also have significant effects near the poles due to the low sun angles. During this period of shadow, temperatures can drop dramatically to below 100 K. This is about 100 K below the freezing temperature for Li-ion batteries. In the absence of power for heaters, these temperatures lead to system failures that inevitably result in mission termination.

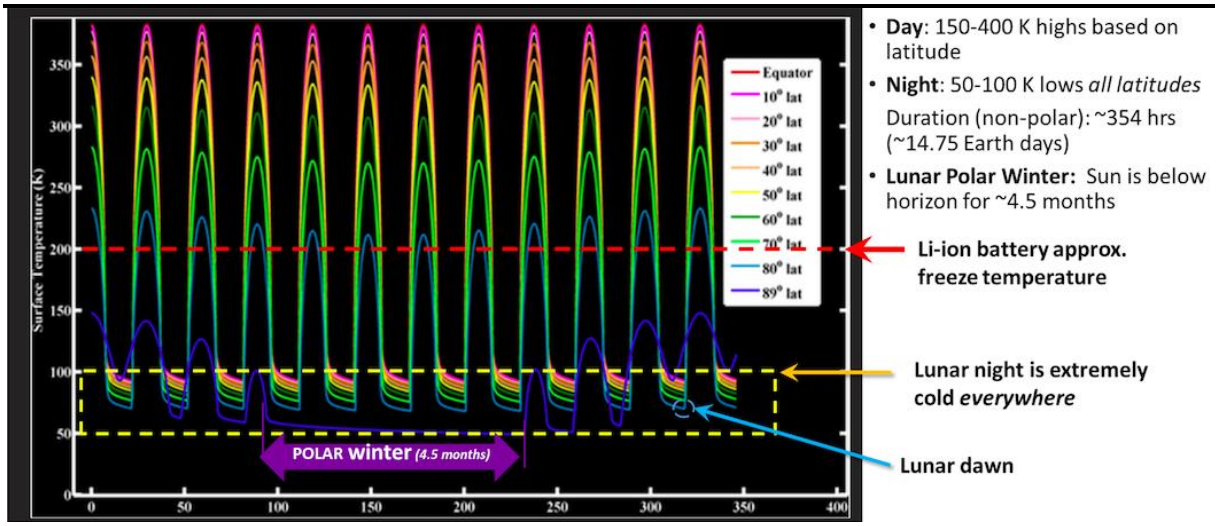

Figure 2: Monthly and Annual Lunar Surface Temperature Variations at Various Latitudes

[credit: LRO Diviner presentation CLPS 2022 Survive the Night Technology Workshop – Dec 2022]

As a result, most current robotic lunar missions are limited to a relatively short duration of 7 to 14 days. This restricted mission timeframe also means that the exploration area covered by a single mission is confined to a few hundred meters around the landing site. If mission duration were to be extended, the rover would need to find areas on the lunar surface that receive sunlight or carry incredibly heavy batteries, significantly reducing the mission's flexibility.

All in all, the limitations described above cause exorbitant mission costs, stemming from the inherent inefficiencies of relying on a single rover operating within a constrained timeframe. Extending these missions would increase the science return and further justify the large costs. Extending mission durations could done a couple of ways. One way would be to equip the rover with larger batteries to support extended operations. However, this approach leads to a substantial increase in system mass, consequently amplifying the costs associated with launching payloads into space. An alternative approach involves establishing charging stations on the lunar surface, which could potentially alleviate the mass-related challenges. However, such charging stations would impose constraints on mission mobility and flexibility, particularly when venturing into unexplored terrains. These charging stations would also be limited to areas where there is adequate sun illumination. Consequently, there exists a critical need for remote power supply solution that can effectively address these constraints in a comprehensive manner. In short, these missions need a power solution that can follow them into the dark.

By implementing an energy-as-a-service system tailored for the lunar environment Lunar Spark is offering remote power services to customers of varying sizes. The costs associated with individual robotic missions can, therefore, be reduced, along with the overall complexity of these missions. The establishment and success of a company offering such services in the lunar market hinge upon the prevailing market demands, primarily focusing on market size and attainable market share within realistic parameters.

3. The Lunar Market

The Lunar Market is experiencing a surge of interest as multiple nations, including the United States (Artemis program) and China (Chang'E project), intensify their efforts to explore and leverage the Moon's resources. With the International Space Station (ISS) set to retire by the 2030s, the lunar market presents a promising avenue for the establishment of a sustainable lunar economy. In-situ resource utilization holds immense potential, enabling the extraction of valuable resources from the lunar surface. The competitive landscape among these actors drives technological advancements and fosters innovation. Infrastructure development and exploration initiatives are gaining momentum, creating exciting opportunities for collaboration and investment in this evolving market. The growing interest in lunar exploration underscores the critical need for reliable and sustainable power sources. Looking beyond the International Space Station (ISS) era, the lunar economy holds great potential. To realize this potential, addressing the power requirements is essential.
Investing in lunar power infrastructure unlocks possibilities for extended stays, human settlements, and sustained scientific research on the Moon. The pursuit of power solutions propels the growth of the lunar market, offering exciting investment prospects and ushering in a new era of space exploration and development.

Within the Lunar power market, there is a variety of users with varying power demands for their activities. For large and stationary installations on the lunar surface, power supply can be provided the most efficient also with a stationary solution. For mobile in

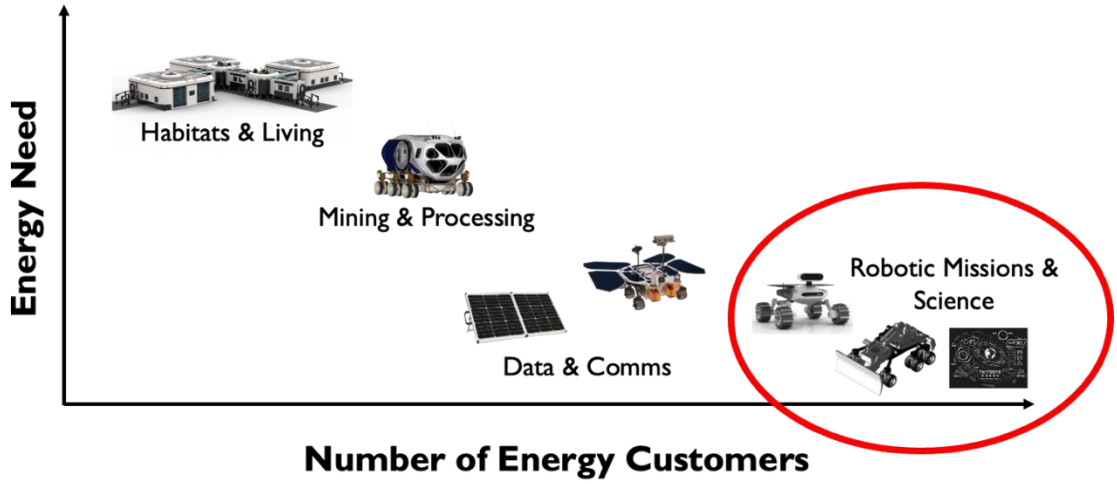

Figure 3: Target market

Based on the Lunar power market analysis, the robotic and scientific exploration missions are identified as an attractive target market, that can be served with an innovative power supply solution.

4. Customers and Stakeholders

In the dynamic landscape of the lunar market, where reliable power access is crucial for success and sustainable growth, a diverse customer base plays a vital role. Lunar Spark customers include government space agencies, private enterprises, and research institutions, all of whom have unique power requirements. To meet their needs, Lunar Spark forges meaningful partnerships, creating a thriving lunar ecosystem.

To better understand the power needs of customers, the vehicle power profiles of planned missions were analysed. The largest rover mission is the Artemis VIPER mission (Volatiles Investigating Polar Exploration Rover). The VIPER rover is expected to require around 80 W of power to sustain itself in hibernation mode while it survives the lunar night. The average and maximum power numbers for VIPER were derived by looking the power required for traverse and during periods of working [NASA reddit]. The small vehicle numbers are based on the planned Chang'E 7 mission. The total power available to their payloads is advertised as 50 Watts [csna.gov]. Estimating that survival needs would be 20% of that yields 10 Watts. Intuitive machines Nova-C lander advertises an available 200 Watts for payloads on the lunar surface. [intuitivemachines.com]. Taking 20% of that yields 50 Watts for survival power. Results from the full analysis are summarized in the table below. The table provides valuable information on the minimum, average, and maximum power requirements for different

vehicle sizes. This data allows tailoring of solutions and ensures reliable power access for each type of vehicle.

Vehicle Profile	Minimum Power	Average Power	Maximum Power
Small Vehicle	10 Watts	50 Watts	80 Watts
Medium Vehicle	50 Watts	200 Watts	250 Watts
Large Vehicle	80 Watts	350 Watts	500 Watts

Table 2: Vehicle profiles and identified power needs for each size

Lunar Spark has decided to focus on delivering 80 Watts as the minimum viable product. This will allow for the largest vehicles to survive the lunar night and also supports a variety of smaller vehicle configurations. The system will scale from the minimum viable product of 80 Watts.

Understanding the specific power needs of each vehicle category is essential for developing tailored solutions that address the challenges of the lunar market. By collaborating closely with regulatory bodies, space organizations, investors, and the public, Lunar Spark aligns objectives and builds a foundation for sustainable growth. This interaction between customers and stakeholders fosters innovation and drives the development of novel technologies and infrastructure, positioning Lunar Spark as pioneers in the lunar market.

5. The Lunar Spark Company

To satisfy the customer and stakeholder needs, the Lunar Spark company is established and registered under the laws of Germany. All former SpaceTech participants are founders of the company with an equal share of 10% of the company. An internal organization is agreed as follows:

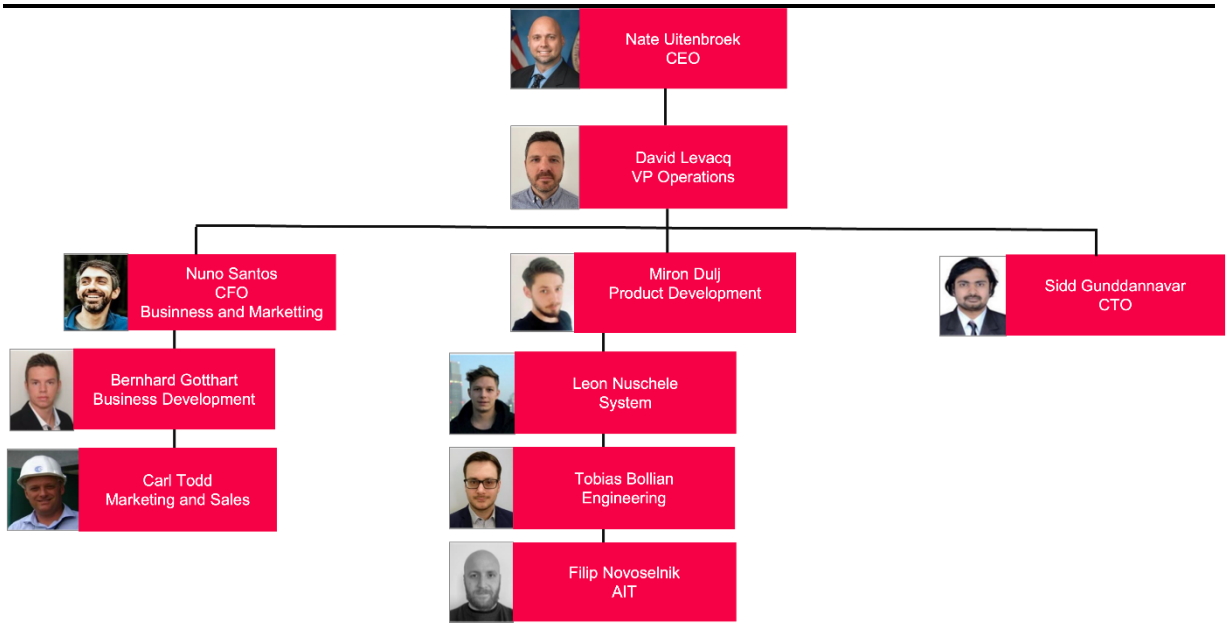

Figure 4: Lunar Spark Organizational Structure

An advisory board with the former SpaceTech Coaches, Dr. Wiley Larson, Dr. Jeff Austin, Dr. Peter van Wirt, Ulrike Fricke and Peter Schrotter is selected, supporting the company on a voluntary basis in the first years.

The company is dedicated to developing the Lunar Spark system, to operate the system and deploy the technology in the lunar market by acquiring customers for the energy as a service product. The Lunar Spark company will solve the customers constraints for robotic exploration missions on the lunar surface, therefore the following vision and mission is defined:

Vision

Lunar Spark is dedicated to effortlessly providing power to customers on the moon, reducing the entry barrier for smaller missions into the lunar market and opening up new opportunities for a flexible and long-term exploration of the moon.

Mission

Lunar Spark offers the best option for exploring the moon without restrictions. With our products and services, the customer can operate independent of the illumination conditions and without restricting mobility. Our goal is to achieve this with minimum effort for the customer. Lunar Spark provides:

- *Readily available hardware for power reception and conversion*
- *Integration support of the hardware into the customer vehicle*
- *Automatic locating and tracking of our customer on the lunar surface*
- *On-demand power*

6. Mission Objectives

Based on a proven systems engineering approach, user needs have been collected within stakeholder interviews, thus validating the problem statement summarized in chapter 2. Based on these user needs, the mission statement of the Lunar Spark company has been defined. This is further broken down into five main mission objectives to fulfil the stakeholders' expectations and run a commercially successful company.

Mission Objective 1:	Provide sufficient energy to enable stationary users on the lunar surface to survive the lunar night (min 80 W continuous).
Mission Objective 2:	Provide an end-to-end power delivery solution from space to user electrical power system interface.
Mission Objective 3:	Autonomously detect the user on the lunar surface within the service area.
Mission Objective 4:	Provide coverage to customers at the lunar south pole region.
Mission Objective 5:	Provide scalability in order to accommodate multiple customers and/or higher energy transmission.
Mission Objective 6:	Minimize receiver size and mass not to constraint user mobility.

The mission objectives are used to select the most suitable system architecture and measure the system effectiveness throughout the design, implementation, and operational phases of the mission.

7. Alternative Architectures

To serve the mission objectives, several power supply approaches were considered for the Lunar Spark project and being assessed according their fit for the Lunar Spark Stakeholders:

1. Solar Farm
2. Rover Solar Panels
3. RTG (Radioisotope Thermoelectric Generators)
4. Fuel Cells
5. Nuclear Power Plant
6. Space Based Beaming

All the approaches were evaluated by the same criteria that include mobility, illumination conditions, power capacity, and multi-mission infrastructure capabilities. Each technology's advantages and disadvantages are summarized in the following table.

Technology	Provides mobility	Works in darkness	High Power capacity	Multi-Mission Infrastructure
Solar Farm	−	−	+	+
Rover Solar Panels	+	−	−	−
RTGs	+	+	+	−
Fuel Cells	+	+	+	−
Nuclear Power Plant	−	+	+	+
Space Based Power Beaming	+	+	+	+

Table 3: Alternative Power Technologies

a. **Mobility:** Early actors on the lunar surface require mobility for exploration and prospecting. Fixed solar farms and nuclear power plants are not ideal due to limited range and the need to return for recharging.
b. **Illumination:** Lunar orbital mechanics result in long lunar nights and low sun angles at the poles where resources are targeted. Solar panel solutions are limited by darkness, affecting mission plans and objectives.
c. **Power Capacity:** Different vehicle categories have varying power needs. Fixed solutions like RTGs (Radioisotope Thermoelectric Generators) and fuel cells score high for power generation. Solar panels have limitations for small rovers but can provide higher power for larger rovers.
d. **Multi-Mission Infrastructure:** Most of the future lunar activities require infrastrucutre for long-duration operation that can serve multiple missions. Rover solar panels, RTGs and, fuel cells are not capable of providing multi-mission infrastructure support.

Space-based power beaming, where energy is collected and beamed from a lunar polar orbit, excels in all categories. It enables mobility, is not limited by illumination, provides adequate capacity, and offers 100% renewable energy. Based on the evaluation, the Space-Based Power Beaming approach has been selected for the Lunar Spark system, as it meets all key criteria effectively.

There are several alternative concepts for energy harvesting and transmission in the context of satellite-based systems. Four main concepts are considered: the single satellite solution, the train of satellites solution, and ground-based solar array farms with satellite-based distribution. They are shown in a figure below.

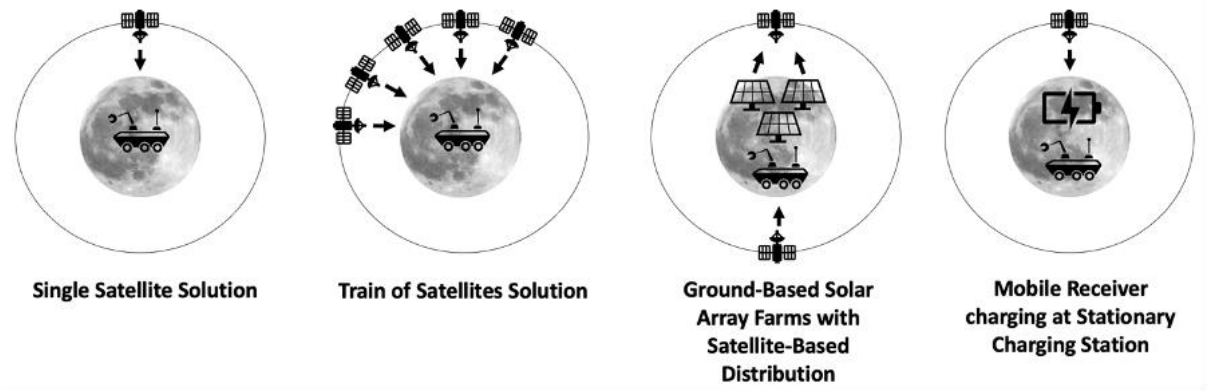

Figure 5: Alternate Mission Concept Options

The single satellite solution involves launching a single satellite that can provide high power and serve multiple customers from the beginning. This approach offers advantages such as lower maintenance and operation requirements. However, it also has drawbacks, including a high impact in case of failure, the need for a heavy and complex satellite, and potential health and safety issues due to high energy levels.

The train of satellites solution adds satellites to reduce the time between charging contacts. This approach offers advantages such as redundancy, increased charging opportunities, scalability, and potential cost savings through mass production. However, it requires multiple launches and may result in higher maintenance and operation costs due to the need to control more satellites. Lunar Spark has chosen to build an automated, scalable system, starting with two satellites that will be accommodated by one launcher. The system will scale from there to increase capacity.

8. Proposed Technical Solution

The overall system, concept of operations, and the system components are introduced in the following sub-chapters.

8.1. System Overview

The Lunar Spark team chose to develop a Space-based solar power (SBSP) technology to provide power for rovers on the Moon. Lunar Spark will deploy two satellites in a 700 km altitude polar orbit, each being capable to serve customers with a need for continuous power of 80 W. This capacity will easily power large rovers in hibernation mode or several small rovers. Each rover will have a Lunar Spark receiver with a beacon for localization. Laser power transmission was chosen, as

it is more suitable than other waveforms for lunar use cases, because laser technology allows for smaller apertures and targeted beams. The receiver uses a laser panel energy receiver for energy absorption. Laser receivers are photovoltaic arrays tuned for a very specific wavelength for optimized laser reception. Under cold temperature these laser receivers can achieve efficiencies higher than solar panels. The system is highly automated with a small team of operators monitoring the spacecrafts and coordinating lunar surface vehicle needs. Operators configure the spacecraft for power delivery, monitor automated localization and vehicle delivery selection, as well as command required obit manuevers and troubleshoot any problems.

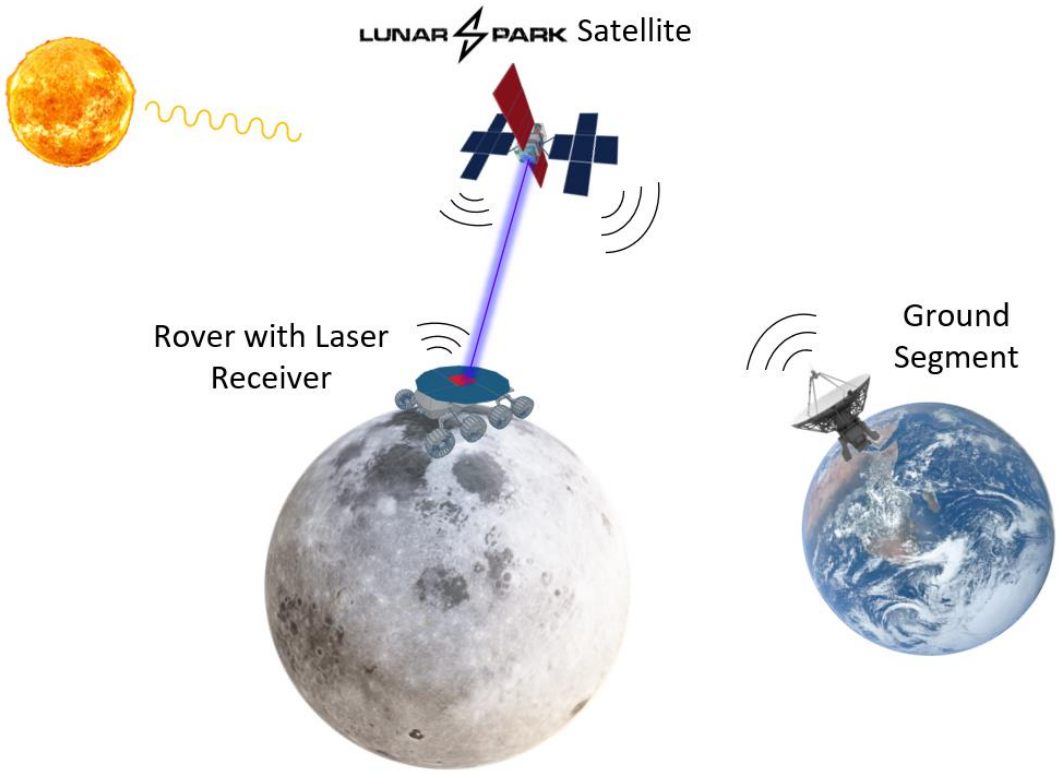

Figure 6: Lunar Spark Space-Based Power Delivery System

8.2. Concept of Operations

The fundamental concept of the Lunar Spark system is to collect energy from the sun while orbiting the moon and provide that power to vehicles on the surface as the satellites fly over. The two satellites in the system are capable of meeting continuous power needs of the rovers on the moon by alternating delivery as they fly over. The overall concept of operation is given below.

8.2.1. Power Delivery Concept of Operations

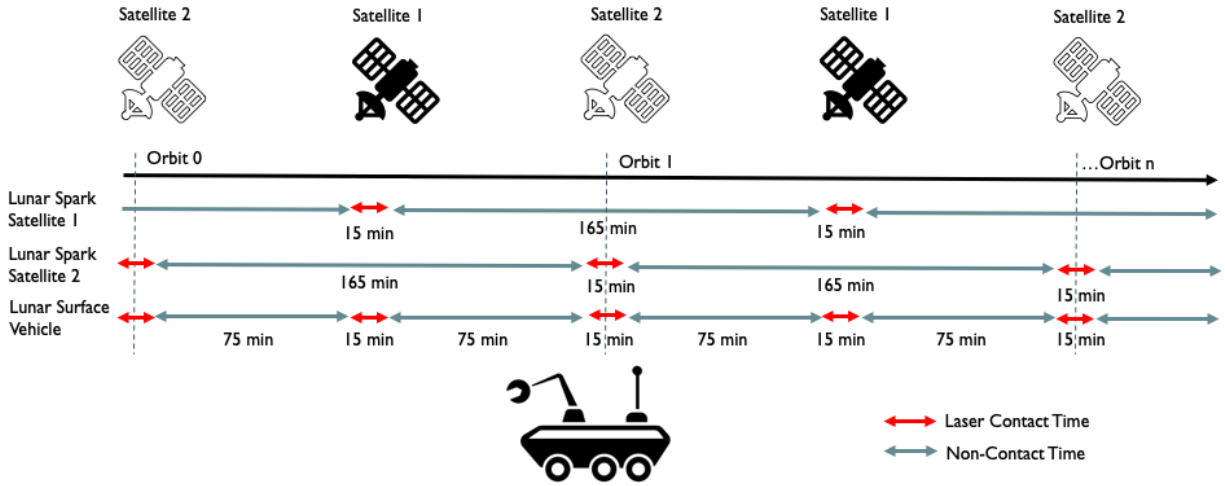

Figure 7: Cyclic Operations Timeline for Power Delivery

The proposed system initially consists of two satellites to provide power delivery to the south polar regions, which encompasses latitudes between 80 and 90 degrees south. These satellites exhibit orbital anomalies that are positioned 180 degrees apart from each other. During their 180-minute orbital period, each satellite offers a 15-minute contact time with the south polar region rovers. This contact time alternates between the two satellites. The objective of this configuration is to ensure a continuous power delivery window of approximately 15 minutes every 75 minutes for the designated south polar region. Power delivery is executed when the elevation angle between the rover location and the satellite is above 45 degrees, as this allows for more efficient laser panel energy conversion. In this configuration each satellite can satisfy the 80 W continuous power requirement on the surface.

8.2.2. Communication Concept of Operations

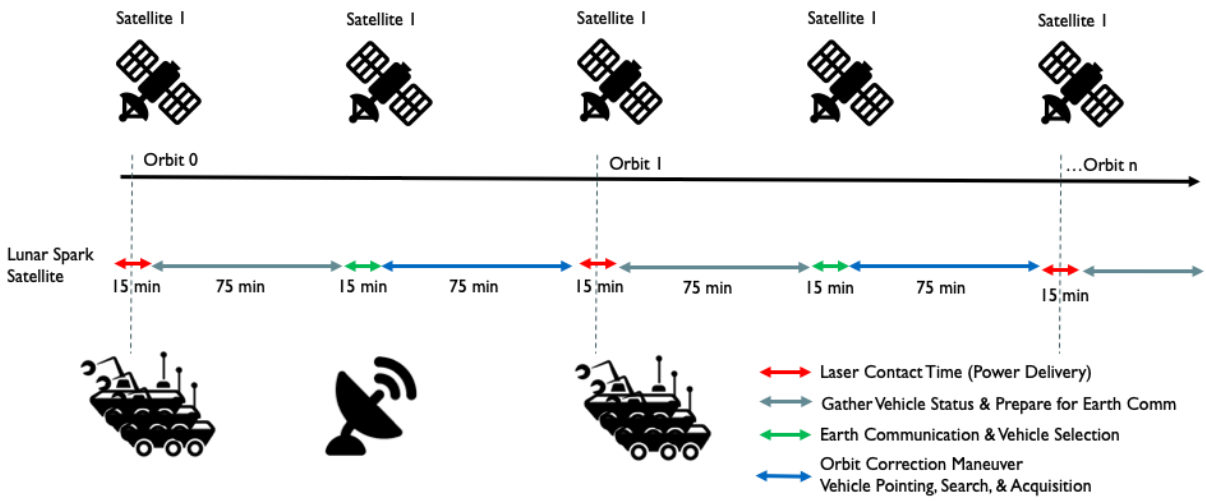

Figure 8: Cyclic Operations Timeline for Communication and Tasking

Satellites collect information regarding the power status and location of surface vehicles as they depart from the south polar region. Through automated algorithms, these satellites determine the vehicle with the lowest time-to-live (TTL) and then determine which vehicle is the target for power transmission on the next south pole fly over. Subsequently, the power statuses, locations, and the selected vehicle are transmitted to mission controllers as the satellite traverses the lunar north pole. While the automated selection process is typically reliable, mission controllers may intervene and override the automatic selection by choosing an alternate vehicle or confirming the automated choice. This provides a human element in the decision-making process, allowing for careful consideration of any additional factors or specific requirements. As the satellite departs the north polar region, it performs any necessary orbit correction maneuvers, and then aligns its orientation towards the selected vehicle's location. As the satellite enters the line-of-sight of the rover, search and acquisition algorithms are executed. These algorithms perform the necessary actions to precisely lock onto the target vehicle, aligning the spacecraft and laser for efficient power delivery. The search and acquisition process completes as the elevation angle approaches 45 degrees, where the power transmission process begins. Overall, this systematic approach, combining automated algorithms with human oversight and precise search and acquisition techniques, ensures the effective and reliable transfer of power to vehicles, ultimately supporting their operations and mission objectives.

8.3. System Capabilities

The primary capability of the Lunar Spark system is to deliver power to rovers on the moon. The designed satellite system can provide 2100 W per day of power per satellite to the lunar surface which allows the operation of a system with a continuous power demand of 80 W. With two satellites the system has the capacity to deliver a total of 4200 W. How this power is distributed could vary depending on the number and locations of rovers in the service area. One scenario would have one large rover in hibernation with 80 W of additional capacity to service several smaller rovers (up to 8 rovers at 10 W each). Another scenario might support two large rovers in hibernation (160 W). With rovers at various locations, each will see a slightly different illumination environment. Some rovers will be in sunlight while others are in the lunar night. Some rovers may be in permanent darkness looking for resources inside craters. Determining the actual power delivery configuration also takes into account margins and the criticality of each rover and balances the power and risk appropriately. The allocation of which user is served in which orbit is an automated process based on the customer energy status and their projected power draw. The energy status of each user is transmitted every flyby by the receiver panel to the Lunar Spark spacecraft. Manual interactions with to prioritize different users are possible and can be uploaded to the system once every orbit. Automated user localization and tracking using the Lunar Spark power receiver and beacon is another key capability of the system which allows for autonomous operation with no need for an interface to the customers ground operations team.

8.4. Lunar Spark Laser Receiver

As one of the mission objectives is to provide an end-to-end solution, it is required to design and integrate a part of the Lunar Spark system on the customers vehicle Lunar Spark Receiver.
The hardware employed in our system plays a dual role: firstly, it converts the optical energy from the laser beam into electrical power to charge the rover, and secondly, it establishes the RF link with the Lunar Spark spacecraft, enabling precise localization and closed-loop feedback necessary for spacecraft fine pointing.

In terms of power conversion, the receiver is illuminated by a laser beam with a wavelength of 445 nm and a beam intensity of 6193 W/m2. Laser cells meticulously tuned to this specific wavelength facilitate a remarkable 60% power conversion efficiency from laser to electric power. Considering a 10% internal system loss, a receiver area with a diameter of 75 cm is required to provide the necessary power for the rovers to operate at a continuous power level of 80 W.

Localization and closed-loop tracking are accomplished through the utilization of an RF Beacon. This beacon serves as a communication interface between the spacecraft and the system, enabling the spacecraft to respond to signals sent during a spiral search. Additionally, information such as the battery status of the vehicle, project power draw, and power levels received by the four laser cell modules is transmitted.

The battery status and power draw information is crucial for spacecraft-level decision-making regarding the allocation of power to different users in various orbits. The information about the power level received in each quadrand, on the other hand, facilitates fine pointing on the spacecraft. To enable this, a four-quadrant geometry is established to measure the power distribution over the receiver panel and close the feedback loop to the spacecraft. Those functions result in the following physical architecture:

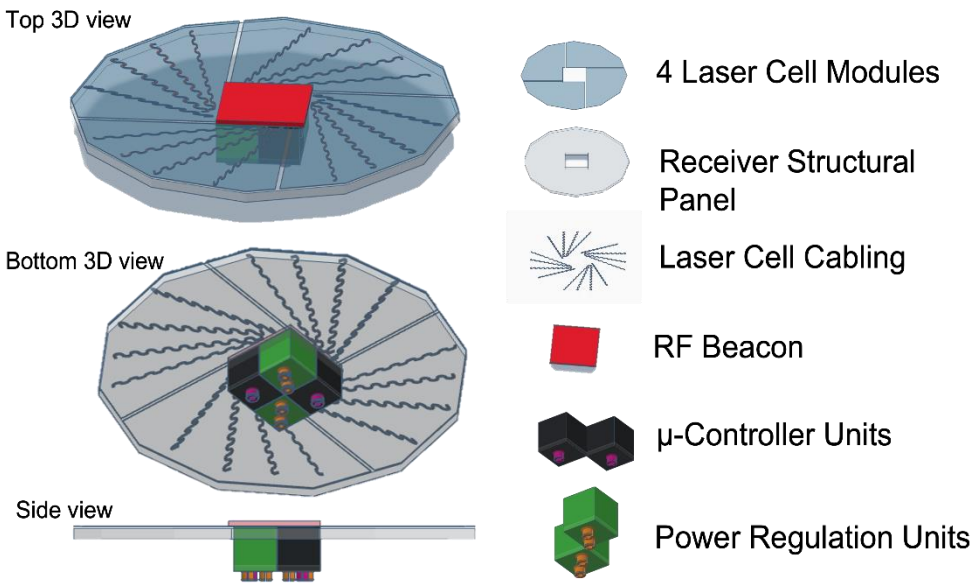

Figure 9. Receiver physical architecture

8.5. Space Segment

Lunar Spark's space segment is composed of two identical spacecrafts in the first operational phase of the company. Each spacecraft is designed for a mission lifetime of 8 years and carries a high-power laser payload following a double redundant concept and it follows a polar Lunar orbit with an altitude of 700 km. In the following sections, the most important subsystems will be addressed and some details provided. First, the steerable high-power laser payload is addressed. Subsequently, the satellite bus will be explored and some words will be shared on the critical subsystems, such as electrical power

system, thermal control system, pointing and attitude control subsystems. The complete picture of all the spacecraft subsystems is given below.

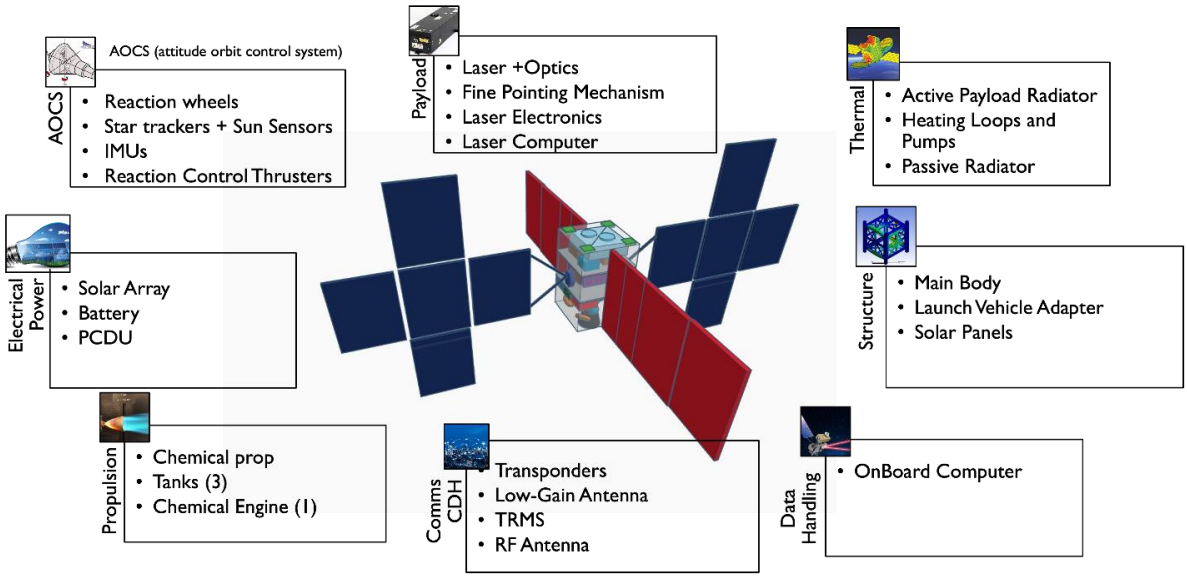

Figure 10: Spacecraft physical architecture

Each spacecraft has a total wet mass of 3145 kg and a main body in the size of 2 x 2 x 3 m with two deployable solar arrays of 25 m^2 each and two deployable thermal radiators in the size of 18 m^2 each.

8.5.1. Payload: Steerable High-Power Laser

Lunar Spark's payload is responsible for pointing and beaming energy towards the customer rover on the lunar surface. The concept is based on a combination of multiple semiconductor lasers and laser combiners to achieve the required output power. On the figure below, an illustration of the payload components is presented.

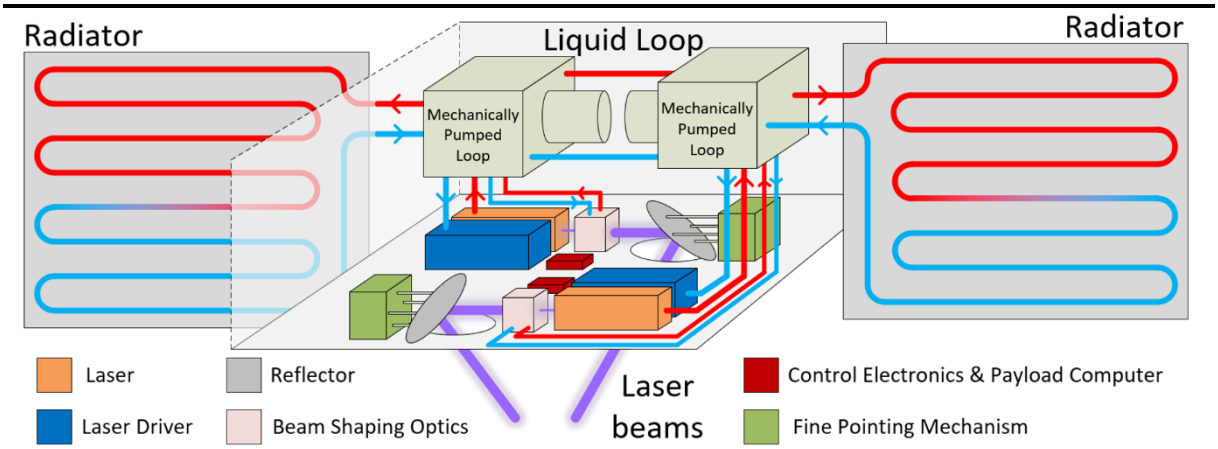

Figure 11: An illustration of the laser payload main components including thermal control system

The payload laser wavelength has been selected to be 445 nm (blue) based on state-of-the-art research on lunar regolith dust reflectance properties and the fact that the received power increases with the square of the decreasing wavelength, which can be mathematically proven. This is an important rationale for choosing a wavelength that is as low as (technically) possible for wireless energy transmission. The 445 nm wavelength also has favourable divergence properites.

In terms of optical engine, the payload is complemented by a steerable beam shaping lens stage, based on a Galilean beam expander, which is illustrated below. On the left: Reflecting a collimated is representative of power beaming configuration. On the right: Reflecting a divergent or out-of-focus is representative of rover spiral-scanning configuration. This is achieved by reducing the distance of the objective lens and consequently the laser beam will further expand into a divergent configuration. The illustrations not to scale.

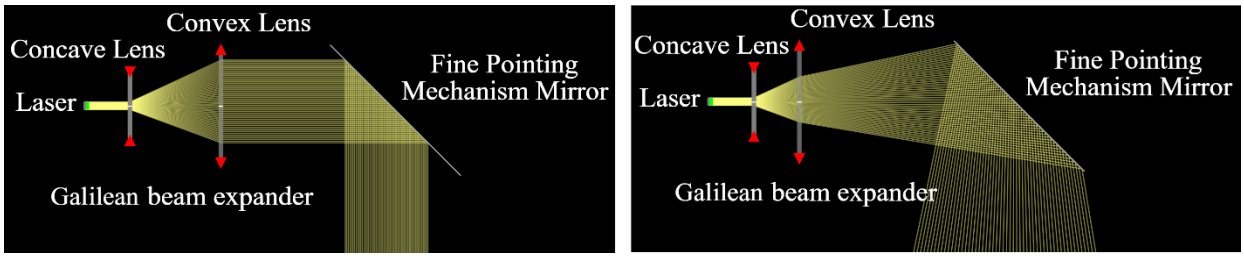

Figure 12: Conceptual illustration of a Galilean beam expander and reflective mirror

The payload specifications are summarized in the table below.

Laser Payload	
Laser Type	Gallium Nitride (GaN) semiconductor

Input Power	42.7 kW (electrical)
Output Power	12.8 kW (optical) / 29.9 kW (thermal)
Laser Efficiency	Conservative 30% (Can go up to 48.5%)
Wavelength	445 nm
Redundancy	Double redundancy concept
Estimates	
Mass	233 kg (20% margin + redundancy)
Volume	0.79 m^3 (75% margin)
Dimensions	1.3 x 1.2 x 0.5 meters (LxWxH)

Table 4: Laser payload specifications and estimations

8.5.2. Satellite Bus

To support the payload operation, the Lunar Spark's satellite bus is specified and its main challenges and solutions to those are described in the following. The approach is aimed at procuring a standard satellite bus that is suitable for the mission goals. Nonetheless, there are several elements that will be customized for the mission.

8.5.2.1. Electrical Power Subsystem

Due to the Lunar Spark purpose of power transmission, the electrical power subsystem is a key element of the spacecraft to enable the mission. The spacecraft's average power demand of 7.8 kW during the 180 minutes orbit is in fairly standard range compared to telecommunication satellites. But the high peak power demands of 50 kW required for the power transmission need to be handled autonomously on the spacecraft and create a big challenge to be solved. The power needs to be provided on demand to the payload when being in sight of the customer’s vehicle. High efficiencies are required to avoid thermal impacts on the payload. Therefore, the spacecrafts batteries need to be charged during the illumination period and the set of batteries shall provide the energy for eclipse as well as for the transmission period. The power system generation and storage capabilities are sized as the following:

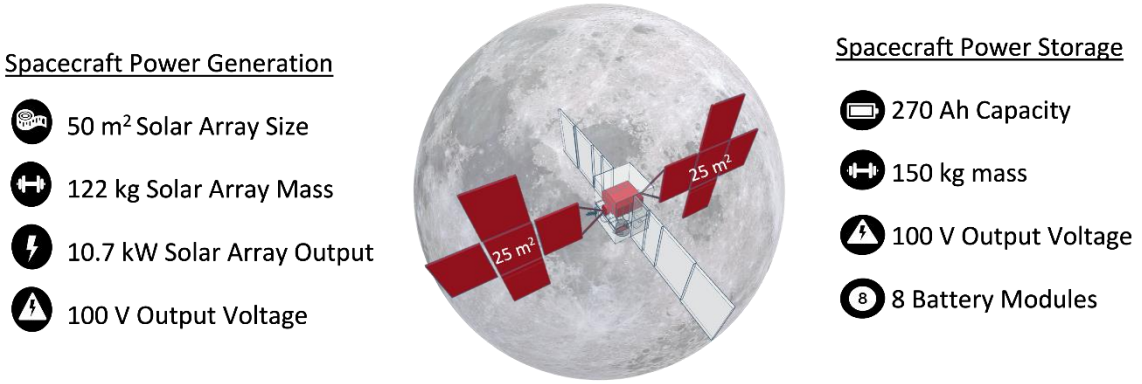

Figure 13: Lunar Spark spacecraft electrical power system sizing

The power distribution within the spacecraft needs to be highly efficient but still cost effective. This is achieved by having a dual bus voltage based on the ECSS standards. All subsystems are powered with a 28 V regulated bus, centrally regulated and distributed by a Power Control and Distribution Unit (PCDU). This voltage allows to use standard subsystem components, which are already qualified for space. The payload is operated using a 100 V unregulated bus voltage directly provided by the 8 battery modules to the payload, protected with Latching Current Limiters (LCLs) and Shunt Regulators. This allows to turn on and of the laser power in demand with minimum power losses within the spacecraft. From thereon, the laser electronics convert the provided power and operate the individual lasers. A total EPS (Electrical Power System) efficiency better than 81% shall be achieved to limit thermal impacts on the payload.

8.5.2.2. Thermal Control Subsystem

Lunar Spark's Thermal Control System (TCS) design requires special attention. More specifically, the payload thermal control poses a complex technical challenge. The laser payload will generate approximately 30 kW of thermal power during the laser operation, which needs to be dissipated away from the most critical components, namely the laser and fine pointing mechanism. The spacecraft thermal control system is divided in three parts: Payload, Bus, and Solar Arrays. The spacecraft bus relies on passive thermal control whereas the payload relies on active thermal control with liquid loops. In-between, there is a thermal isolation layer. The solar panels rely on standard passive thermal control.

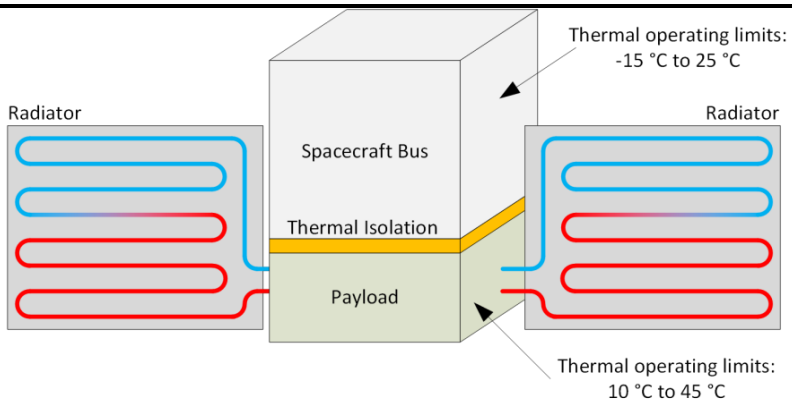

Figure 14: Simplified illustration of the TCS design approach for Lunar Spark.

Below an illustration of the payload thermal control system with redundant payload.

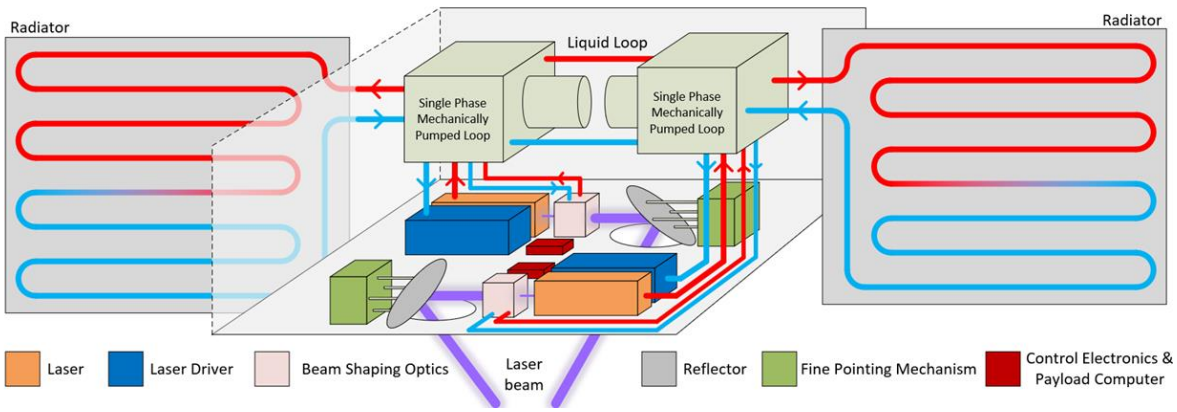

Figure 15: Payload illustration with double redundant laser and thermal control systems

The payload uses a single-phase mechanically pumped loop (1θ-MPL). Ammonia was selected as cooling fluid, due to its low density. This approach requires a double-layer radiator with a wingspan of 14 meters as illustrated below. Several improvement techniques have been used to optimize the radiator performance.

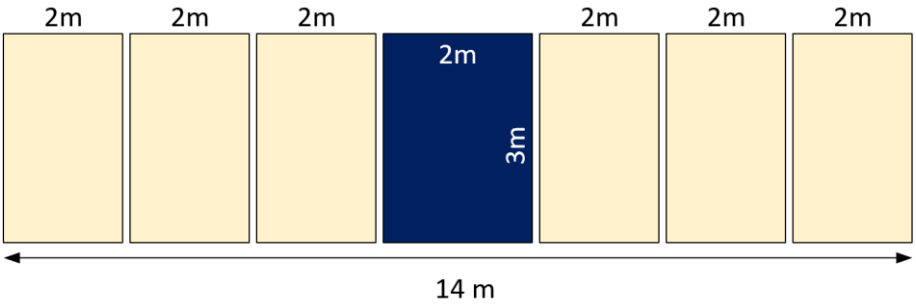

Figure 16: Lunar Spark radiator wingspan

The thermal control system specifications are summarized in the table below.

Payload Thermal Control	
Type (Active)	Single -Phase Mechanically Pumped Loop
Load Capacity	Can radiate 30.5 kW
Cooling Fluid	Ammonia (58kg of NH3)
Total Mass	320 kg (10% margin)
Redundancy	Dual pump concept

Table 5: Thermal Control system specifications and estimations

8.5.2.3. Pointing Strategy

The laser pointing concept for the Lunar Spark satellite involves a two-step strategy to ensure accurate beam alignment with the receiver on the lunar surface. The overall goal is to maintain precise pointing direction and angle to enable successful power transfer between the satellite and the user rover.

The first step is coarse pointing, which is achieved through the satellite's Attitude Determination and Control System (ADCS). Prior to the transmission window, the satellite slews to orient its laser beam towards the receiver location. The specific user rover to be serviced is determined during each pass over the lunar pole, and its localization data from the previous orbit is used. Once the user to service will be in the field of view of the satellite with a sufficient elevation angle, the RF beacon of the user will be woken up and the user localization system will provide the real-time relative vector between the spacecraft and the receiver. This will allow the ADCS to refine the attitude of the spacecraft. A total coarse pointing accuracy of +/- 2 mrad is achieved. This defines the search angle for the second pointing step, the fine pointing.

The second step relies on a Fine Pointing Mechanism (FPM) and closed-loop feedback from the receiver/beacon. The FPM is responsible for accurately steering the laser beam towards the receiver and maintaining alignment over the duration of the transmit window. It operates in two degrees of freedom, allowing precise control of the reflective mirror's angle to adjust the beam direction. The FPM must have a resolution finer than 623 nrad to achieve the required pointing accuracy. To account for margins, a resolution of +/- 400 nrad and an angular range of +/- 2.5 mrad are specified for the FPM. The closed-loop feedback from the receiver/beacon utilizes the segmented laser panel. Power received by each of the four quadrants is provided back to the spacecraft. The differences in power production between the four quadrants helps identify pointing errors. Correcting these errors continuously adjusts the FPM's position based on real-time information, ensuring that the laser beam remains on target.

By employing this two-step pointing concept, the Lunar Spark satellite can achieve the necessary accuracy to steer the laser beam towards the user rover on the lunar surface and maintain precise alignment for the duration of the transmit window. This enables efficient and reliable power transfer between the satellite and the lunar surface.

Pointing main specifications are provided in the table below.

ADCS pointing accuracy	**+/- 1.75 mrad**
User localization accuracy	+/- 0.25 mrad
Total coarse pointing accuracy	+/- 2 mrad

Fine pointing mechanism resolution	**+/- 400 nrad**
Fine pointing mechanism range	+/- 2.5 mrad

Table 6: Coarse and fine pointing key characteristics

8.5.2.4. User Localization

For the coarse localization stage, the satellite utilizes a RF link between a microwave antenna on-board the satellite and a radio frequency beacon mounted onto the customer's hardware. As the satellite flies over the service area, it periodically transmits a wake-up signal. This signal is then received by the RF beacon of each customer located on the ground within the current antenna footprint, where it triggers the generation of a response signal (transponder-like behaviour). Once the RF antenna on the satellite captures the beacon's response signal of the visible customers, it is possible to estimate the relative angular direction using a technique called monopulse. The satellite is hereby able to

distinguish the response of each customer that might arrive simultaneously and applies the monopulse to each received signal. The result of this process is a vector that can be utilized in the coarse pointing algorithm for corrections.

8.5.2.5. Attitude Determination and Control System (ADCS)

The Lunar Spark ADCS subsystem pursues 4 major objectives:

1. Stabilize the Spacecraft after launcher separation.
2. Maintain desired orbit/trajectory as specified by the mission requirements.
3. Control spacecraft attitude to:
    1. Maximize solar energy collection by orienting solar panels towards the sun.
    2. Perform coarse pointing during energy beaming.
    3. Orient TT&C Low-gain antennas towards the Earth during communication windows.
4. Ensure safe state of the spacecraft at any time, including emergency and anomaly situations.

Architecture of the Attitude Determination and Control Subsystem is illustrated in the figure below.

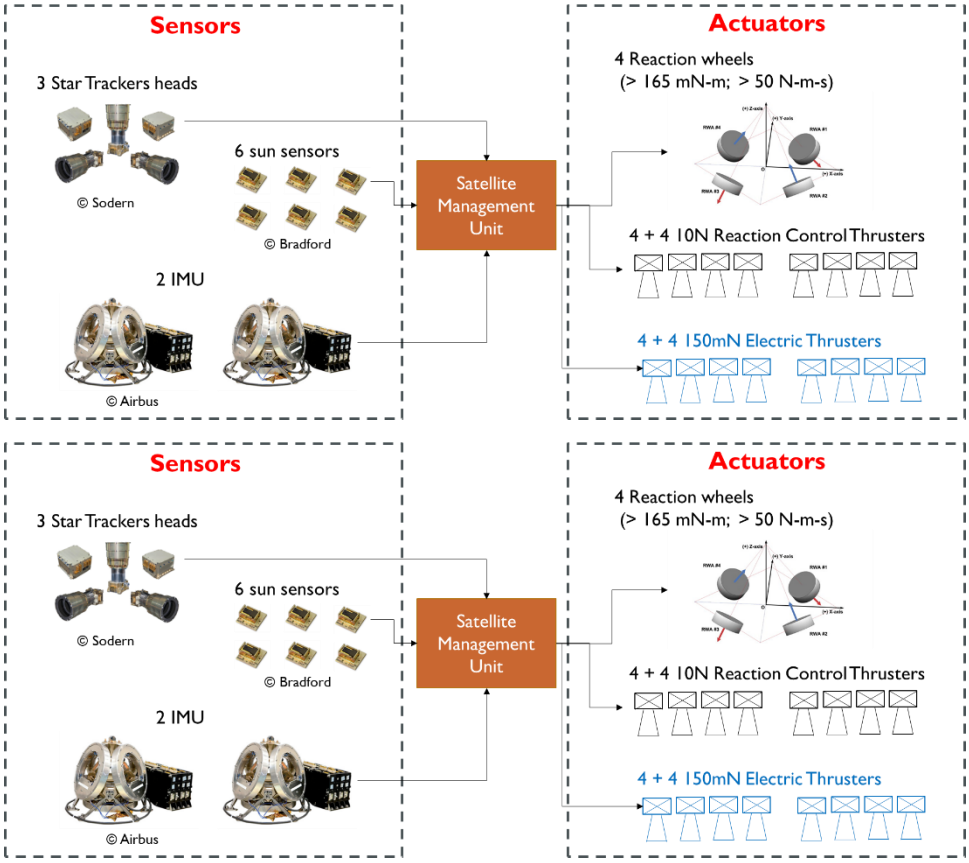

Figure 17: Attitude Determination and Control Subsystem Architecture

Attitude sensing will combine star trackers (3 heads in hot redundancy) with Inertial Measurement Unit (2 units in cold redundancy). Six sun sensors are used for Sun direction determination and attitude sensing in safe mode.

The required coarse pointing accuracy of 1.75 mrad will be achieved with a zero-bias active attitude control based on 4 hot redundant reaction wheels in a pyramid configuration. Those will be the primary attitude control actuators in nominal mode when orbiting around the Moon.

Electric thrusters (4 nominal + 4 redundant in cold redundancy) will be used for orbital manoeuvres (initial orbit acquisition, station keeping, end-of-life deorbiting), reaction wheels desaturation and end of life manoeuvres.

Reaction Control Thrusters (4 nominal + 4 redundant in cold redundancy) will be used for attitude control before/during and after Liquid Apogee Engine burn and in safe mode, and for spacecraft detumbling after launcher separation.

8.5.3. Spacecraft Launch and Maneuvers

While there are over 30 launchers capable of launching satellites into space, only a few are sufficiently robust to support the demanding requirements of Lunar Spark's interplanetary trajectory. This spacecraft launch mass is 3.5 tons of wet mass. Since the Lunar Spark system consists of two such spacecrafts, the total mass that must be delivered to the Moon's orbit is around 7 tons. Launchers such as Atlas V, Falcon Heavy, and Delta IV Heavy are capable of performing launches including Trans-Lunar Injection (TLI) maneuvers needed for Lunar Spark. Considering its significant capacity of 17 tons for trans-lunar trajectories, Falcon Heavy has been chosen as the primary launcher for Lunar Spark, with New Glenn serving as a reliable backup option.

When it comes to transfer options from Earth to the Moon, there are several strategies that balance energy requirements, transferred mass, and travel time. The three most common methods are direct transfer, low-energy transfer, and low-thrust transfer. Although each has its advantages and disadvantages, the direct transfer method emerges as the most viable for Lunar Spark, despite its substantial V costs. This is due to the long travel times and high radiation exposure risks associated with low-energy and low-thrust transfers.

Once the Lunar Spark spacecraft reaches Low Earth Orbit (LEO) via the chosen launcher, a Trans-Lunar Injection (TLI) maneuver is initiated to set it on its lunar trajectory. TLI maneuver is energy intensive with a ΔV demand of 3200 m/s and is provided by the upper stage of the launcher. This transfer time to the Moon is a function of the lunar phase and typically varies between 4 and 5 days. After launching onto the trajectory, a mid-course correction is performed at T + 24h to correct any launch vehicle errors. The final maneuver, the Lunar Orbit Insertion (LOI) with ΔV of 750 m/s happens at T + 72h and results in the spacecraft being captured by the Moon's gravity. Detailed timeline with all the maneuvers performed is shown below.

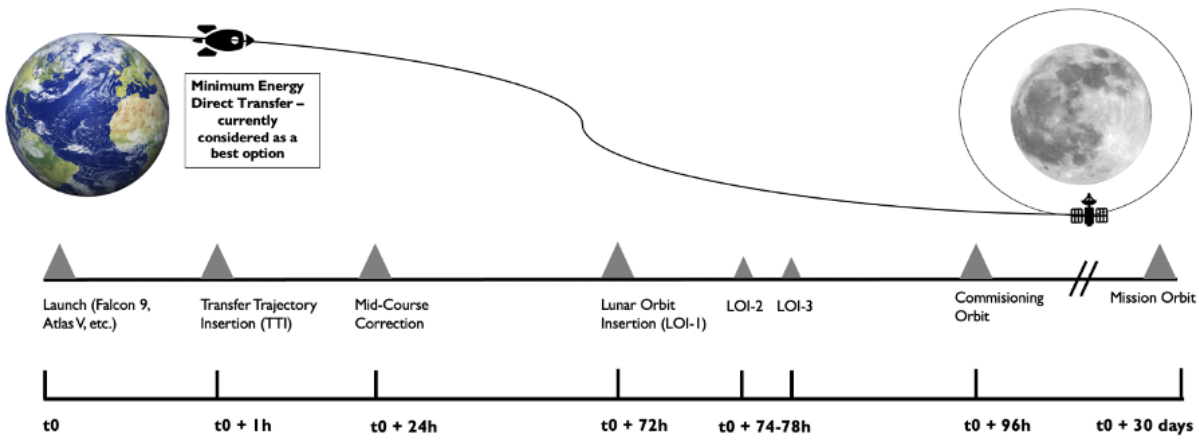

Figure 18: Direct lunar transfer maneuvers and timeline

The propulsion system's design and choice of propellant have effect on the spacecraft's mass, dynamics, and overall performance. For Lunar Spark's spacecraft, a bi-propellant propulsion system is used to perform the LOI maneuver. The propulsion system includes a high-thrust Liqui Apogee Engine and 8 low-thrust thrusters. An essential factor considered was the choice between monopropellant and bipropellant. Monopropellant has a specific impulse (ISP) of 240 seconds and the trade study revealed that the bipropellant, with an ISP of 310 seconds, could save approximately 400 kg of fuel, making it a more feasible choice for the LOI maneuver. The selected fuel is mono-methyl hydrazine (MMH), while the oxidizer is dinitrogen tetroxide (N2O4). Total estimated V budget for Earth to the Moon transfer is summarized in the table below.

Manoeuvre (Lunar Transfer)	ΔV [m/s]
Mid-course correction	30
Lunar orbit insertion (LOI-1)	750
LOI-2	150
LOI-3	120
Unallocated margin	50
Total	**1100**

Table 7: Lunar transfer ΔV budget

Once the spacecraft is successfully inserted into lunar orbit, it must perform station-keeping maneuvers to maintain its altitude over an extended period. These maneuvers use electric propulsion, which is more efficient than chemical propulsion, particularly given the spacecraft's ample electric power supply. The orbit maintenance includes orbit station-keeping, momentum unloading and deorbiting (end-of-life maneuver). The electric propulsion system includes 8 Hall Effect Thrusters, each capable of producing up to 150 mN of thrust. With the spacecraft's lifespan estimated at 8 years, the required V is estimated to be 104 m/s or 13 m/s per year based on a simulation performed in GMAT (General Mission Analysis Tool). The summary of orbit maintenance delta-V budget is given in the table below.

Manoeuvre (Orbit Maintenance)	ΔV [m/s]
Station-Keeping	104 (13 m/s per year)
End-of-Life manevour	100
Unallocated margin	50
Total	**254**

Table 8: Orbit maintenance ΔV budget

8.6. Ground Segment

The ground segment consists of multiple contracted ground stations around the Earth to provide communication to the lunar orbiting satellite assets. These ground stations are all connected to one Mission Control Center operated by a team of about dozen Lunar Spark operators with a mix of space operations and software skills. Satellites communicate with Earth one time per orbit as they pass over the lunar north pole.

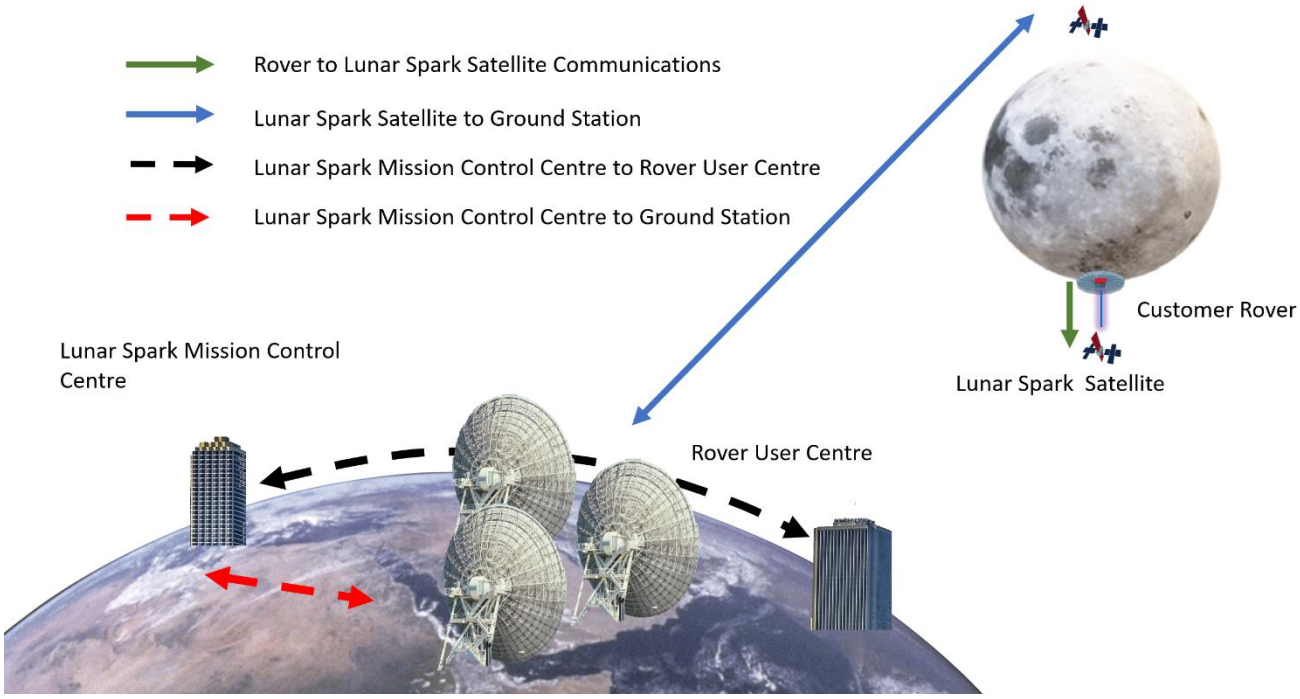

Figure 19: Lunar Spark communication links

There are four main communication links:

1. Rover to Lunar Spark Satellite Communication: The lunar Spark Satellite receives a status message from the rover, this contains power and various status information. This link is also used to measure localization errors.
2. Lunar Spark Satellite to Ground Station: The ground station receives and transmits the RF signal to the Lunar Spark satellite. The ground stations are rented by the Lunar Spark company. The ground stations provide uplink and downlink access to the Mission Control Center.
3. Lunar Spark Mission Control Center to Rover User Center: The status from the rover is augmented with the transmitted power and the location information of the rover, derived by the satellite. This information is then transmitted to the Rover Operations Center. Requests for a manual intervention, cancelling or requesting power delivery can also be sent via this link.
4. Lunar Spark Mission Control Center to Ground Station: The telemetry and telecommands from the Lunar Spark satellites are received at the Lunar Spark Mission Control Center. The ground station is responsible for the RF link to the satellite. Telecommands from the Lunar Spark User Center are converted and sent to the satellite. Telemetry from the satellite is converted to baseband and sent to the Lunar Spark Mission Control Center. General commanding and status messages from the ground segment are managed over this link. The power delivery process is completely automated with software onboard the satellite and receiver. This

software coordinates surface vehicle localization using the vehicle beacons and selects the appropriate vehicle to service each orbit. The operations team's primary power delivery responsibility is to monitor these automated power delivery algorithms, confirm that surface vehicle power needs are being met, and ensure that the satellite systems are healthy. The operations team can configure the vehicle selection algorithms and override the automated selection if unforeseen scenarios arise. The operations team also monitors the satellite orbit and commands orbit corrections that are performed each orbit

8.7. System Measures of Effectiveness

Sun illumination is the most limiting constraint when it comes to lunar surface mission planning. The VIPER mission is interested in sites that have permanently shaded regions because that's where the volatiles will be preserved. At the same time, they need to be near high mountains and ridges that remain illuminated when the sun dips low on the horizon. This results in just a few sites scattered across the lunar south pole. With Lunar Spark, VIPER could remove sun illumination as a constraint and really focus on the areas where resources are most likely to be found. This independence from sun illumination is a major benefit of using the Lunar Spark power delivery system.

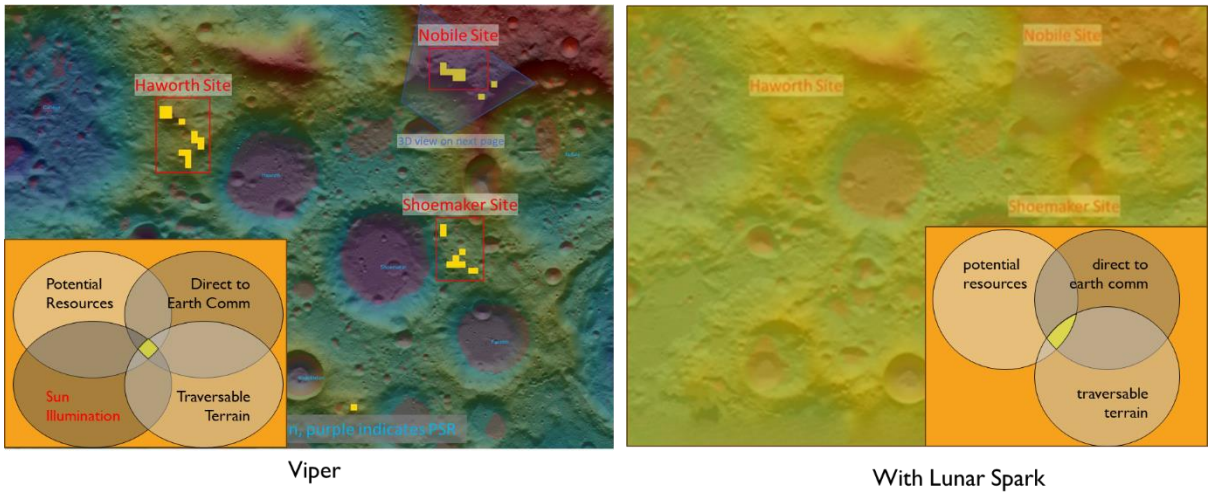

Figure 20: Removing sun illumination as a constraint increases VIPER mission flexibility

The following Measure of Effectiveness (MOE) metrics have been established to assess the performance and success of the designed system in meeting mission objectives. The table below summarizes the benefits Lunar Spark could provide to a mission like VIPER.

1	**Provides survival power (0 W to 80 W)**	**Power**
2	Increase working time from 19% to 42%	Flexibility
3	Increase potential exploration diameter from 3km to 600km	Mobility
4	Extend m ission from 100 days to 1+ years	Extension

Table 9: VIPER mission improvements with Lunar Spark

Power: The Lunar Spark system demonstrates its capability to provide survival power to customers requiring 80 Watts while they are in the dark.

Flexibility: By utilizing the Lunar Spark technology, the system enhances the rover's flexibility by significantly increasing its working time. There is no need to chase the sun light and find safe havens. The estimated improvement for VIPER (Volatiles Investigating Polar Exploration Rover) is from 19% to 42% working time. This increase is achieved by eliminating the need for the rover to traverse to a safe haven with suitable illumination, which accounts for 23% of the previous operational profile. With Lunar Spark, VIPER could keep working as the sun is setting over the horizon and then hibernate in place. The Lunar Spark solution eliminates the need for safe havens all together, which make previously unavailable areas of lunar surface available for exploration and increases the launch opportunities to include lunar winters.

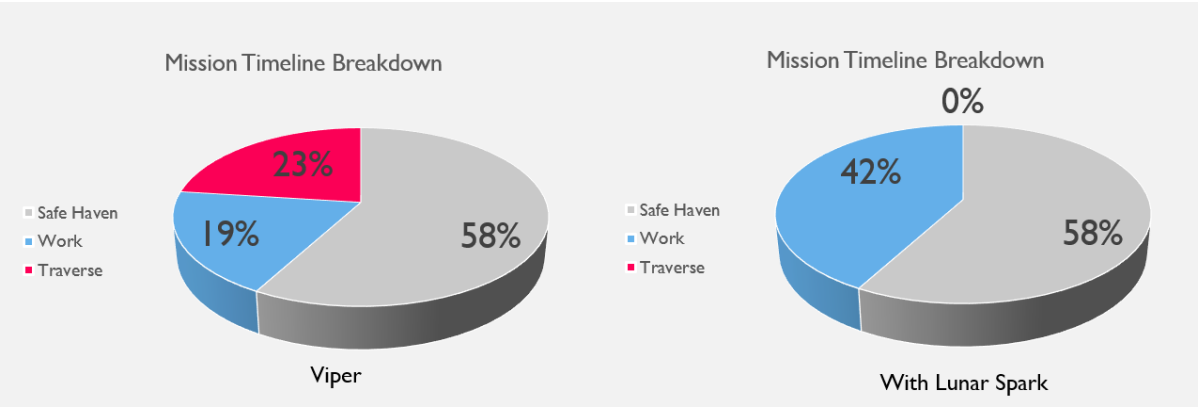

Figure 21: Eliminating the need to traverse to safe havens more than doubles work time for VIPER

Mobility: The Lunar Spark solution revolutionizes the rover's mobility capabilities. While the Viper mission showcased a radius of mobility limited to 3 km due to the need to remain close to safe havens, the implementation of the Lunar Spark technology empowers the rover to explore a vast region around the lunar south pole, spanning an impressive diameter of approximately 600 km as they no

longer limited by sun illumination. This expanded range unlocks unprecedented opportunities for scientific exploration and data collection. Without the limitation of sun illumination, vehicles are free to explore the entire south polar region, including inside dark craters. The system could also support potential north polar missions

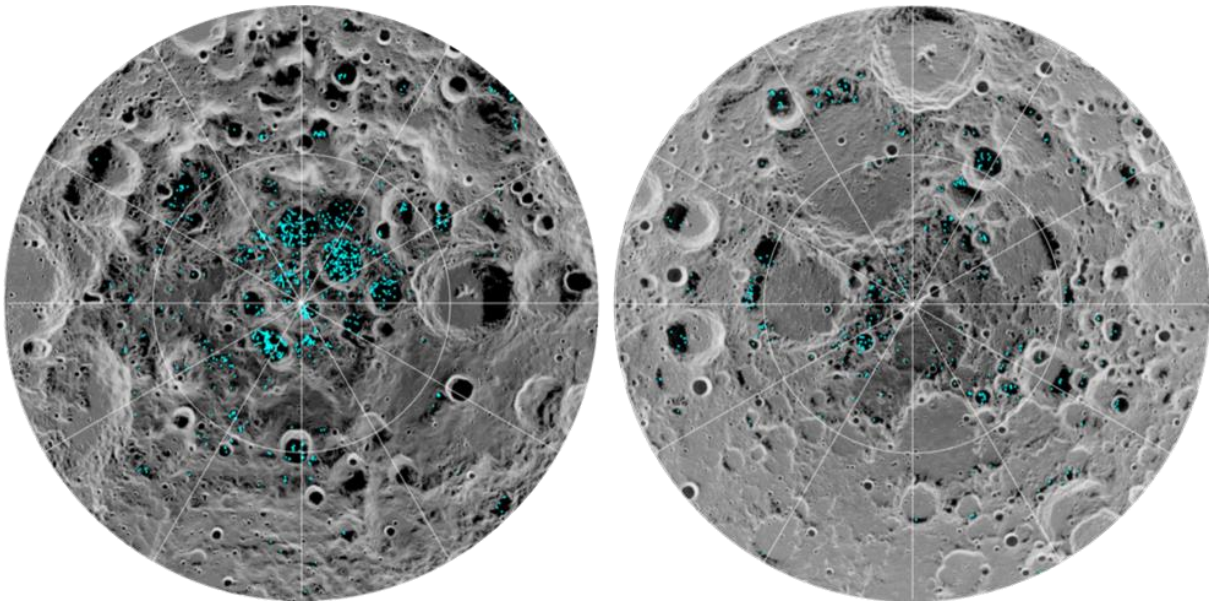

Figure 22: Lunar south and north poles with potential resource site marked in blue

[credit: NASA https://www.nasa.gov/feature/ames/ice-confirmed-at-the-moon-s-poles]

Mission Extension: Traditionally, lunar rovers have been designed to operate for a limited duration of 7-15 days, depending on when the first lunar night falls. However, the integration of the Lunar Spark technology offers a significant extension to the mission's lifespan. With this solution, the mission duration can be extended to the limits of the hardware, enabling prolonged exploration and scientific investigations on the lunar surface. The customer can have lifetime as long as their hardware lifetime.

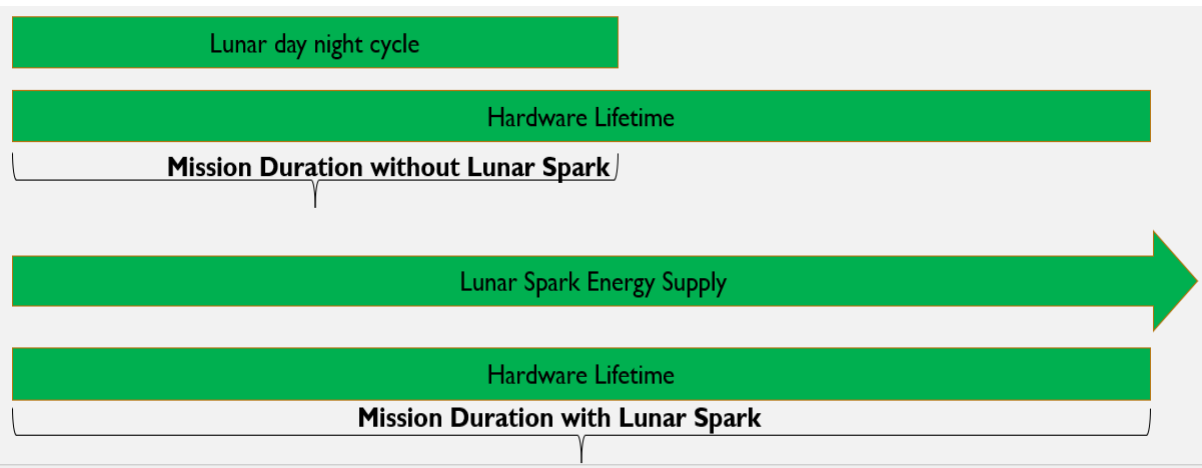

Figure 23: Mission Duration with Lunar Spark extends to the hardware lifetime

These Measure of Effectiveness metrics serve as essential indicators to evaluate the system's performance and its alignment with the mission objectives. The Lunar Spark system demonstrates its capacity to provide survival power, increase flexibility and working time, enhance mobility for extensive exploration, and achieve a substantial extension of the mission's duration. These capabilities position the system as a highly effective solution for future mission requirements, unlocking new horizons in lunar exploration and research.

9. System Customer Interfaces

Lunar Spark aims to provide an end-to-end solution. The first interaction with the customer is through sales and the engineering support provided with the Lunar Spark Receiver. To implement the Lunar Spark solution within the customer mission, the collaboration between both companies shall start at least 3 years prior to launch. Lunar Spark can provide support in system design to define the mechanical and electrical interfaces for the receiver integration. In addition, support in mission planning and operation based on the power supply is offered to the customers.

The receiver hardware will be delivered around two years prior to launch and is fully tested and qualified for space operations. Receiver integration support and system user manuals are included.
The collaboration ends with the end of the customer mission, whereas already planned and scheduled power supplies still will be charged to the customer. The customer is in charge of the disposal of the Lunar Spark receiver as part of his system

During the mission, the system is automated with spacecraft implemented localization and tracking functions that require no active ground operation interface to the customers ground operations team. Customers can send long term planning requests and report any issues to the Lunar Spark Mission control center using a dedicated web interface. This allows the Lunar Spark operations team to check availability and monitor the automated planning of the onboard software.

If a customer would like to change or stop the provision of power for a particular reason, or request additional power, this can also be done through the online tool. There is an emergency number provided for customers, in case of urgent need, this service will be available 24/7.

10. Implementation Plan

The following section gives an overview of the system implementation for the Lunar Spark satellite and receiver. Due to the innovative character of the mission and the complex system setup, a project

setup to be implemented in the Lunar Spark company is selected to follow the space mission design processes, which are well known and established in the business.

10.1. Project Breakdown Structures

The Lunar Spark Project is broken into eleven elements. The following figure shows the details of elements broken into subsystems, components, documents, functionality. The project breakdown structures are detailed below.

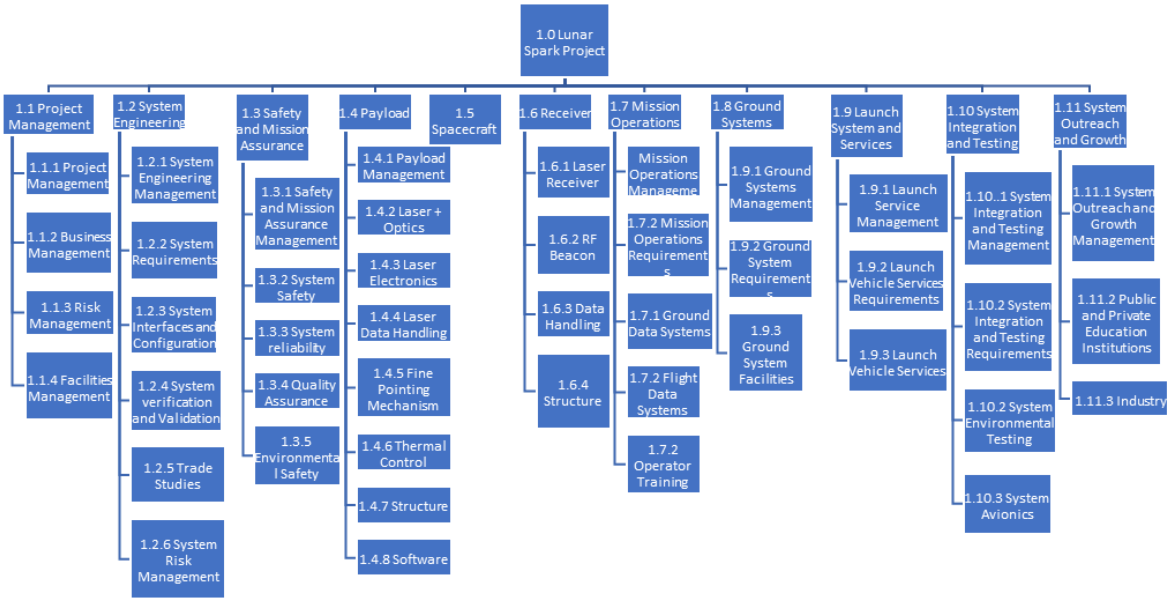

Figure 24: WBS (Work Breakdown Structure) to Level 3

10.2. Work Package Description

Within the Lunar Spark Project, the following Work Packages are defined:

1.1 Project Management

All activities associated with business and administrative planning, organizing, directing, coordinating, analyzing, controlling, status reporting, and approval processes used to accomplish overall project objectives. This includes Business, Risk and Facilities Management.

1.2 System Engineering

This is the technical management for controlling the engineering effort for the project. This is responsible for all hardware and software development.

Main tasks include requirements engineering, preliminary design specifications, interface control documents and preparing the main system engineering reviews.

1.3 Safety and Mission Assurance

This element is responsible for controlling the safety and mission assurance elements of the project. This element includes design, development, review and verification. This function includes the Product Assurance oversight of the subcontractors.

1.4 Payload

This element is responsible for the full Lunar Spark Laser development, from the prototype to the final flight ready payload. This includes all system engineering reviews and contract monitoring. This element includes the special-purpose equipment, Ground Support Equipment (GSE) needed to support system integration and test.

1.5 Spacecraft

The Spacecraft is the platform for carrying the Lunar Spark Payload. This element is responsible for the full Lunar Spark Spacecraft development. The spacecraft bus will be procured from a satellite manufacturer with Lunar Spark providing the payload. This element is responsible for all system engineering reviews and contract monitoring.

1.6 Receiver

This element is responsible for the full Lunar Spark Rover Receiver development, from the prototype to the final flight ready unit delivered to customers. This includes all system engineering reviews and contract monitoring. This element will work closely with the Payload manager.

1.7 Mission Operations

The management of the development and implementation of personnel, procedures, documentation, software and training required to conduct mission operations. This element includes tracking, commanding, receiving/processing telemetry, analyses of system status, trajectory analysis, orbit determination, maneuver analysis, target body orbit/ephemeris updates, and disposal of the Lunar Spark satellites at end of life.

1.8 Ground Systems

This element includes the management of equipment, hardware, software, networks, and mission-unique facilities required to conduct mission operations. This includes all the infrastructure, computers, communications, operating systems, and networking equipment needed to interconnect

and host the Mission Operations software. This element includes the design, development, implementation, integration, test of the ground system, including the hardware and software needed for processing, archiving, and distributing telemetry and telecommands. This element also includes the use and maintenance of the project test beds and project-owned facilities.

1.9 Launch System and Services

This element covers the management of the launch service contract to place Lunar Spark into the Trans Lunar Injection. This element includes the launch vehicle, launch vehicle integration, launch operations, any other associated launch services, and associated ground support equipment.

1.10 System Integration and Testing

This element includes the hardware, software, procedures, and Lunar Spark owned facilities required to perform the integration and testing of the systems, payloads, spacecraft, launch vehicle/services, and mission operations.

1.11 System Outreach and Growth

This element includes management and coordinates activities related to education, public outreach and media support.

10.3. Model Philosophy

The model philosophy proposed to support the verification and validation approach is the Proto-Flight Model philosophy. This is widely used to reduce the cost associated with the use of a full qualification model and flight model. In this approach qualification tests are carried out on the flight model. However, in some key areas driven by risk, other models are needed to support this.

These are related to the laser and laser thermal control system where there will be a Qualification/Engineering model that will be used for ground testing and in the STM (Structural and Thermal Model) (Structural and Thermal Model). The STM will be used to validate the thermal and mechanical models. For these elements only acceptance testing is performed on the PFM, Protoflight Model. The STM tests shall be completed before System CDR.

There will be a “flat sat” for the development of software and the functional verification. Likewise, a similar bench will be used for the Lunar Spark receiver. The Engineering Model (EM) units, primarily to be used in the benches, will be made of commercial grade components with the same specifications as those intended for flight. The qualification models will make use of high reliability space grade components.

	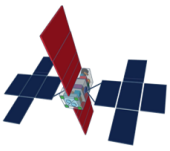 Satellite	 Payload	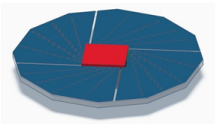 Receiver
Engineering Model (EM)	✓	✓	✓
Structural Thermal Model (STM)	✓	✓	
Qualification Model (QM)		✓	✓
Protoflight Model (PM)	✓		
Flight Model (FM)	✓	✓	✓

Figure 25: Model philosophy for Lunar Spark System Components

11. System Development Plan

The following section presents the basic concepts contained in the System Development Plan. The overall lifecycle follows the ESA standard approach detailed in the ECSS standards.

11.1. Schedule

The overall development flow is summarized below. The space segment development is represented as the 1st Generation Satellite Development below.

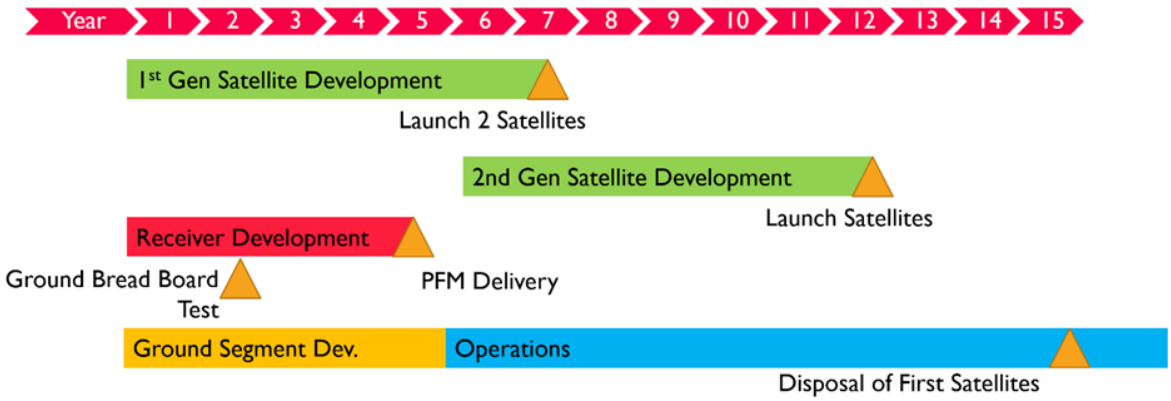

Figure 26: Overall Development Schedule Logic

Below is the preliminary schedule for the Lunar Spark System and Space Segment activities. It is noted that there is eight months margin with respect to the launch date. This is needed due to the risks involved in the overall project. The highest risks are attributed to the payload and its interfaces with the platform, i.e. power and thermal. For clarity only one platform, payload, spacecraft and receiver are shown. The development will consider the first spacecraft as a proto flight model, which is used for qualification. The second model will go through only acceptance testing.

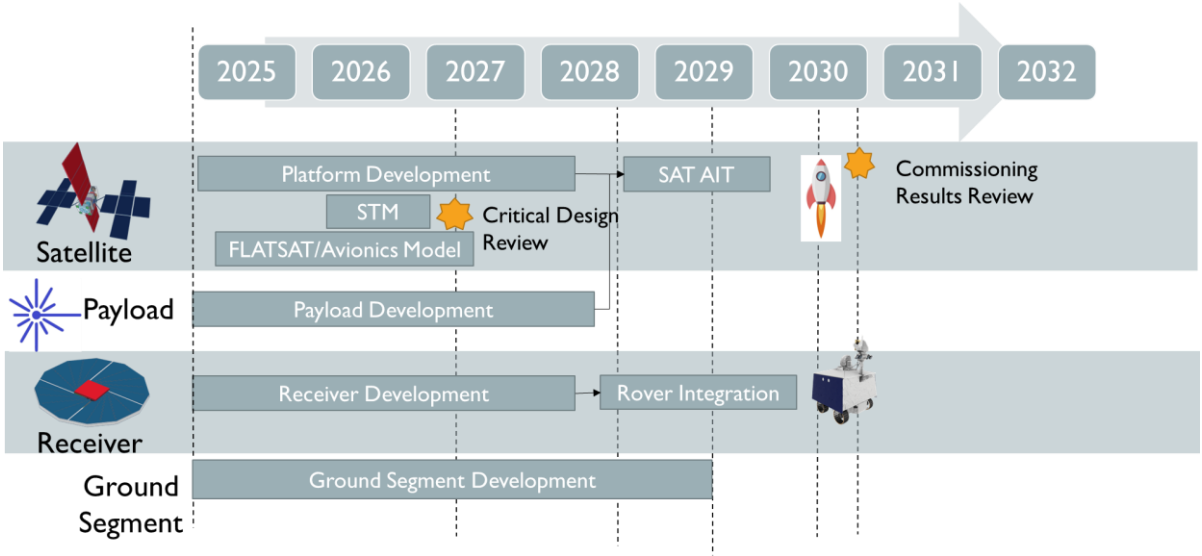

Figure 27: Lunar Spark System and Space Segment Schedule

The acronyms for the reviews follow ESA nomenclature found in ECSS standards, the only difference is the Lunar Spark project has a combined QR, Qualification Review, and AR, Acceptance Review.

11.2. Spacecraft Integration

The payload is separated, as much as possible, to allow parallel integration. The payload is accommodated on the top of the satellite. The satellite is broken into three main layers with a center section consisting of the propulsion module including tanks and the chemical engine for lunar orbit injection. Two outer side panels are used to mount the solar arrays and the two other side panels are used to mount the radiators and antennas. The top panel of the payload will contain the RF antennas for customer receiver detector, the laser and laser pointing mechanism.

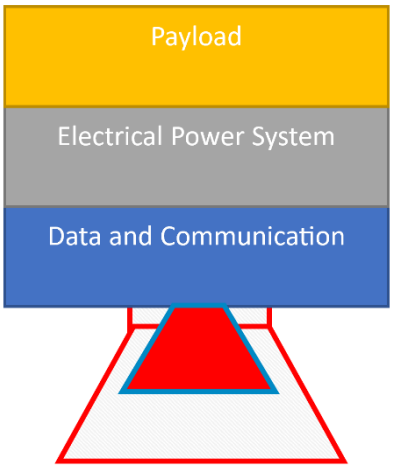

Figure 28: Spacecraft Sub-Assemblies

11.3. Spacecraft PFM AIT Flow

The Lunar Spark System AIT flow for the spacecraft PFM is described in the figure below. The sequence starts with the integration of the payload and spacecraft bus. After this activity the full functional testing is performed. This is followed by the mechanical and thermal tests. An alignment test, covering ADCS and the payload laser, is performed before and after the mechanical testing to check that the necessary alignment tolerance will be maintained after launch. The testing is completed with the electromagnetic compatibility test and the compact range test for the x-band low gain antenna.

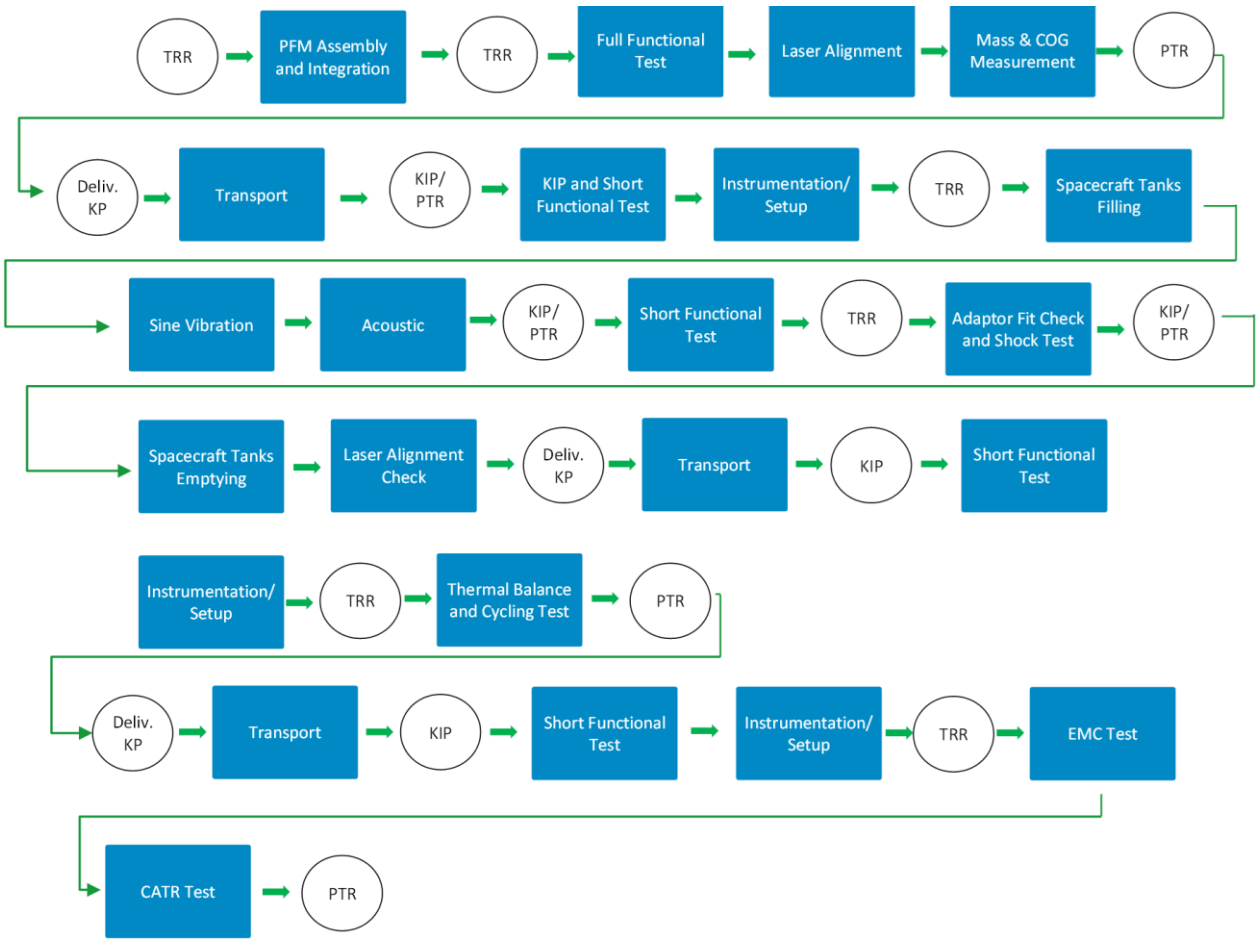

Figure 29: PFM AIT Flow

12. Business Plan

Lunar Spark's objective is to provide a reliable backup power solution for lunar missions, ensures the survival of rovers and remote science installations during the challenging lunar night. Our product consists of an energy receiver module and a reliable source of energy transmitted from our Lunar orbiting satellites. For this purpose, we offer two key products and a service that fully meets the customer need that we identified during several interviews with key stakeholders. Further, our pricing structure is carefully crafted to provide flexibility and attract customers to our system.
This section details the products, services and pricing structure of Lunar Spark.

Firstly, we provide a hardware receiver designed specifically for receiving energy from our Lunar Spark satellite. This hardware seamlessly integrates into our customers' systems, facilitating efficient communication and power transfer between their equipment and our satellites, and is priced at 20 million EUR. Our second revenue stream is the one-time access fee of 5 million EUR that allows for access to Lunar Spark's power infrastructure. In addition, this access fee also includes support with the integration of the receiver into the customer's system, during which the customer will benefit from the comprehensive support and expertise of the Lunar Spark team.

With our power delivery service, we offer a reliable supply of power from our satellites, ensuring continuous operation of survival heaters throughout the lunar night. To incentivize adoption and provide an attractive value proposition, we have set an initial price of 200,000 EUR per kWh delivered for the first five years of service. This competitive pricing model aims to drive customer interest and enable them to benefit from our cost-effective solution. After the initial five years, the price per kWh delivered will increase to 400,000 EUR. This price is very attractive compared to past solar-powered lunar mission costs, which averaged around 1 million euros per kWh. Lunar Spark will offer the power in monthly packages and the customer will pay for the maximum delivered daily power needed.

Lunar Spark's value proposition is a reliable and wireless power delivery service, offering increased mobility, flexibility, and extended mission lifetimes. By eliminating the need for heavy and cumbersome batteries, our solution simplifies systems and reduces associated costs. Mission operators can concentrate on lunar exploration rather than being limited by illumination conditions and vehicle survival.

13. Financial Plan

One of the cornerstones of Lunar Spark is the financial planning. This section details how the financial model has been setup and what were the strategic choices in managing the finances from the moment the company is newly created until 15 years in the future.

Lunar Spark's operations will require significant levels of funding in the first seven years. The main cost drivers until launch are:

- R&D for technological demonstration (excluding salaries): 2.5 Mio EUR
- Flat Payload (year 3-4): 7.3 Mio EUR
- Payload EQM (year 4-5): 60 Mio EUR
- Year 5-6:
    - Total Cost per Satellite Bus (Bus, Integration of Payload, Testing): 100 Mio EUR
    - Total Cost per Satellite Payload: 100 Mio EUR
- Year 7:
    - Launch of two satellites for 100 Mio EUR
- Salaries for the Lunar Spark work force (figure below), as well as corresponding tax and social security contributions for the first 7 years: 45 Mio EUR

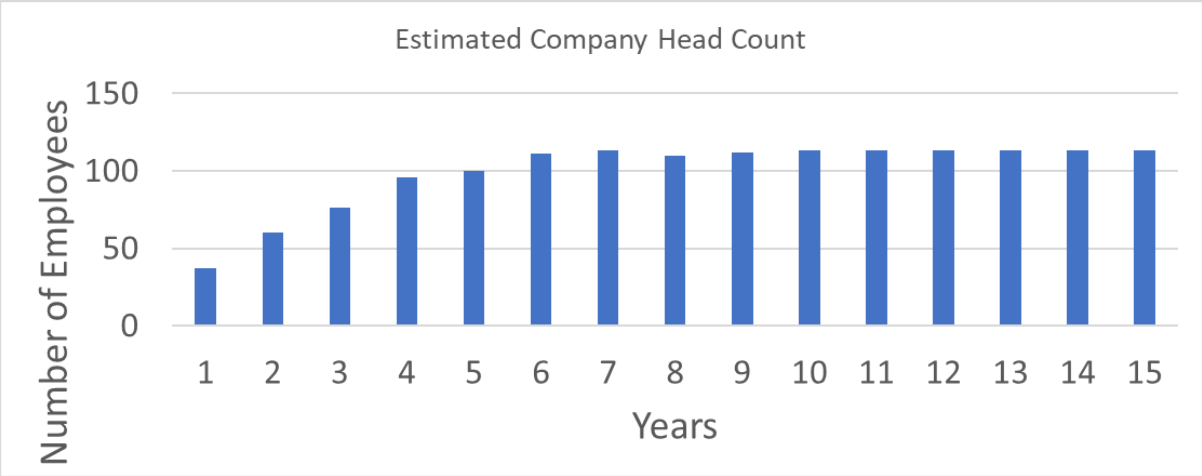

Figure 30: Lunar Spark employee count

The figure below shows the operative cashflow of the company, which follows the typical J-curve for the first 8 years. The large dip occurring during year 5 and 6 is due to the large investment in the production of the first two satellites. The operative cashflow recovers in year 7 after the launch, which initiates the recurring revenue from direct energy provision. Further increases in the operative cashflow are achieved by means of launching the next generation of satellites in year 12.

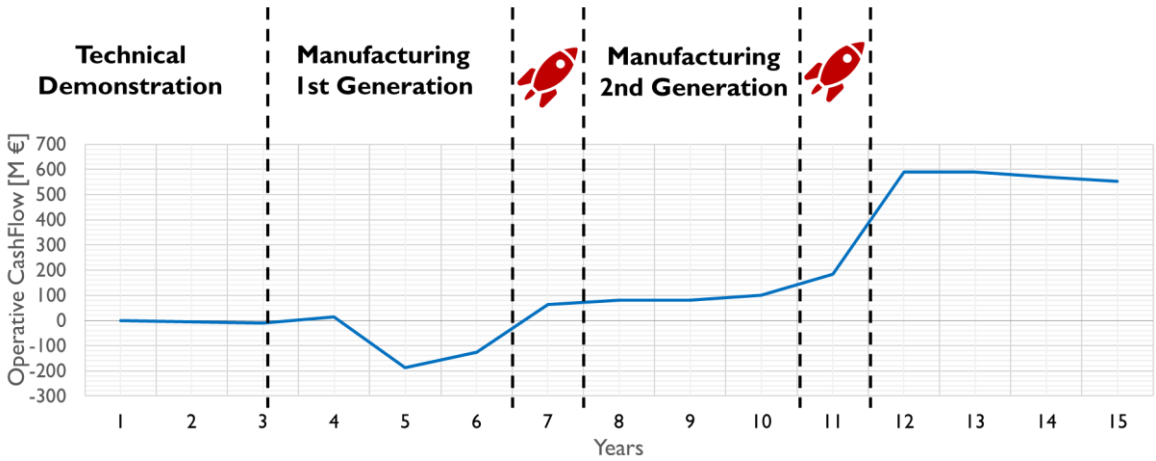

Figure 31: Operational cashflow

It is evident that Lunar Spark requires a large initial funding to cover the expenses of the first 7 years until the first generation of satellites produce a revenue. The captured investment is shown in the figure below. The assumptions on the investments are:

- Year 1-3 (Technological Demonstration)
  - Sweat Equity
  - Own contributions from funders, friends and family of 300.000 EUR
  - Institutional grants worth 35 million EUR
- Year 3-6 (Manufacturing 1st Generation)
  - Institutional grants worth 30 million EUR
  - Investor money worth 120 million EUR
  - Sales of one-time access fee and receiver hardware
- Year 6 (Pre-Launch)
  - Bank loan worth 156 million EUR

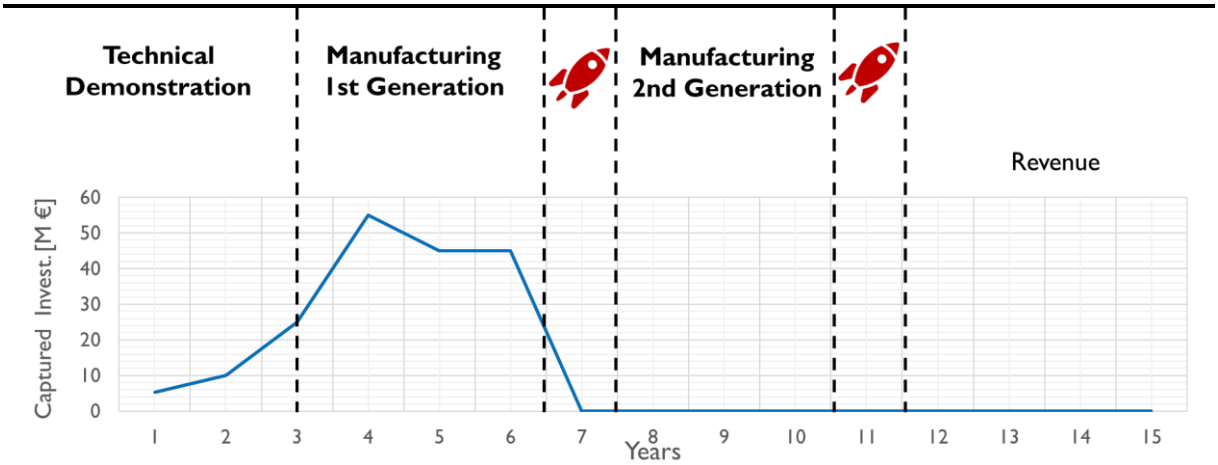

Figure 32: Captured investment

The resulting revenues and expenses are shown in the following figure, indicating a break-even after year 6.

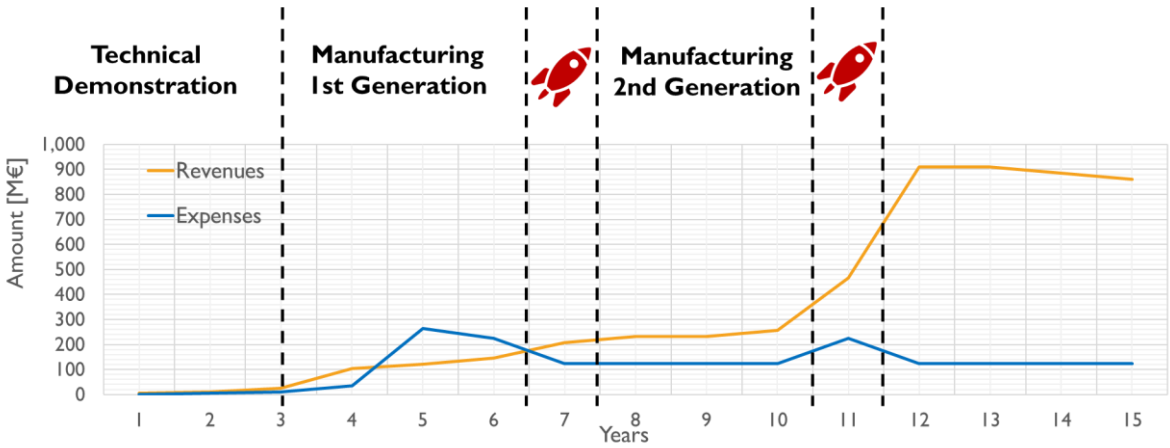

Figure 33: Revenue and expenses

The next figure shows that the resulting cashflow remains positive and yields an investor return of 11.3-12.8 (depending on time of investment). Lunar Spark is thus a very attractive investment.

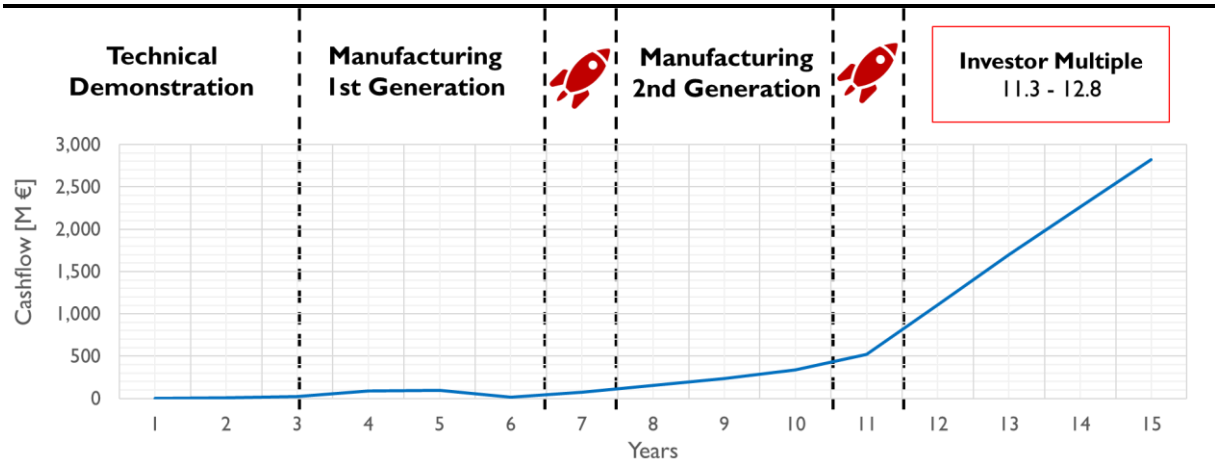

Figure 34: Cashflow resulting in investor multiple of 11.3 – 12.8

In addition to the financial planning above, Lunar Spark performed a sensitivity analysis and analyzed the impact on the financial model. The following scenarios were investigated.

- Satellite utilization of only 30% (instead of 60% baseline utilization) (first figure below)
- Loss of one satellite two years after launch (next figure below)
- Delayed launch (last figure below)

The sensitivity analysis revealed that even in the assumed worst case, Lunar Spark returns investors a multiple of five.

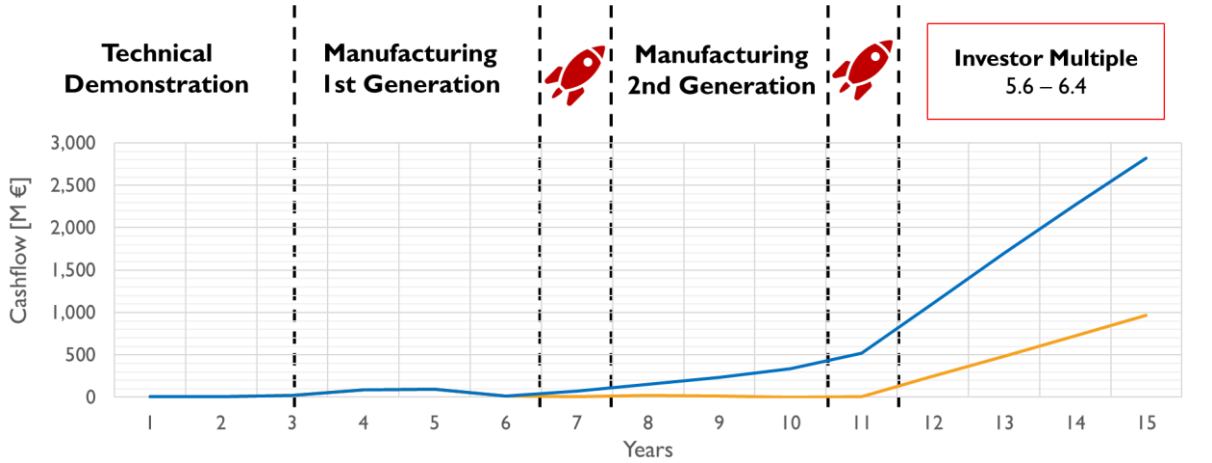

Figure 35: Sensitivity analysis: baseline scenario vs scenario with 30% satellite usage

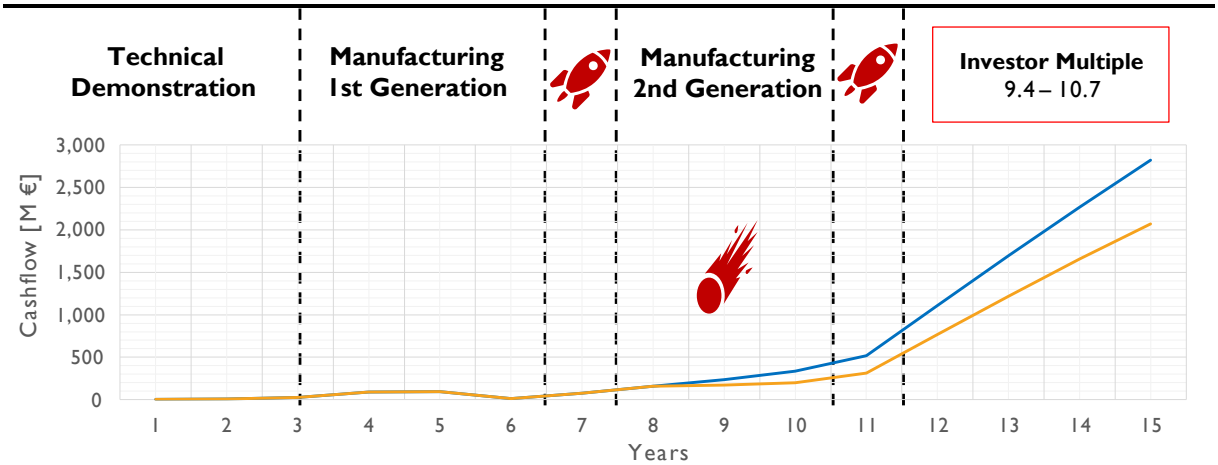

Figure 36: Sensitivity analysis: baseline scenario vs scenario with satellite loss after year two

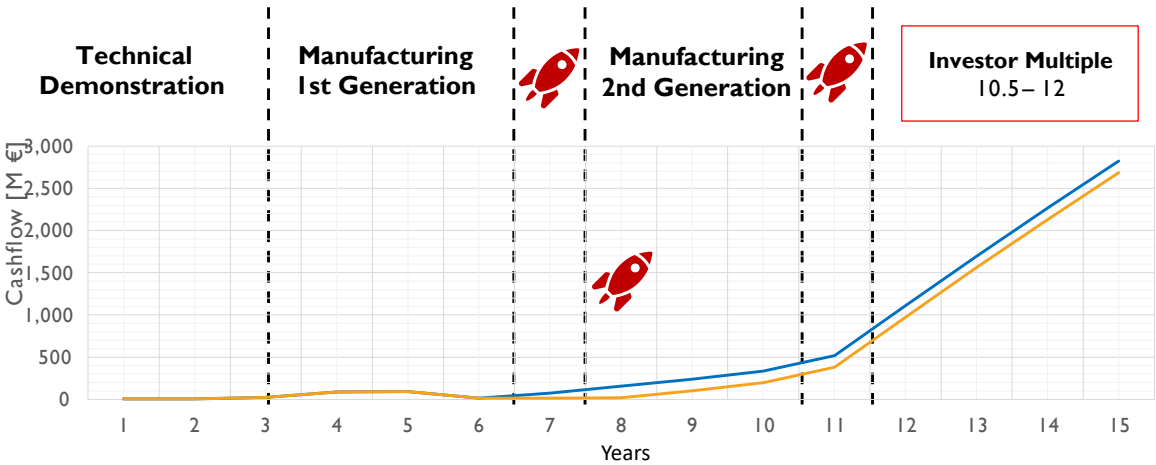

Figure 37: Sensitivity analysis: baseline scenario vs scenario with launch delay

14. Risks

This document presents an abstract of the risk register for the Lunar Spark project, outlining the identified risks along with their respective mitigation strategies. The risks captured in this register have the potential to impact the project's cost, schedule, and technical feasibility. By proactively addressing these risks, Lunar Spark aims to minimize their impact and likelihood, ensuring the successful execution of the project.

14.1. Risk Register

The following table provides a comprehensive overview of the identified risks and their corresponding mitigation actions.

ID	Title	Risk	Mitigation
TR1	Pointing control loops interferences	Given that the laser and laser drivers must be driven with very high power levels, then there exists the possibility that the laser lifetime is shorter than expected	Stability of combined coarse/fine pointing control system shall be carefully analyzed in the first phase of project development via simulation and terrestrial demonstration
TR2	Laser lifetime too short	Given that the laser and laser drivers must be driven with very high power levels, then there exists the possibility that the laser lifetime is shorter than expected	Laser payload component selection with long lifetimes and laser payload redundancy
TR3	Active thermal control system too large	Given than the Lunar Spark satellite must dissipate a large amount of heat, then there exists the possibility that an active thermal control system must be too large and heavy to be able to dissipate the thermal load and keep the satellite and payload within the specified thermal limits	Usage of a single-phase mechanically pumped loop based on ammonia and usage of several improvement techniques to optimize the radiator performance
BR1	Lack of funding	Given that lunar SBPS is a project with a long term vision, then there exists the possibility that our company, Lunar Spark, will not be able to capture enough funding for the business idea.	By finding alternative sources of funding like crowdsourcing or angel investors the risk of getting not enough funding could be reduced. Forfeiting as a last resort especially when only a certain amount is missing.
BR2	Not enough customers in the early phase	Given that lunar SBPS is a project with a long term implementation roadmap, then there exists the possibility that our company Lunar Spark will not be able to find enough customers in the early phase to	The main building blocks of our mitigation strategy to avoid this risk are: define most valuable customers, educate customers and collaborate with institutions on critical missions.

		enable a ramp up and thus end up with lack of financing in the early phase until the first constellation is deployed.	
BR3	Time to market and first revenues at wrong time frame.	Given that lunar SBPS implementation might have a time based sweet spot to take place (neither too early nor too late), then there exists the possibility that the time to market and the generation of first revenues might occur at the wrong time frame.	To reduce the risk of bad time to market we are constantly measuring time to market and we had an initial definition of the project which help identify and mitigate major risks early on.
RR1	Lack of consensus on regulatory framework	Given that the currently existing regulatory framework is not widely widespread, accepted or does not create adoption consensus among the adopting countries, there exists the possibility that we might not be able to operate effectively with our business over an international market without major resources being committed to allow global and potentially specific regional regulatory compliance.	We have to accept that risk, but we will engage with regulators and policymakers: This can help us to better understand the rationale behind disagreements, regulatory changes and influence the direction of policy development.
RR2	Changes in governmental regulatory	Given that the governmental regulatory framework is either non-existent or shifting, then there exists the possibility that we might not be able to operate the system as planned.	This is a risk that we will accept, our mitigation strategy in response to changes in regulatory frameworks and collaborate with space agencies to get their early safety assessment and backing in the regulation decision making.

Table 10 :Risks and mitigations

This risk register is subject to regular review and update throughout the course of the Lunar Spark project to ensure its effectiveness in mitigating risks.

14.2. Risk Conclusion

The risk register for the Lunar Spark project provides a comprehensive overview of the identified risks and their corresponding mitigation actions. By following a structured risk management process and proactively addressing these risks, Lunar Spark aims to safeguard the project's cost, schedule, and technical feasibility. Continuous monitoring and adjustment of mitigation strategies will be performed to ensure the successful execution of the project and minimize any potential adverse impacts.

15. Conclusion and Outreach

Our lunar rover power system utilizes cutting-edge laser transmission technology to provide wirelessly transmitted power from a lunar orbit to lunar rovers on the Moon's surface. This innovative approach enables enhanced mobility, increased mission flexibility, and prolonged mission durations for lunar exploration. Lunar Spark is poised be a significant contributor to future exploration of the lunar surface.

To ensure the system's outreach and growth, we have identified key strategies and growth options that encompass increasing spacecraft capacity, exploring potential use cases, and expanding system capabilities.

Raising Awareness and Stakeholder Engagement: Our outreach activities will focus on raising awareness about the Lunar Spark power system among potential users and stakeholders. This includes active participation in international space conferences and workshops, where we will showcase our research findings and demonstrate the system's capabilities. By engaging with experts, investors, and strategic partners, we aim to generate interest and foster collaboration opportunities to drive system adoption and growth.

Increasing Spacecraft Capacity with Advanced Payload Systems: To meet the evolving needs of lunar exploration, we will invest in research and development to enhance spacecraft capacity with a more advanced payload system. This will involve increasing the power transmission capability and range, improving the efficiency of the laser transmission technology. By scaling the system's capacity, we can reach out to a larger users and aim to gain a higher market share.

Exploring Potential Use Cases: In addition to providing power to lunar rovers, our system has the potential to serve as a power relay system for ground-based operations. By establishing a ground-to-orbit-to-ground power relay infrastructure, we can scale the system to be also used for higher power levels for users being less mobile.

GNSS and Communication as Add-ons to System Capabilities: We recognize the importance of seamless navigation and communication for lunar exploration missions. As an add-on to our satellite constellation, we will explore integrating GNSS (Global Navigation Satellite System) and communication capabilities. By providing precise positioning and reliable communication channels, we can enhance the overall efficiency and effectiveness of lunar rovers, further attracting potential users and stakeholders.

Application of Technology for Satellite-to-Satellite Charging: Expanding the application of laser transmission technology, we will explore the feasibility of satellite-to-satellite charging. Enabling satellites in space to recharge or transfer power using our laser transmission system will unlock new growth opportunities also in the terrestrial space market. By reducing the reliance on traditional power sources and increasing mission endurance, this extension of our technology's capabilities will attract collaborations with satellite manufacturers and space agencies.

Utilizing Laser Payload for Pulsed Laser Debris Removal: Addressing the growing concern of space debris, we can leverage our laser payload system for pulsed laser debris removal. By developing and implementing a debris removal system utilizing our existing laser technology, we contribute to the sustainability of space activities. This addition to our system's capabilities presents an attractive value proposition and opens doors for partnerships with organizations involved in space debris mitigation efforts.

Our system's outreach and growth will be achieved through strategic efforts to raise awareness, scale the system's capacity, and adapt to evolving needs. By increasing spacecraft capacity, exploring potential use cases, and expanding system capabilities with GNSS, communication, satellite-to-satellite charging, and debris removal, we position ourselves as a key player in the lunar exploration domain. Through collaboration, innovation, and stakeholder engagement, we aim to enable and advance lunar missions with a sustainable and efficient power solution for lunar rovers.